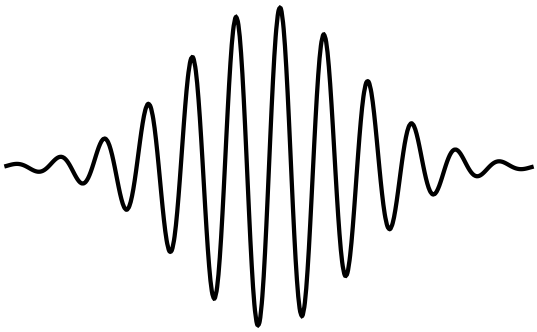

Analysis and Design of a Low Noise, Small Area Inductorless Oscillator for RF Applications

Masterthesis

Patrick Schulz

Fachgebiet Mixed Signal Circuit Design
Fakultät IV Elektrotechnik und Informatik
Technische Universität Berlin

Analysis and Design of a Low Noise, Small Area Inductorless Oscillator for RF Applications

Masterthesis

Patrick Schulz
342 197

19. Juni 2017

Supervisor:

Prof. Dr. Friedel Gerfers
Prof. Dr. Roland Thewes

Eidesstattliche Erklärung

Hiermit erkläre ich, dass ich die vorliegende Arbeit selbstständig und eigenhändig sowie ohne unerlaubte fremde Hilfe und ausschließlich unter Verwendung der aufgeführten Quellen und Hilfsmittel angefertigt habe.

Berlin, 19. Juni 2017

Patrick Schulz

This research was conducted in cooperation with NXP, Hamburg.

Zusammenfassung

Für unsere modernen Kommunikationssysteme wie WiFi oder mobile Kommunikation (Handy) sind hohe Bandbreiten und damit ein hoher Datendurchsatz erstrebenswert. Da die verfügbaren Sendefrequenzen limitiert sind, müssen diese Systeme in ihrer Leistungsfähigkeit zunehmen, um dem zunehmenden Fortschritt der Verwendung von Technologien gerecht zu werden. Wichtige Fragen beim Entwurf von Kommunikationssystemen sind, neben anderen, das generierte Rauschen sowie der ökonomische Wert. Je niedriger das Rauschen ist, desto enger können einzelne Kanäle zueinander platziert werden, was es einen höheren Datendurchsatz in einem Frequenzband ermöglicht. Je günstiger Systeme entworfen werden, desto mehr können produziert werden.

Ein wichtiger Baustein in Kommunikationssystemen ist der Oszillator, welcher benötigte periodische in gewünschter Frequenz erzeugt. Aktuell bilden Oszillatoren basierend auf Kapazitäten und Induktivitäten (LC-Oszillatoren) den Goldstandard in der Hochfrequenzindustrie. Die Induktivitäten nehmen allerdings einen wesentlichen Teil der Fläche der integrierten Schaltungen ein. Während alternative Oszillatortopologien existieren, bleibt das niedrige Rauschen von LC-Oszillatoren unübertroffen. Diese Eigenschaft ist in einigen Fällen wichtiger als die hohe verbrauchte Fläche. Es ist daher von großen Interesse, eine Alternative zu finden, die ein ähnlich gutes Rauschverhalten wie LC-Oszillatoren aufweist, dabei aber weniger Fläche benötigt.

In dieser Arbeit wird ein möglicher Kandidat vorgestellt. Diese Oszillatorstruktur basiert auf aktiven Induktivitäten. Während diese üblicherweise mehr Rauschen als ihre passiven Gegenstücke erzeugen, kann ihr Qualitätsfaktor viel höher sein. Da Oszillatorrauschen stark mit diesem Parameter verknüpft ist, könnten durch Oszillatoren, die auf aktiven Induktivitäten basieren, Systeme entworfen werden, deren Rauschen gleich oder besser ist als das von LC-Oszillatoren. Außerdem wäre hier die benötigte Fläche deutlich kleiner. Der implementierte Oszillator zeigt vielversprechende Ergebnisse – obwohl er LC-Oszillatoren nicht übertrifft – die viel Potential für weitere Verbesserungen aufweisen. Zusätzlich präsentiert diese Arbeit eine theoretische Analyse von Oszillatoren, die auf aktiven Induktivitäten basieren.

Abstract

In our modern communication systems, such as WiFi or mobile phones communications, high bandwidth and therefore high data throughput is desirable. Since the available frequencies for transmission are limited, these systems must improve in performance to keep up with the advance in technology usage. Important topics in designing communication systems are, besides many others, the noise that is generated as well as the economical value. The lower the noise, the more tight transmission channels can be placed, hence more data can be transmitted in the same frequency band, since security spacing can be reduced. The cheaper systems can be designed, the more can be produced.

A part of great importance in communication systems are oscillators, which generate needed periodic signals. Currently, the gold standard in the radio frequency industry are oscillators built from capacitors and inductors (LC oscillators), where the latter consume a big portion of the area of the respective integrated circuits. While there are many different oscillator topologies, none match the low noise of LC oscillators, which in some cases is the most important parameter, even with regard to chip area. It is therefore of great interest to find an alternative, which can keep up with the performance of LC oscillators.

In this work, a possible candidate is presented. This oscillator structure is based on building active inductors. While these generally produce more noise than their passive counterparts, their quality factor can be much higher. Since oscillator noise is highly related to this parameter, oscillators based on active inductors could introduce systems, whose noise performance is equal to or better than LC oscillators while requiring less space. The implemented oscillator shows promising results – though not outperforming LC oscillators – which also show great potential for further improvements. Additionally, a theoretical analysis of oscillators based on active inductors is performed.

Acknowledgments

I wish to thank Professor Friedel Gerfers for his support and trust in me. He introduced me into the wonderful and challenging world of analog integrated design and was a great source of knowledge during my last two years at university. He always took the time to support me during student projects, answering all my questions. I want to thank him very much for great discussions and, of course, for opening the possibility of doing my masterthesis at NXP in Hamburg.

In Hamburg, I would like to thank Martin Ehlert for giving me the opportunity to work at NXP during the preparation of my thesis. My supervisor Ulrich Moehlmann supported me by giving me many insights into the art of PLL-design and general advices and I am grateful for his interest in my workings and ideas. Then I want to thank Saeed Milady for long and interesting talks about every little problem and question I had, including very theoretical topics perhaps not that important for this work. Additionally, Alexander Sanchez shared his expertise on oscillator design with me. Furthermore, thanks go to Said Shahmoradi and Nina Huels for inviting me to off-work activities like christmas market events and lunch breaks. Also, I would like to thank the whole staff of the BU Auto group at NXP for making my work there very enjoyable. From the first day on I was included as part of the team, which I appreciate a lot.

Then I want to thank my university colleages, who accompanied me during my years at TU Berlin. Thank you for all the great and interesting conversations, lunch in the cafeteria, important reminders and leisure activities: Urs Hecht, Christiane Schiller, Özgü Dogan, Zenit Music, Marius Kaufmann-Bühler, Marcel Meinersen, Sophia Bauknecht, Robin Piper and The-Thu Tran. I wish you all the best for finishing your studies and your life after university. I hope we will all see us again.

Furthermore I would like to thank my family: My parents for making it possible for me to follow my studies free of financial problems. Their advice was always appreciated as well as their house being a home for me anytime. Thanks go also to my sister for being available whenever I needed to talk to her. I wish her all the best for her graduation and her many projects at our parent's house.

Finally, I want to thank Tony, who supported me during my thesis while she herself had to prepare for her final exam. Thank you for all the great days we spent together, celebrating our free time. And thank you for keeping my head from exploding in the final days of writing my thesis.

Contents

List of Figures

Chapter 1.

Introduction

In our world today, wireless communication plays a more and more important role in our daily life and society. Probably one of the most important technologies for day-to-day activities is the smartphone. Receiving mail, planning schedules, playing games, all while always being "online". Usually, mobile communication is expected by its users to provide all demanded functions and data, preferably with high data rates and no connection issues. Only events like New Year's Eve show the limits of our current communication technology, where it is often unlikely that a proper connection between two users can be established.

Our communication technology affects not only daily life but also industry, medical applications and many more. There is public radio, mobile phones, television, satellite (for example GPS), Wi-Fi and also household objects such as light control or entertainment systems. Implanted devices for medical diagnosis and treatment can now be checked and operated without removing them from the body. It is safe to say that our current life is not thinkable and would be very different without wireless technology. How is it possible that wireless communication devices are increasing with data rates and accessibility also improving simultaneously?

The increasing technology pushes the boundaries of possibilities and imposes new requirements on performance of communication systems. One major issue in the design of these systems is noise. It limits the minimal detectable signals and disturbes other communication channels and standards. With the current advance in technology, this demands a great noise performance of these systems. As will be shown in the course of this work, oscillators (which are needed for modern communication concepts) play an important role in determining the noise performace of entire communication systems.

Besides opening up more and more fields of applications, the existing technologies also demand to improve. Cellular mobile communication has now been around for some years, but there still are many developments of new wireless standards. This is not surprising: As of 2015, roughly $1.4 \cdot 10^9$ smartphones have been sold world-wide, all needing small, reliable and efficient communication circuits. Besides mobile communication, these devices also make extensive use of internet resources. This yields an increase in the amount of used data, which somehow has to get to the phone and back again. For this, wireless standards are extended and improved (or created) to provide the needed data rates. Examples are *EDGE* and *LTE*.

It is, obviously, not enough to define new standards, they also have to be implemented. For this, new systems and circuits have to be developed in order to enhance previous system performances.

Furthermore, not only signal processing is now done by digital architectures, but also "classical" analog domains are becoming increasingly digital.

As will be seen in the course of this work, electronic noise plays in important role in high throughput communication systems.

1.1. Motivation

Figure 1.1 shows the die photographs of an two different LC oscillator, both operating in the same frequency range (around 1 GHz). Even without any knowledge of integrated circuits and chip design, one would immediately notice the coils on the chips, which take a significantly amount of space. In factor, almost half of the chip area is occupied by them, perhaps even more for the chip in the right image.

The oscillators shown here consist of a resonator and some active circuitry, furthermore a buffer to provide a low output impedance. The resonator is made from a coil (the "balanced inductor" in the left image) and a capacitor (the "varactor" and the "switched-cap array", both also in the left image), whereas the buffer and the active circuitry are implemented with transistors. Since

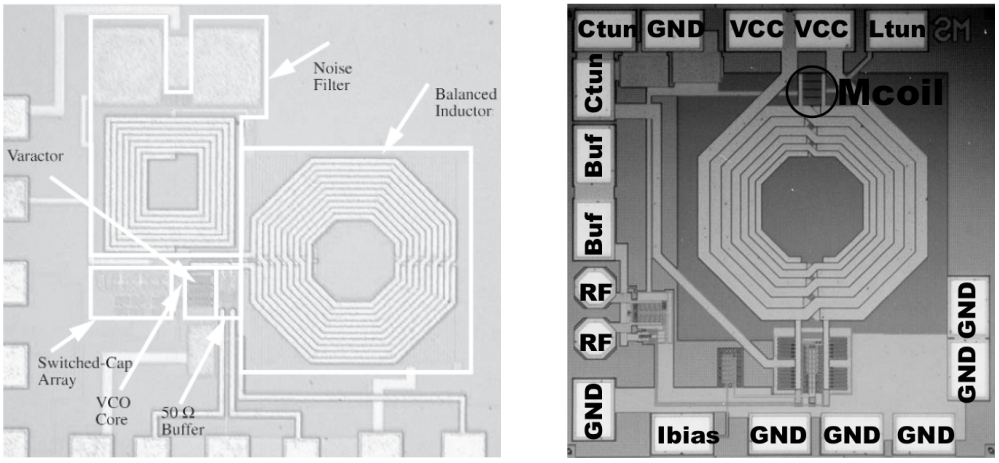

Figure 1.1. – Die photographs of two different LC oscillators of approximately the same operating frequency (1 GHz). Left image: [HSA01], right image: [Tie06]

transistors can be used in order to build complex circuits and signal processing units, it seems excessive to allocate so much space for one device (the inductor) and not use this space to build interesting and useful systems. Now, why is so much chip area "wasted" by the inductor? What purpose does it serve and why can't it be replaced by something substantially smaller? This

work will try to answer these question and provide some insights on alternative designs where bulky inductors are not needed.

1.2. Overview

This work is structured as follows: First, some basic concepts about modern communication systems and frequency synthesizers will be presented. Furthermore, fundamental mathematics used will be discussed. The second part is an extensive treatment of oscillators. This includes mathematical models, topologies and an more in-depth discussion on phase noise. These concepts will be shown by studying simple examples. The following chapter will discuss passive and, more importantly, active inductors to be used in oscillators. After this, oscillators using active inductors will be presented. Here, a specific topology will be presented, which results will be shown in the following chapter. Lastly, a conclusion will be drawn as well as further prospects.

Chapter 2.

Foundations

This chapter will give a short overview of modern communication systems. For this, general information on communication concepts will be given as well as a basic introduction to phase-locked loops.

2.1. Introduction to modern communication systems

What is wireless communication and how does it work? For the user of communication systems, the inner mechanisms are abstract and unknown, maybe somewhat "magical": The data goes in one device and appears (more or less instantly) at another. The data can be anything from images, speech signals, texts and more. Figure 2.1 shows this structure. The transmitter needs

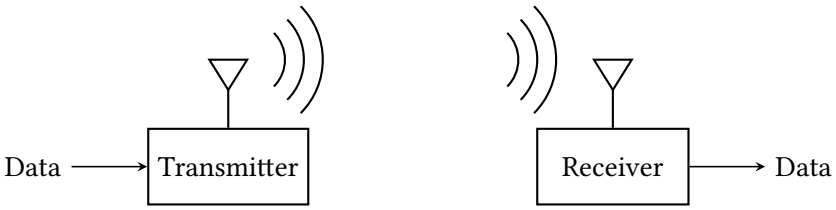

Figure 2.1. – Basic structure of wireless communication

to process the data and impose it on a *carrier signal* or simply carrier. This is a special signal which acts as a transporter and brings the data from the transmitter to the receiver. There, the data gets extracted from the carrier signal and is again available to the user. There is more to the whole picture, of course, but here only a few important aspects shall be covered.

The carrier is a periodic signal and therefore can be characterized by its frequency. The frequency distribution of carrier signals is significant in todays communication systems, where the allowable ranges for different types of communication (for example WiFi or radio) are specified by wireless communication standards. This means that different standards operate in different frequency intervals or *bands*.

An important mechanism is *up-/downconversion*, which describes moving the signals of interest to a different frequency band. This is for several reasons: First, this can be used to achieve

much more efficient communication since losses in transmission depend on the frequency of the transmitted signal. Secondly, it is impossible to transmit signals, which *basebands* (the spectrum of the data) include DC values ($f = 0$), so in these cases a conversion is needed. Furthermore, shifting baseband signals to different frequencies allows simultaneous use of different communication standards, which themself consist of many channels. Therefore, a much higher data throughput can be achieved by using conversion of frequencies.

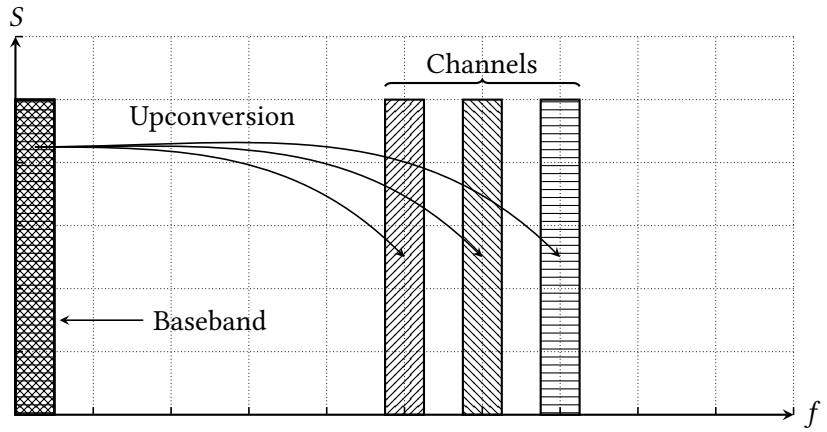

Figure 2.2. – Frequency translation of baseband signals (upconversion)

Figure 2.2 reveals this principle. Three competing transmissions with the same baseband (the data is different, but needed bandwidth is the same) are shown. If there is a different channel for each transmitter, the data can be transmitted simultaneously without interference. A receiver has to pick the right channel, read out the channels after each other or use more than one signal path for simultaneous reception. This shows that receivers must be selective in frequency which usually leads to systems being sensitive only to specific frequency bands. Broadband systems incorporating a large frequency range are in general harder to implement and less efficient.

The conversion process is done through a *mixer*, which generates periodic signals with the sum and the difference of the frequency of the input signals (and possible more harmonics with all thinkable integer frequency combinations ($n\omega_1 + m\omega_2$). A simple mixer can be built from multiplying two signals ($u(t)$ is a generic signal):

$$\begin{aligned} u(t) &= u_0 \cos(\omega_s t) \\ u_m(t) &= u(t) \cdot \cos(\omega_m t) \\ &= \frac{u_0}{2}\Big(\cos\big((\omega_m - \omega_s)t\big) + \cos\big((\omega_m + \omega_s)t\big)\Big) \end{aligned} \tag{2.1}$$

The mixing process generates two new (translated) signals at the frequencies $\omega_2 - \omega_1$ and $\omega_2 + \omega_1$, therefore creating one signal with higher and one with lower frequency. The unwanted signal (depending on up-/downconversion) can easily be filtered out. An upconverted signal can be downconverted by the same process, in this case filtering out the high frequency part. Note

that it is of no importance whether the mixing frequency is higher or lower than the signal frequency.

The described conversion process can be used in two different ways: Direct or *homodyne* conversion and *heterodyne* conversion.[1] Homodyne conversion shifts signals directly from the baseband to the transmission frequency and back, where heterodyne architectures use an *intermediate frequency (IF)*. This has some advantages over the direct principle: In tuned receivers many different frequency channels and bands can be detected, but by converting them all to a common frequency band (the intermediate frequency) the exact same post-processing circuitry can be used for all signals. Furthermore, this allows higher selectivity, since filters for lower frequencies can be implemeneted with narrower bands.

The two main building blocks of communication systems are the receiver and the transmitter (often combined as *transceiver*). They serve the complimentary purposes: The transmitter takes a signal, converts it to a higher frequency and transmits the converted signal with the means of an antenna. The receiver senses a signal at the antenna and downconverts it back to the baseband. The baseband signal in both systems is usually processed by a digital unit.

Figure 2.3 shows a typical heterodyne receiver. In the high frequency part of the system (the RF part), there is the antenna, which picks up the transmitted signal. This signal gets filtered to remove all out-of-band signals. Then, the remaining signal gets amplified by a low noise amplifier (LNA) and downconverted through the mixer which is driven by the local oscillator (LO). Now the signal lies in the intermediate frequency and gets further processed here, for example through a demodulator. Afterwards, the baseband signal carrying the actual information is processed. The last two steps are often combined, in this case the signal after the downconversion is converted to the digital domain by the means of an analog-to-digital converter (ADC), so that the demodulation and the processing both take place in the more robust digital world.

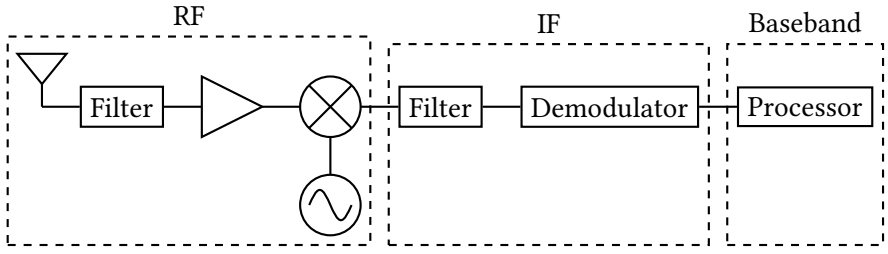

Figure 2.3. – Structure of a modern heterodyne receiver

[1] The term homodyne originates from the greek words *homo* (same) and *dyne* (mixing), *hetero* means different.

2.2. Frequency synthesizers: Phase locked loops

In figure 2.3, many important building blocks of communication systems can be seen, which all are not trivial to design. This work will focus on the local oscillator. In order to select many different channels and even different frequency bands of different communication standards, the oscillator must provide a very frequency-stable signal, since fluctuations in frequency directly relate to errors in downconversion. Furthermore, the oscillator needs to be *tunable* for the selection of a channel. While it is possible to build a relatively stable *fixed* oscillator, it is hard to acchieve both stability and tunability. How is this acchieved in modern communication systems? The answer to this question is to build a *frequency synthesizer*, which is based on a *phase-locked loop*.

A phase-locked loop is a negative feedback system controlling frequencies. It works by comparing a (tunable) signal two a fixed reference signal and adjusting the tunable signal until both match.

Figure 2.4 shows a generic model of a phase-locked loop. This model consists of four basic building blocks: First, a phase detector, which produces the phase difference of the two signals ϕ_1 and ϕ_2 as output. This output signal incorporates both high and low frequency contents, therefore a filter is used to remove unwanted signals. The output of the lowpass filter is then fed into a signal-controlled oscillator (SCO), producing a periodic signal, whose frequency is dependent of the phase difference of the two input signals. The divider makes it possible for the SCO to use higher frequencies than the reference signal.

This structure forms a negative feedback loop: in the case of ideal components, the frequency of the output signal will be the frequency of the input signal multiplied by the division factor. The

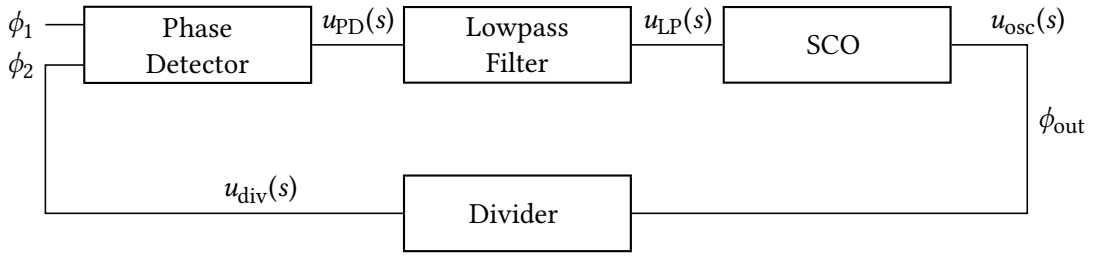

Figure 2.4. – Blockdiagram of a phase-locked-loop

signal-controlled oscillator can be controlled in many different ways; typical implementations are a *voltage*-controlled oscillator (VCO) or a *digitally*-controlled oscillator (DCO), but other types are possible (for example current-controlled oscillators).

The phase detector produces a signal proportional to the phase difference of the two signals ϕ_1 and ϕ_2:

$$u_{PD}(s) = k_{PD} \cdot (\phi_1 - \phi_2)$$

This signal gets shaped by the lowpass filter, which also removes unwanted high frequency components created by the phase detector. The corresponding output is found by multiplying the signal with the transfer function of the filter:

$$u_{\mathrm{LP}}(s) = H_{\mathrm{LP}}(s) \cdot u_{\mathrm{PD}}(s) = H_{\mathrm{LP}}(s) \cdot k_{\mathrm{PD}} \cdot (\phi_1 - \phi_2)$$

The signal-controlled oscillator produces a periodic signal with a *frequency* proportional to the input signal. Frequency and phase are related to each other through differentiation/integration: The phase is the time-domain integral of the frequency. A signal with constant frequency will have a phase variing linearily in time. Therefore, in phase domain, the oscillator operates as integrator:[2]

$$u_{\mathrm{osc}}(s) = \frac{k_{\mathrm{osc}}}{s} H_{\mathrm{LP}}(s) \cdot k_{\mathrm{PD}} \cdot (\phi_1 - \phi_2) \tag{2.2}$$

The divider simply adds another factor N:

$$u_{\mathrm{div}}(s) = \frac{1}{N} \cdot \frac{k_{\mathrm{osc}}}{s} H_{\mathrm{LP}}(s) \cdot k_{\mathrm{PD}} \cdot (\phi_1 - \phi_2)$$

This signal $u_{\mathrm{div}}(s)$ is exactly ϕ_2, so we can calculate a transfer function from the input signal ϕ_1 to the output signal ϕ_2:

$$\begin{aligned}
\phi_2 &= \frac{1}{N} \cdot \frac{k_{\mathrm{osc}}}{s} H_{\mathrm{LP}}(s) \cdot k_{\mathrm{PD}} \cdot (\phi_1 - \phi_2) \\
\iff H(s) &= \frac{\frac{1}{N} \cdot \frac{k_{\mathrm{osc}}}{s} H_{\mathrm{LP}}(s) \cdot k_{\mathrm{PD}}}{1 + \frac{1}{N} \cdot \frac{k_{\mathrm{osc}}}{s} H_{\mathrm{LP}}(s) \cdot k_{\mathrm{PD}}} \\
&= \frac{\frac{1}{N} \cdot k_{\mathrm{osc}} H_{\mathrm{LP}}(s) \cdot k_{\mathrm{PD}}}{s + \frac{1}{N} \cdot k_{\mathrm{osc}} H_{\mathrm{LP}}(s) \cdot k_{\mathrm{PD}}} \\
&= \frac{1}{1 + s \frac{N}{k_{\mathrm{osc}} k_{\mathrm{PD}} H_{\mathrm{LP}}(s)}}
\end{aligned} \tag{2.3}$$

As can be seen, the exact type of transfer function depends on the type of loop filter. For a low-pass filter, the derived transfer function will also show a low-pass characteristic.[3]

Equation 2.3 shows the transfer function from ϕ_1 to ϕ_2, which is approximately 1 for low frequencies. Therefore, if the phase of the reference signal and the (divided) phase of the synthesized signal are equal, the phase is *locked*[4]. If the phases are the same, also the frequencies

[2] Admittedly, this "proof" lacks formality. For this discussion, however, this analysis is sufficient. The integrating nature of the oscillator for phase signals will be addressed again later on. See section 2.3.2 and 3.7.4.

[3] Imagine the simplest case: A one-pole filter. The pole of this filter will shift in frequency but stay a pole.

[4] There may be a constant offset.

of the two signals will be equal. This means that (mentally moving before the divider) the output signal of the PLL (the signal coming out of the oscillator) has a N-fold frequency of the input signal. If the reference signal is perfect, the non-idealities of the SCO play are not of concern. Now, why is this sensible to do? Why not directly use a reference signal with the right frequency? The key here is the divider. Since the output of the PLL is a signal with *increased* frequency, a PLL with a variable (programmable) divider provides a system which performs programmable frequency multiplication. Therefore this configuration is called a frequency synthesizer.

An major property of a phase-locked loop is that it stabilizes the frequency of oscillators due to its negative feedback. This has several important consequences: Any static frequency error of the oscillator due to process mismatch and other non-idealities is fixed. The control signal of the SCO will be adjusted accordingly, so that again the phases of the two signals match.

The oscillators (both the reference and the SCO) exhibit noise in the phase domain, the so-called phase noise. In general, the power spectral density of this noise gets shaped by the corresponding transfer function of the PLL. Here, the transfer function from the reference to the output and from the SCO to the output are analyzed. The first transfer function is already known: It simply is the transfer function that was previously derived.

The second transfer function (from the SCO to the output) is given by the following equation, which is derived from equation 2.2 with $\phi_1 = 0$ and an addition of a noise signal (ϕ_N):

$$\begin{aligned} \phi_{\text{out}} &= -\frac{k_{\text{osc}}}{s} H_{\text{LP}}(s) \cdot k_{\text{PD}} \cdot \phi_{\text{out}} + \phi_N \\ \iff \phi_{\text{out}} &= \phi_N \cdot \frac{1}{1 + \frac{k_{\text{osc}}}{s} H_{\text{LP}}(s) \cdot k_{\text{PD}}} \end{aligned}$$

The simplest low-pass filter is of the form

$$H_{\text{LP}}(s) = \frac{1}{s + \omega_c}$$

With this, both transfer functions can be written as

$$\begin{aligned} H_1(s) &= \frac{k_{\text{PD}} k_{\text{osc}} N}{k_{\text{PD}} k_{\text{osc}} + sN + s^2 \frac{N}{\omega_c}} \\ H_2(s) &= \frac{Ns + s^2 \frac{N}{\omega_c}}{k_{\text{PD}} k_{\text{osc}} + sN + s^2 \frac{N}{\omega_c}} \end{aligned}$$

$H_1(s)$ shows a low-pass characteristic, while $H_2(s)$ has a high-pass behaviour. This means that phase errors from the input (the reference) are filtered out at high frequency ($H_1(s)$) and phase

errors coming from the SCO are suppressed at low frequencies. Phase noise is a type of phase error and therefore gets shaped by the corresponding transfer function. Figure 2.5 shows a typical phase noise profile of the output signal of a phase-locked loop. The dashed lines show the unfiltered phase noise of both the reference oscillator and the SCO with the SCO showing a higher amount of noise. The dotted lines are the respective phase noise profiles after filtering, the solid line depicts the total phase noise of the frequency synthesizer. As can be seen, the

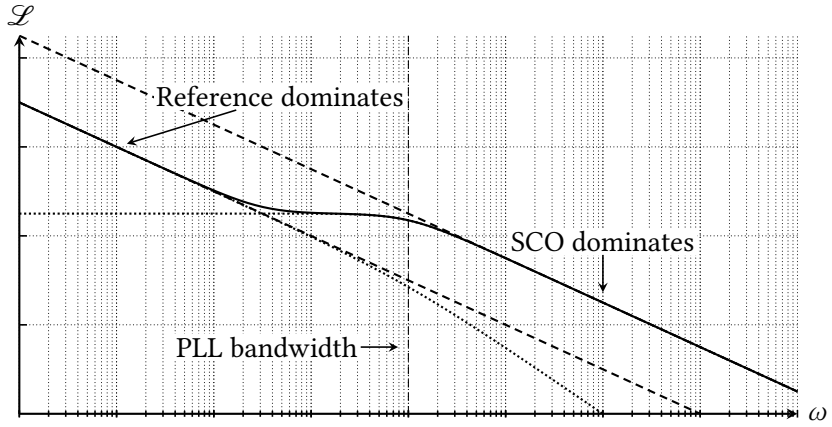

Figure 2.5. – A typical phase noise profile of a phase-locked loop

reference phase noise is significantly lower than the phase noise of the SCO. This is a sensible assumption, since the reference is used as stable signal, to which the synthesized signal can be compared to. Note that the phase noise of the SCO gets filtered out below the PLL bandwidth and becomes flat while the reference phase noise get filtered out at frequencies above the PLL bandwidth. Therefore, the slope here increases. More information on phase-locked loops can be found for instance in the book by Roland Best ([Bes07]) or the book by Floyd Gardner ([Gar05]). A quick overview with basic information is also provided in Razavi's RF microelectronics book ([Raz12]), which serves well as a light introduction.

2.3. Basic concepts in communication

In this section a short overview of important aspects of wireless communication will be given. Some aspects are not directly related to the design of oscillators, but do add constraints to it. Furthermore, it helps in understanding RF circuits and design choices.

2.3.1. Multiple access techniques

How do many users of a certain wireless standard (for example GSM) operate simultaneously? Since there may be thousands of users but not so many channels, there has to be a different approach for solving this problem. The usual techniques incorporate some sort of division

of available ressources of which there are basically three. This is best illustrated by an often used analogy (see for example [Raz12]): Imagine a group of people in a room talking to each other, perhaps at a party. Now there are several different ongoing discussions involving smaller groups. How do the groups distinguish between the message meant for them and the message from another group? The obvious answer is *power* (volume), and its property of decreasing with increasing distance to the transmitter. However, this is not the approach which will be discussed here. One way to communicate properly would be to only speak at certain times: Every group gets a time slot in which they are allowed to talk, perhaps through the use of an object to symbolize the right to speak (a *token*). Another possibility would be that every group has to speak in a different pitch, so you can concentrate only on voices with a low or high pitch. Lastly, the groups could speak in different languages for separation of content.

The three mentioned methods are used in wireless communications and are called *time-division multiple access* (different times), *frequency-division multiple access* (different pitches) and *code-division multiple access* (different languages). Frequency-division multiple access or FDMA was already introduced: The use of different channels within a designated frequency band. As explained before, this is often not enough.

With time-division multiple access or TDMA only one transmitter is active at a time. The individual transceivers receive a time slot, in which they are allowed to make a transmission. For this, clever techniques for finding the time slots have been developed, including for example a random waiting time with sensing for a free channel.

Lastly, code-division multiple access or CDMA assigns different codes to the baseband signal of different transmitters. With the right encoding scheme, it is possible that the unwanted components are canceled out and therefore ignored by the receiver. This technique can be combined with FDMA by periodically switching the transmission channel according to code. This is called *frequency hopping*.

2.3.2. Modulation schemes

Modulation is the process of imposing a baseband signal onto a carrier in order to shift its spectrum in frequency. It is therefore highly related to upconversion and demodulation, which reverses the process of modulation, is related to downconversion. Here, basic analog modulation schemes are presented with a short discussion of digital modulation. The three basic analog modulation types are *amplitude* (AM), *phase* (PM) and *frequency* (FM) modulation.

Amplitude modulation changes the amplitude of a carrier signal $y_c(t)$ according to a modulation signal $y_m(t)$. There are two main types of amplitude modulation, one in which the carrier is transmitted, one where it is not. This difference is simple in mathematical terms: General amplitude modulation can be expressed by:

$$\begin{aligned} y_{\mathrm{AM}}(t) &= \big(1 + y_m(t)\big) A_0 y_c(t) = \big(1 + y_m(t)\big) A_0 \cos(\omega_0 t) \\ &= A_0 \cos(\omega_0 t) + A_0 y_m(t) \cos(\omega_0 t) \end{aligned} \tag{2.4}$$

The first part of equation 2.4 is simply the carrier signal, the second part shows the modulated signal. If the carrier is not transmitted (using so-called double-sideband supressed-carrier transmission), the first part reduces to 0 and only the modulated signal remains. The multiplication of the modulation signal with the carrier signal translates the spectrum of the modulation signal (the *baseband* signal) to center frequencies of $-\omega_0$ and ω_0.

Phase and frequency modulation are similar in both influencing the momentary phase or frequency of a carrier, but they have subtle differences. The distinction depends on the argument of the cosine in equation 2.5 and 2.6.

$$y_{\mathrm{PM}}(t) = A_0 \cos(\omega_0 t + \phi(t)) \tag{2.5}$$

$$y_{\mathrm{FM}}(t) = A_0 \cos(\omega_0 t + \int_{-\infty}^{t} \phi(\tau)\,\mathrm{d}\tau) \tag{2.6}$$

The argument of the cosine is a phase Φ (with its unit of rad) and the instantenous frequency can be found by taking the derivative:

$$\omega(t) = \frac{\partial}{\partial t}\Phi$$

For linear modulation signals $\phi(t) = \phi_0 t$, the difference between PM and FM is clearly visible:

$$\omega_{\mathrm{PM}}(t) = \omega_0 + \phi_0$$
$$\omega_{\mathrm{FM}}(t) = \omega_0 + \phi_0 t$$

While the instantenous frequency of the phase-modulated signal stays constant, it varies over time in the case of the frequency-modulated signal. It is therefore said that for PM the so-called *excess phase* is proportional to the modulation signal while for FM the so-called *excess frequency* shows this property. The excess phase and frequency are the additional part of the cosine argument and its derivative, respectively. See the treatment on analog modulation in [Raz12].

Phase and frequency modulation both yield a complex spectrum, which is not easily calculated. There is a common narrowband-FM approximation where it is assumed that the modulation is small compared to the total phase argument of the cosine. In this case, FM and PM yield a frequency translation similar to amplitude modulation where the baseband signal is centered around the carrier frequency with its original bandwidth.

This treatment of modulation is very brief and only covers analog modulation. The digital counterparts of the here introduced modulation concepts have slightly different names but are basically the same. The difference lies in the nature of the baseband signal, where in one case its analog and in the other its digital. The digital counterparts of AM, PM and FM are called “amplitude shift keying” (ASK), “phase shift keying” (PSK) and “frequency shift keying” (FSK). Digital signals and -modulation are used because they offer advantages in their lower susceptibility to noise. Also, if digitally modulated signals are used, many parts of the

transceiver chain operate in the digital domain, which offers the usual benefits of digital over analog design.

2.4. Mathematical foundations

2.4.1. Review of system theory

A system can be any abstraction of a physical entity, where an input and an output can be assigned. In this work (and generally in electronics), the term system refers to a circuit or a collection of circuits. This abstraction is useful in order to simplify the analysis and to seperate problems and their solution into *system level* and *implementation level*.

Linear, time-invariant systems

A linear, time-invariant system has two important properties: A scaled input signal yields a equally scaled output signal and a sum of two input signals yields the sum of the two corresponding output signals. This is called *linearity*:

$$y(t) = S\{ax_1(t) + bx_2(t)\} = aS\{x_1(t)\} + bS\{x_2(t)\}$$

The second property concerns time-invariance: It is of no significance if a input signal is inserted into the system now or tomorrow. The time of appliance does not alter the response, only shifts it in time:

$$y(t - t_0) = S\{x_1(t - t_0)\}$$

The response of a LTI system to an input signal is related to its *impulse response* $h(t)$, which is, as the name implies, the response of the system to an dirac impulse at the input. With this, the response for arbitrary input signals can be found by using convolution:

$$y(t) = h(t) * x(t) = \int_{-\infty}^{\infty} h(t - \tau)x(\tau)\,\mathrm{d}\tau$$

In the laplace domain the convolution becomes a multiplication and the impulse response becomes the *transfer function* $H(s)$. This function is characterized by three parameters: Static gain, poles and zeros. It can be written as a rational function:

$$H(s) = H_0 \frac{\prod_{i=1}^{N_z}(s - z_i)}{\prod_{i=1}^{N_p}(s - p_i)}$$

The location of the poles and zeros relates to important properties of the system, most dominantly *stability*. Poles in the right half-plane (zeros and poles are complex, therefore for poles where $\mathrm{Re}(p) > 0$), the system becomes unstable. This is especially critical in closed-loop systems, since there poles can vary their position depending on loop gain.

Another important property of LTI-systems is the fact that they don't change the frequency content of a signal. Though the amplitudes of existing signals will be changed, there will never be new frequencies introduced. This means that if a LTI-system is driven by a sinusoid of a frequency ω_0, the output of the system will also be a signal of the frequency ω_0 (with possible different amplitude and phase).

Non-linear and time-varying systems

In a time-variant system, the response to a stimulus depends on the time the stimulus is applied. The output due to the same input signal applied today and tomorrow can be different. This does not necessarily mean that linearity does not hold. A system can perfectly be linear, but time-variant. This can be modeled by using a impulse response, which depends on the time the input is applied. The convolution integral still holds for computing the output of the system as response to an input, but it changes slightly:

$$y(t) = h(t, t_0) * x(t) = \int_{-\infty}^{\infty} h(t - \tau, t_0) x(\tau)\,\mathrm{d}\tau$$

Since there are now many (infinite) impulse responses, there is no need to shift the "original" impulse response in time. Therefore, some authors omit the time shift within the convolution, assuming the $h(t, t_0)$ is "at the right time" ([HL98], [Raz12, page 569]):

$$y(t) = \int_{-\infty}^{\infty} h(t, \tau) x(\tau)\,\mathrm{d}\tau$$

Different from LTI-systems, linear time-variant systems *can* create different frequencies than present in the input. This is not that surprising: If the impulse response changes with time, it also changes within the convolution integral. If now the input signal varies with time, the response does too, but in a possible different manner.

A non-linear system (but perhaps time-invariant) has transfer characteristics, which can't be expressed by linear functions. Often, these systems are approximated as linear systems in certain operating regions, which is called small-signal analysis or approximation. This is an important circuit design technique, for example for amplifier design. Here, the system is approximated as linear and the validity of this assumption is checked later on, possible resulting in a redesign.

While the small-signal analysis is a powerful tool, it comes at a price. There are certain phenomena, that can't be explained or predicted with small-signal models. Care has to be

taken in order take this into consideration during design. As will be shown later, oscillators are inherently non-linear systems.

Similar to time-variant systems, a non-linear system can create harmonics, therefore alter the frequency content of input signals. Take for instance the system below with a non-linear transfer characteristic:

$$y(t) = a\,x(t) + b\,x^3(t)$$

Here, $y(t)$ is the output signal of the system with an input signal of $x(t)$. a and b are constants. If this system is driven by a pure sinusoid of the frequency ω_0, the output will also contain higher frequency components:

$$\begin{aligned} y(t) &= a\cos(\omega_0 t) + b\cos^3(\omega_0 t) \\ &= a\cos(\omega_0 t) + \frac{b}{4}\big(3\cos(\omega_0 t) + \cos(3\omega_0 t)\big) \\ &= \left(a + \frac{3b}{4}\right)\cos(\omega_0 t) + \frac{b}{4}\cos(3\omega_0 t) \end{aligned}$$

Besides altering the amplitude of the main frequency component (ω_0), a new component with the threefold frequency occurs. Therefore, a standard test of linearity is the analysis of the frequency components of the output of a system. For this, a single-tone or a two-tone test can be used, where the latter is specifically useful in narrow bandwidth systems, since the harmonics (which have a significantly higher frequency) of a single tone are possibly filtered out already at observation frequencies. See [Raz12, page 14—35] for a deeper discussion on non-linearity.

Chapter 3.

Oscillator Fundamentals

In this chapter, an overview about general oscillator concepts such as the barkhausen criterions and amplitude stabilization will be given. More important for this work, phase noise will be explained and analyzed as well. The second half of the chapter deals with different implementations of oscillators with a focus on on-chip implementations.

3.1. Introduction

What exactly *is* an oscillator? It is a system generating periodic waveforms of a specific kind. It is important to notice that it does this in a deterministic and controllable way. A negative feedback system can become unstable, but this results in unwanted behaviour. Here, precautions have to be taken in order to ensure stability. This is usually done by analyzing the phase or gain margin of associated blocks within the system. However, since negative feedback systems should be stable and any instability is undesired, the generation of parasitic oscillations is not considered as oscillator. For proper oscillators, similar design methodologies can be used, but as will be shown, the systems have fundamental differences to classical negative feedback systems.

3.2. Feedback Model

Consider the basic feedback model in figure 3.1. It is often use to explain feedback mechanisms and mostly applied for negative feedback. However, oscillators can be conveniently abstracted in this manner.

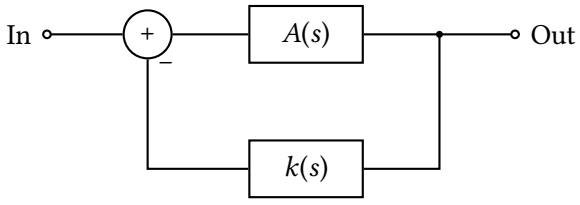

Figure 3.1. – Block diagram of basic feedback model

The system consists of a forward path with the transfer function $A(s)$, a feedback network which changes the signal by its transfer function $k(s)$ and a summing point. Here, the difference (since the polarity of the feedback signal is reversed) of the input and the feedback signal is obtained and fed into the forward path. Using basic system theory, the transfer function from input to the output of the entire system is obtained:

$$H(s) = \frac{\text{Out}}{\text{In}} = \frac{A(s)}{1 + k(s)A(s)}$$

While designing negative feedback systems, the transfer function must be stable, which means that a bounded input signal produces a bounded output signal (BIBO stability). Now, this system should become unstable in order to generate periodic signals. For this, the denominator of $H(s)$ should become 0. In order to satisfy the condition $1 + k(s)A(s) = 0$, we must consider the complex nature of both $k(s)$ and $A(s)$. The above condition is met if both the product of the magnitudes is 1 and the overall phase shift is a multiple of 180°:

$$\begin{aligned} 1 + k(s)A(s) = 0 &= 1 + \left|k(s)A(s)\right| \cdot \exp\left(j \cdot \angle\, k(s)A(s)\right) \\ \left|k(s)A(s)\right| &= \left|k(s)\right|\left|A(s)\right| = 1 \\ \angle\, k(s)A(s) &= n \cdot 180^\circ \qquad n \in \mathbb{N} \end{aligned}$$

These two equations are called "barkhausen criteria". This is straightforward: In order to ensure stable[1] oscillations, the magnitude of the signal should not change by passing through the loop, therefore the loop gain should be exactly 1. Furthermore, at the summing point the two signals need to be exactly out-of-phase (180° difference) in order to subtract two signals of opposite phase.

Since an oscillator should produce a waveform with a constant amplitude, the argument of the functions above in the laplace domain becomes a pure sinusoidal frequency ($s = j\omega$). If the argument had a real part, the amplitude of the output of the system would be either increasing ($\text{Re}(s) > 0$) or decreasing ($\text{Re}(s) < 0$). Therefore, the closed-loop system must have its poles lying on the imaginary axis to be working as an oscillator.

3.3. Non-linearities

The previous descriptions showed how a system can oscillate under specific conditions regarding linear analysis. There is, however, no discussion of oscillator start-up and amplitude. Additionally, it was shown that the poles of the closed-loop system lie on the imaginary axis, which seems prone to errors. How can the position of the poles be guaranteed, while any small disturbance causes the oscillation to develop unwanted instabilities or decay with time? This question will be answered in this section.

[1] "Stable" in this context means undamped, predictable oscillations, not stable in system theory sense. Still, the amplitude should be bounded and well defined, for this reason this expression is used.

Consider the following three pole-zero-diagrams in figure 3.2[2], which show the same system (with the same pole-zero-distribution) at different values of loop gain. The left graph shows a damped system, here all poles lie in the left half plane. It shows a *stable*[3] system. This means that for whatever reason occurring oscillations will decrease until a steady-state is reached. The right graph shows the opposite: here the existing poles lie in the right half plane. This means that present oscillations will grow in amplitude unbounded.[4] The remaining graph in the middle shows the third case, where existing oscillations will be neither damped nor amplified. This system *preserves* oscillations at some frequencies. This, as was already shown in the previous section, ensures stable oscillations and is the behaviour of an oscillator.

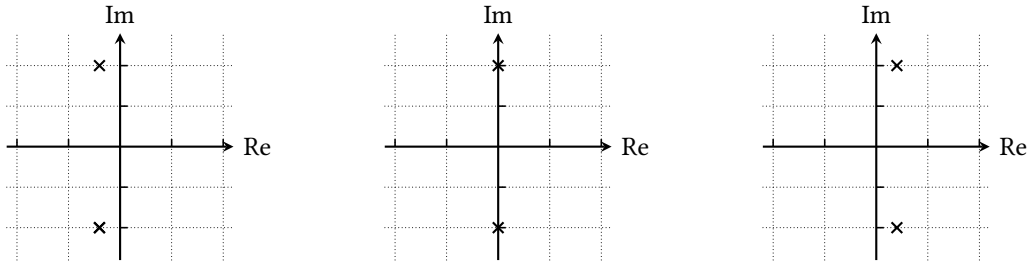

Figure 3.2. – Pole-Zero-Diagram of a feedback system in three different states

Now consider the root-locus plot in figure 3.3. There are three poles in this (closed-loop) system, which is stable for low values of loop gain (the initial position of all poles lies in the left half-plane). Varying their position with the loop gain (or the feedback factor), the two rightmost poles eventually shift into the right half plane and the overall loop becomes unstable. With this, any occurring signal at the right frequency will be amplified infinitely. At certain amplitudes however, the loop gain will degrade due to clipping and operation out of the bounds of the operating point. This reduction of loop gain pushes the poles back into the left half plane. Now the loop gain is again too small and the oscillation amplitude decreases, which in turn again shifts the poles towards the right half plane. On average, the poles are located at exactly the imaginary axis. This ensures a steady-state oscillation.

Next, consider the trajectory of a closed-loop system in state-space. Figure 3.4 shows the state-space trajectory of an system with two state variables, in this case x and y. These state variables could be, for example, the voltage at the terminals of an inductor and the current trough it within a LC oscillator. The two images show a damped system (left) and an unstable system (right). In the damped system (which is stable in the sense of system theory), the energy of the state variables will eventually be dissipated and the system will enter a stable state where both state variables are zero. In the unstable system, however, the energy of the state variables will rise infinitely. Here, both curves show spirals, which is due to the sinusoidal waveform and the change of amplitude. A perfect sinusoidal waveform with two state variables yields a circle. Other types are possible, and more likely.

[2] These are *closed-loop* poles.
[3] In system theory sense.
[4] In real systems there will be some limiting factor since the described case is obviously not possible.

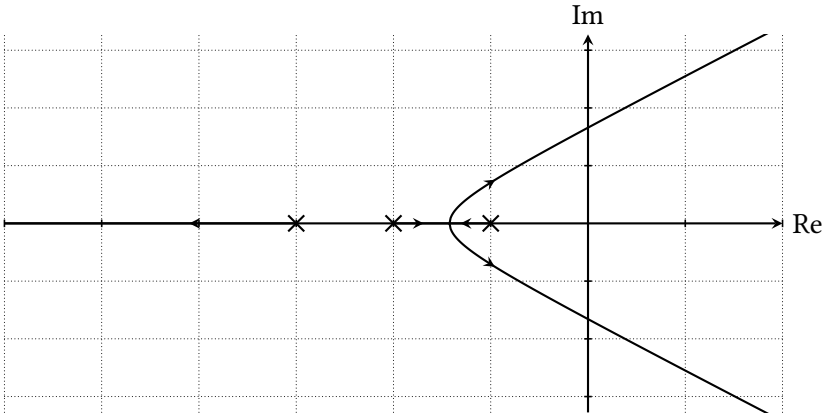

Figure 3.3. – Root locus plot

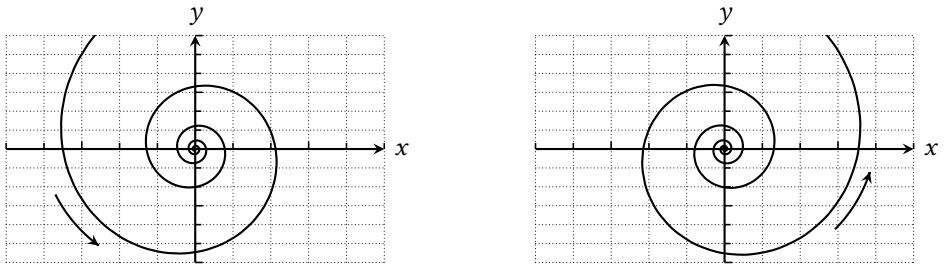

Figure 3.4. – State-space trajectories of damped (left) and unstable (right) systems

To summarize the previous analyzations: In any oscillator, there are poles *near* the imaginary axis, determining the intrinsic frequency of the oscillator. In order to achieve stable oscillations (which again means predictable and controllable oscillations with constant, non-zero amplitude), these poles have to be stabilized to lie – at least on average – *exactly* on the imaginary axis. These two parts will be called the *resonator* and the *energy restoring element*. The latter fundamentally shows non-linearities which are mandatory for the function of every *real-world* oscillator.

3.4. An oscillator introductory study using a simple LC resonator

The observations made up to here will be demonstrated by using a simple oscillator model, which shows basic and elementary concepts of oscillators. For this, a LC resonator will be considered in increasing complexity: First, an ideal tank will be analysed. After that, tank losses and their impact on the oscillation will be introduced. Lastly, a real *oscillator* will be shown by using an non-linear circuit element. This element is, as already shown necessary in order to speak of an oscillator.

3.4.1. The ideal LC resonantor

The left side of figure 3.5 shows an ideal LC resonantor, consisting solely of a capacitor and a inductor. The output voltage is measured across both devices, the output current is assumed to be zero. Therefore, the following differential equation can be derived:

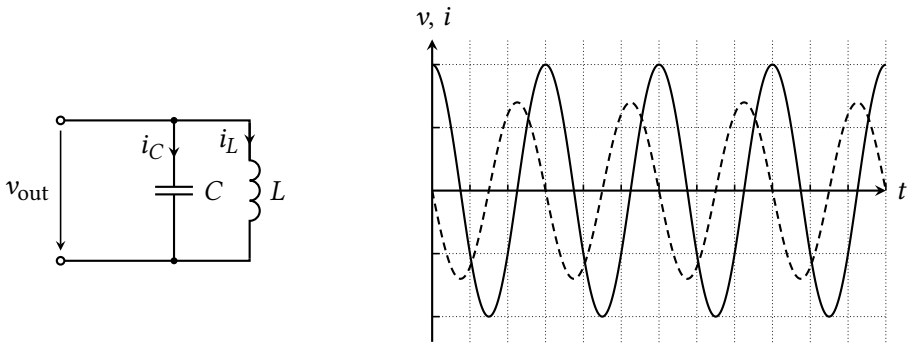

Figure 3.5. – Oscillating system consisting of an ideal inductor and capacitor

$$
\begin{aligned}
i_C &= C\frac{\partial}{\partial t}v_C = C\frac{\partial}{\partial t}v_{\text{out}} \\
v_L &= v_{\text{out}} = L\frac{\partial}{\partial t}i_L = -L\frac{\partial}{\partial t}i_C = -L\frac{\partial}{\partial t}\left(C\frac{\partial}{\partial t}v_{\text{out}}\right) = -LC\frac{\partial^2}{\partial t^2}v_{\text{out}} \\
\Longleftrightarrow\ 0 &= v_{\text{out}} + LC\frac{\partial^2}{\partial t^2}v_{\text{out}}
\end{aligned}
\tag{3.1}
$$

Equation 3.1 can be solved by[5]

$$
\begin{aligned}
v_{\text{out}} &= v_0\cos(\omega_0 t) \\
i_C &= C\frac{\partial}{\partial t}v_{\text{out}} = -v_0 C\omega_0\sin(\omega_0 t)
\end{aligned}
$$

For this solution, an initial condition of the following form was used: $v_{\text{out}}(t = 0) = v_0$ and $i_C(t = 0) = 0$. This sets the amplitude of the oscillation. Figure 3.5 shows the transient response of the LC tank.

If there were an ideal implementation of this LC tank, the capacitor would still have to be charged to an initial voltage in order to provide some energy for the oscillation. Though there are no loss mechanisms in this circuit, there are also no energy restoring elements. For this reason, the circuit consisting of an ideal LC tank can hardly be called an oscillator.

The ideal LC resonator can hardly be viewed as system, but in order to illustrate the system-level consideration of last section, the circuit in figure 3.5 will be analyzed in this manner. For this,

[5]To be formally correct, a more general solution is required. For this discussion, this solution is sufficient.

the current at the terminals of the resonantor will be considered as input of the system, while the voltage across the devices will stand for its output. Therefore, the following holds:

$$\begin{aligned} V_{\text{out}}(s) &= I_{\text{in}}(s) \cdot Z(s) \\ &= I_{\text{in}}(s) \cdot \frac{1}{C} \frac{s}{s^2 + \omega_0^2} \qquad \text{with } \omega_0 = \frac{1}{\sqrt{LC}} \end{aligned}$$

If $I_{\text{in}}(s) = i_0$ (the corresponding time-domain signal is a dirac impulse), the output voltage is the impulse response:

$$v_{\text{out}}(t) = \frac{i_0}{C} \cos\left(\omega_0 t\right)$$

The poles of this system lie at

$$s_{1,2} = \pm j\omega_0$$

which matches the above discussion on system level.

3.4.2. The lossy LC resonator

Now a non-ideal resonator is considered. The loss of the tank is modeled with a parallel resistor R. ALthough there are better and more accurate models, this consideration is sufficient. See section 4.1 for a more detailed discussion.

Again, the differential equation describing the output voltage of the resonantor is derived. Now, the current through the resistor needs to be considered.

$$\begin{aligned} v_{\text{out}} &= v_L = L \frac{\partial}{\partial t} i_L \\ i_L &= -i_R - i_C = -\frac{v_{\text{out}}}{R} - C \frac{\partial}{\partial t} v_{\text{out}} \\ v_{\text{out}} &= L \frac{\partial}{\partial t} \left(-\frac{v_{\text{out}}}{R} - C \frac{\partial}{\partial t} v_{\text{out}} \right) = -\frac{L}{R} \frac{\partial}{\partial t} v_{\text{out}} - LC \frac{\partial^2}{\partial t^2} v_{\text{out}} \\ \Longleftrightarrow 0 &= v_{\text{out}} + \frac{L}{R} \frac{\partial}{\partial t} v_{\text{out}} + LC \frac{\partial^2}{\partial t^2} v_{\text{out}} = \omega_0^2 v_{\text{out}} + 2\zeta\omega_0 \frac{\partial}{\partial t} v_{\text{out}} + \frac{\partial^2}{\partial t^2} v_{\text{out}} \end{aligned}$$

with

$$\begin{aligned} \omega_0 &= \frac{1}{LC} \\ \zeta &= \frac{1}{2R} \sqrt{\frac{L}{C}} \end{aligned}$$

One solution of this differential equation is

$$v_{\text{out}} = v_0 \exp\left(-\zeta \omega_0 t\right) \cos\left(\omega_0 \sqrt{1-\zeta^2}\, t\right) \tag{3.2}$$

The above solution is sensible for values of $\zeta < 1$, for bigger values there will be no oscillation. In the case of $\zeta < 1$, decaying oscillations can be seen. Note that this again requires proper initial conditions to introduce some energy into the tank. As expected, this oscillation is damped, with its rate of decay depending on the resistor R. A larger resistor leads to smaller losses and less damping. Furthermore, as equation 3.2 shows, the oscillation frequency changes with losses compared to the oscillation of the loss-less tank.

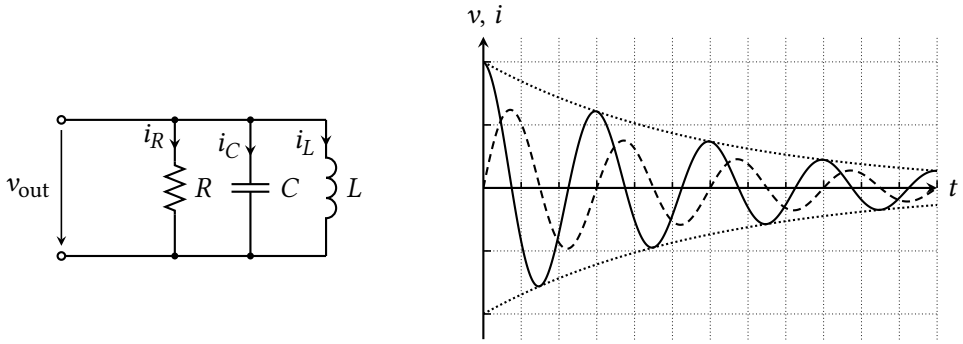

Figure 3.6. – Oscillating system consisting of an ideal inductor and capacitor and a resistor

Again, the circuit is viewed as a system with current as input and voltage as output. The calculation of the transfer function yields

$$H(s) = \frac{sLR}{R + sL + s^2 LCR}$$

with its poles lying at

$$s_{1,2} = \frac{-L \pm \sqrt{L^2 - 4R^2 LC}}{2RLC}$$

Fore reasonable values of L, C and R the term under the square root becomes negative, therefore yielding complex-conjugate poles. This condition is important or otherwise the system would show no oscillation at all, not even damped. This was also assumed in the solution of the differential equation, where this condition was described as $\zeta < 1$. As intuitively expected, the poles of the damped resonator move to the imaginary axis with $R \longrightarrow \infty$, which then is the same circuit as in the previous section.

3.4.3. The lossy LC resonantor with energy restoring element

The previous two section showed the oscillations of an resonator, both ideal and non-ideal. The ideal tank differs from the non-ideal case in that it has no parallel resistor. There, sustainable

oscillations with constant amplitude were possible. Since it is impossible to build circuits without resistive losses, these losses must be compensated. Imagine a *negative* resistor was introduced into the resonantor, which exactly matches the loss resistor. Both would cancel out and leave only the ideal resonator, again producing an oscillation with constant amplitude. However, the problem lies within the need of *exact* matching. How can this be achieved? Furthermore, the question of how to implement a negative resistor remains.

In this section, a fictional negative resistor is used to built a *real* oscillator, where the amplitude is stabilized in a negative-feedback-way. It will be shown how to special properties of this mystical part help in solving two major problems of building oscillators: starting the oscillator and stabilizing the amplitude.

For this discussion the non-ideal resonator of the previous section will be used again. This time, a fourth part will be added, which symbolizes the negative resistor. The circuit in figure 3.7 shows the resulting structure, where the leftmost device denotes the negative resistor. As before, the resonator shows losses in the form of the parallel resistor R.

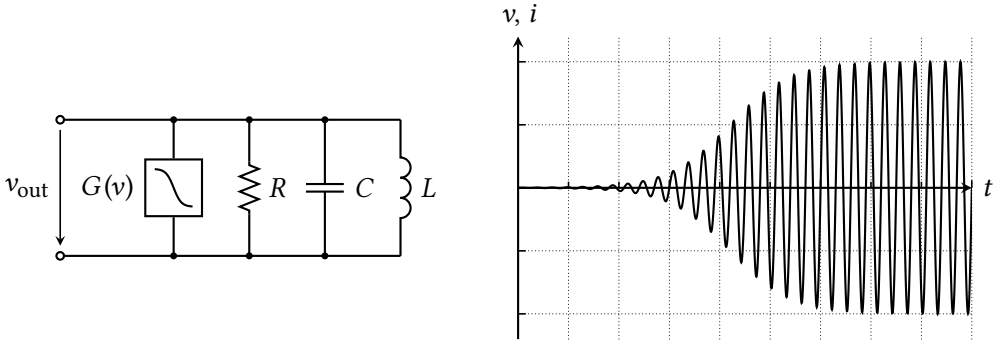

Figure 3.7. – Oscillator built from ideal resistor, capacitor and inductor as well as an nonlinear active element for loss compensation

The non-linear element $G(v)$ is the restoring element which compensates the losses of the tank. Since a negative resistance has a current-voltage characteristic with a negative slope (at least in some region), there are many possibilities in modelling such a characteristic. It will be shown in section 3.5.2 that a sensible model is a inverted bell-shaped resistance profile [6]. For small voltages across the device it has its minimum resistance, which increases for larger voltage amplitudes. The resulting current-voltage characteristic can be modelled by

$$G(v) = -I_0 \tanh\left(\frac{g_m}{I_0} v\right)$$

which has a saturating character for large voltage amplitudes.

[6] Any shape that monotonically decreases for higher amplitudes is fine, for example a rectangular profile. However, a smooth shape is preferable, if only for convergence improvements in simulations. See appendix B for a easy and effective implementation of such a device.

This circuit can now start without any starting voltages or currents (initial conditions). Though it will need some kind of disturbance, the noise of the resistor and the non-linear element will be enough to start the oscillator. For small amplitudes, the non-linear element will introduce energy into the tank which is more than the lost energy in the resistor. Therefore, the amplitude of the oscillator will increase, as can be seen in the right image of figure 3.7. At some point, the lost energy will be the same as the energy introduced by the non-linear element. This is the steady state of the oscillator, where the average transconductance of the non-linear element will be the same as the conductance of the resistor.

The non-linearity of the negative resistor also solves the matching problem of the two resistances. The oscillator will adjust its amplitude in a manner that the average introduced energy by the non-linear element matches *exactly* the lost energy of the tank. This means that the amplitude of the oscillation depends on the amount of lost energy. If the loss is higher (R is lower), but the characteristic of the negative resistor stays the same, the amplitude must decrease. With this, the circuit spends more time in the region of high energy return, which is needed to compensate the loss. Therefore, the circuit in figure 3.7 is resistent to device parameter variations[7]. For oscillations to exist, the only condition is that the minimum negative resistance must be smaller than the loss resistance (amplitude-wise).

Now that the need for non-linear, negative resistor was developed, the next section will introduce a common implementation of such a device.

3.5. Negative Resistances – the Cross-Coupled Pair

All oscillators need some kind of mechanism for compensation of losses. The classical LC-oscillator, for example, consists of a capacitor and an inductor in parallel. Both devices introduce ohmic losses, which can be represented by a resistance. This resistance leads to damping, which needs to be compensated. For this, a negative resistance will be introduced.

There are several methods of implementing negative resistances. They are built around the fact that feedback changes the input and output impedances approximately by the loop gain (division or multiplication, this depends on the type of feedback). If the feedback is positive, the loop gain becomes negative and yields negative input and output resistances (see also [Raz01])

3.5.1. Small signal model

Figure 3.8 shows an implementation of a cross-coupled pair using nmos-transistors, next to its small signal model. Here, two parasitic elements are included, namely the output resistance and the gate-source capacitance of the transistor, since these are major non-idealities. However,

[7] In that sense that the circuit is a proper oscillator. This is only a question of whether an oscillation occurs or not, not a question of quality of the oscillation.

this inclusion is only for completeness, since often approximations can be made that neglect these elements.

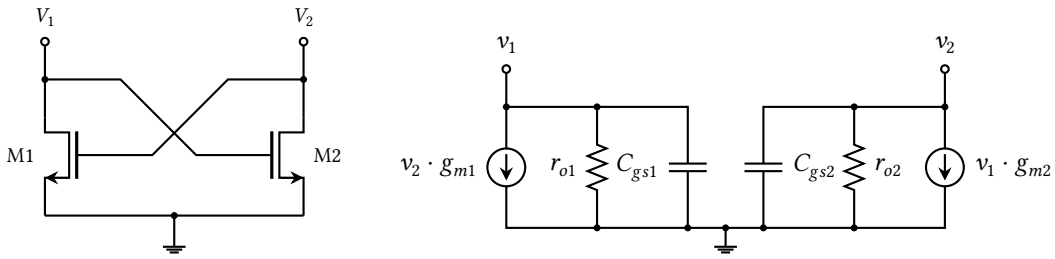

Figure 3.8. – Cross-coupled pair and its small signal model

The small signal model in figure 3.8 can be simplified by assuming that the circuit is symmetric (for example $g_{m1} = g_{m2} = g_m$) and that the circuit is differentially balanced, so $v_1 = -v_2 = v_{\text{in}}$. With this, the circuit reduces to its half circuit (see [Gra+09]), which can be seen in figure 3.9.

$$\begin{aligned} i_{\text{in}} &= -\frac{1}{2} v_{\text{in}} \cdot g_m + \frac{1}{2} v_{\text{in}} \cdot \frac{1}{r_o} + \frac{1}{2} v_{\text{in}} \cdot sC_{gs} \\ i_{\text{in}} &= \frac{1}{2} v_{\text{in}} \left(\frac{1}{r_o} + sC_{gs} - g_m \right) \\ \Longleftrightarrow Z_{\text{in}} &= \frac{v_{\text{in}}}{i_{\text{in}}} = \frac{2}{\frac{1}{r_o} + sC_{gs} - g_m} = -\frac{2r_o}{g_m r_o - 1 - sr_o C_{gs}} \end{aligned} \tag{3.3}$$

Equation 3.3 shows that Z_{in} consists, besides others, of a negative part. Neglecting r_o^{-1} and C_{gs}, Z_{in} is a perfect negative resistor of the value $\frac{2}{g_m}$. Since usually $g_m r_o > 1$, this approximation is reasonable. For large frequencies the resistance becomes positive again. This has to be taken into account so the negative resistance is provided in the wanted frequency range. The corner frequency of the negative resistance, where the magnitude of the impedance starts to change

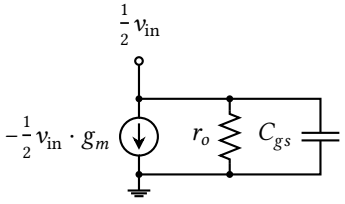

Figure 3.9. – Half circuit of the small signal model of the cross-coupled pair

significantly, can be calculated. For this, it is assumed that $r_o^{-1} \ll 1$.

$$\begin{aligned} \left|g_m - j\omega C_{gs}\right| &< \sqrt{2} g_m \qquad \text{(3 dB-frequency)} \\ \sqrt{g_m^2 + \omega^2 C_{gs}^2} &< \sqrt{2} g_m \\ \omega_{3\,\mathrm{dB}} &< \frac{g_m}{C_{gs}} \end{aligned}$$

The usuable frequency range of the cross-coupled pair as negative resistance is limited by the unity-gain frequency of the transistors. Therefore, the length and overdrive voltages of the transistors needs to be chosen to match the frequency requirements.

3.5.2. Large signal behaviour

With the above small signal model only the input impedance at the operating point can be calculated. If the behaviour of cross-coupled pair were perfectly linear, it could not be used to build oscillators. As shown in section 3.3, non-linear behaviour is essential for oscillators.

Again, consider the circuit in figure 3.8. If the differential voltage increases, for example by rising V_1 and lowering V_2, one of the transistor will eventually turn off, while the other will conduct more and more current (in this example, M1 turns off). Therefore, there are two extremes with either side conducting a large current while the other side is turned off. Of course, there is a

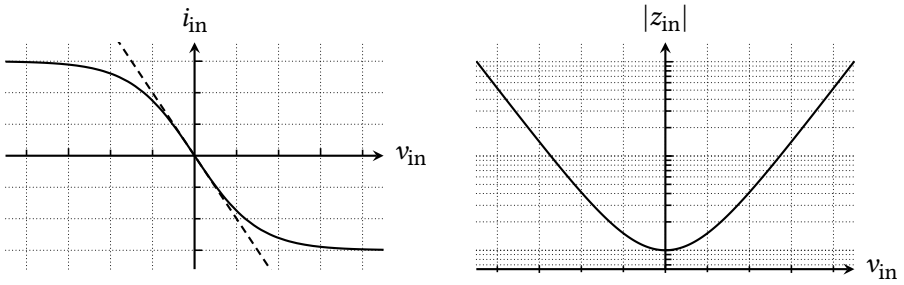

Figure 3.10. – Characteristic curve of the negative resistance

smooth transition into this regions, so that the current-voltage characteristic resembles the curve (left image) in figure 3.10. Here, the dashed line shows the curve of the equivalent (small signal) resistor at the operating point ($v_{in} = 0$). For larger amplitudes, the slope of the curve decreases, which leads to a smaller negative resistance.

The right image in figure 3.10 shows the derivative of the current-voltage characteristic, which is the corresponding incremental resistance. Since the resistance is negative, the magnitude is presented. Remember that a small resistor in a LC resonantor yields big losses, so on the other hand a small *negative* resistor introduces big amounts of energy into the tank.

The voltage-current characteristic can be modeled by a tanh-function:

$$i = -I_0 \tanh\left(\frac{G_m}{I_0} v\right)$$

which results in a incremental resistance of

$$\begin{aligned} z_{\text{in}} = \left(\frac{\partial}{\partial v} i\right)^{-1} &= \frac{1}{G_m}\left(\tanh^2\left(\frac{G_m}{I_0} v\right) - 1\right)^{-1} \\ &= \frac{1}{G_m} \cosh^2\left(\frac{G_m}{I_0} v\right) \end{aligned}$$

As expected, for small values of v, the incremental resistance equals the inverse of the transconductance of the cross-coupled pair, where $G_m = 2g_m$.

3.5.3. Amplitude estimation of oscillators using the cross-coupled pair

The amplitude of an oscillator plays an important role in minimizing noise, therefore it is of interest to calculate or at least roughly estimate it. Two approaches are presented, one based on taylor series, the other one using an assumption of the switching action of the cross-coupled pair within an oscillator.

Recall that for stable oscillation, the average introduced energy must match exactly the average loss. In the case of the simple LC resonator with losses, they same can be achieved by matching the average negative resistance of the cross-coupled pair to the loss resistor of the tank. For not-too-large amplitudes, a taylor approximation can be made of the current-voltage characteristic of the cross-coupled pair. This yields:

$$i \approx \frac{G_m^3}{3I_0^2} v^3 - G_m v$$

For sinusoidal voltages at the inputs of the negative resistance, the produced current is

$$i = \frac{G_m^3}{3I_0^2} v_0^3 \sin^3(\omega_0 t) - G_m v_0 \sin(\omega_0 t)$$

The average transconductance $\bar{G}_m$ can be calculated with the quotient of the average voltage and current in one half of a cycle:

$$\bar{G}_m = \frac{\bar{i}}{\bar{v}} = \frac{\frac{2}{T}\int_0^{\frac{T}{2}} i \,\mathrm{d}t}{\frac{2}{T}\int_0^{\frac{T}{2}} v \,\mathrm{d}t} = \frac{\int_0^{\frac{T}{2}} \frac{G_m^3}{3I_0^2} v_0^3 \sin^3(\omega_0 t) - G_m v_0 \sin(\omega_0 t) \,\mathrm{d}t}{\int_0^{\frac{T}{2}} v_0 \sin(\omega_0 t) \,\mathrm{d}t}$$

$$\bar{G}_m = G_m \cdot \left(2\left(\frac{G_m v_0}{3I_0}\right)^2 - 1\right)$$

In steady state, the average transconductance of the cross-coupled pair matches the loss of the tank, modeled by the parallel resistor R_p.

$$\begin{aligned} \bar{G}_m &= -\frac{1}{R_p} \\ G_m \cdot \left(2\left(\frac{G_m v_0}{3 I_0} \right)^2 - 1 \right) &= -\frac{1}{R_p} \\ \Leftrightarrow \quad v_0 &= 3 \frac{I_0}{\sqrt{2} G_m} \sqrt{1 - \frac{1}{G_m R_p}} \end{aligned}$$

The square-root term may not become negative, so the following condition must be met:

$$G_m > R_p$$

This is clear since G_m models the steepness of the current-voltage characteristic of the cross-coupled pair in the origin. If G_m is smaller than the steepness of the current-voltage characteristic of the resistor, the losses can not be compensated for.

This result can be used to perform an estimation of the voltage amplitude of the oscillator. Keep in mind the assumptions used up to here: The oscillator waveform (voltage) is sinusoidal, the voltage-current characteristic of the cross-coupled pair can be modeled by an tangus hyperbolicus, which, in turn, can be approximated by its third-order taylor series. The last point is important, since this introduces great errors for large amplitudes of the oscillator waveform.

Figure 3.11 shows the transient response of the cross-coupled pair due to a sinusoidal waveform. The left image displays the voltage, the right image the current at the terminals. For small amplitudes the bevahiour is fairly linear, with increasing non-linearities with higher amplitudes. Still, for medium amplitudes, the taylor approximation is sufficient. The validity deteriorates for big values of G_m and small values of I_0. If G_m is large, the slope at the origin is large, therefore quickly showing saturation. This can be compensated by a large maximum current I_0.

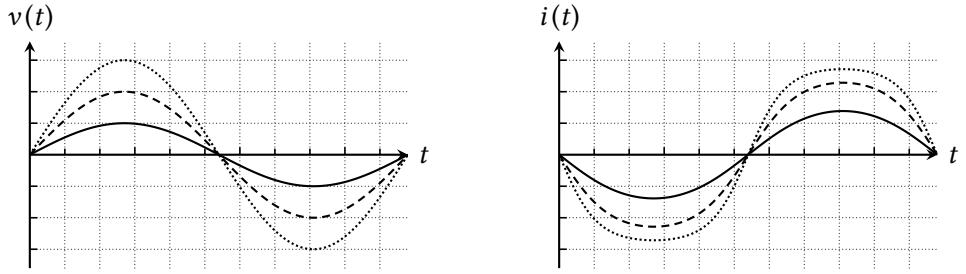

Figure 3.11. – Transient response of the cross-coupled pair excited by a sine wave

While the above analysis gives some insight, it is often not valid in oscillator design. This is because of two distinct operation regions of oscillators, called the “current limited” and the

"voltage limited" regimes (see for example [Lis+14]). To minimize oscillator phase noise, it is preferable to operate in the voltage limited regime, which means that the cross-coupled pair should exhibit hard switching. The individual transistors should be peridically switched totally on and off, which causes the amplitude of the oscillator to reach a maximum. For the voltage limited regime, there is a well-known calculation methodology, which uses frequency analysis.

In the case of large amplitudes, it is assumed that the current at one terminal of the cross-coupled pair shows a rectangular shape (the current at the other terminal shows the opposite, since the sum of both currents is constant). The tank acts as filter, which, at resonance, can be modeled as the parallel combination of an inductor, a capacitor and a resistor. The inductor and the capacitor act as an open circuit for signals at the oscillation frequency, but as a small impedance at other frequencies. Therefore, only the fundamental tone of the current in the oscillator flows through the resistor, generating the oscillator voltage. Hence, only the fundamental tone is responsible of the amplitude of the oscillator.

The current through the tank can be expressed by the following form:[8]

$$i(t) = i_0 \frac{4}{\pi} \sum_{n=1}^{n=\infty} \frac{\sin\big((2n-1)\omega_0 t\big)}{2n-1}$$

As mentioned, only the fundamental tone builds the voltage signal, so the output voltage is of the form:

$$\begin{aligned} v_{\text{out}}(t) &= i_0 R_p \frac{4}{\pi} \sin\big(\omega_0 t\big) \\ \Longleftrightarrow\ v_0 &= i_0 R_p \frac{4}{\pi} \end{aligned}$$

3.6. Performance parameters of oscillators

So far the oscillator was introduced. It was determined, how it runs at a specific frequency, how the oscillation is stabilized, including the inherently non-linear nature of oscillators. However, what performance parameters are important for oscillators? What makes an oscillator a *good* oscillator? In the following, some major parameters are introduced.

3.6.1. Frequency and tuning range

Frequency is on of the main parameter of oscillators, since they are designed to generate a periodic waveform with a certain frequency. This frequency must be stable and exact, since otherwise conversion errors are introduced within receivers and transmitters.

[8] This is a single-sided spectrum representation.

The main use of oscillators in communication circuits is within frequency synthesizers. Therefore, they must be tunable. The required tuning range depends mostly on the application and which frequencies are to be synthesized. It is possible to include multiple wireless standards, therefore requiring a higher tuning range. The frequency band can be preselected through dividers, making it possible to design one oscillator for many bands, targeting at the highest frequency. However, since designing high-frequency oscillators is harder, this may not always be the right approach. Another important factor determining the tuning range are process spread and modellation errors during design. The frequency of the oscillator will never be at exact the value it was designed for, but this is necessary for correct down- and upconversion. A phase-locked loop with the right locking range can compensate for this, all that is needed is a stable and accurate reference oscillator. The tuning range must be large enough to ensure that these compensation mechanism can be used properly.

3.6.2. Amplitude and signal power

The amplitude of an oscillator is of importance, since a large amplitude exhibits a better signal-to-noise ratio. Often, the amplitude is limited by the power supply or the operating regions of circuit components.

3.6.3. Waveform and purity

There are many different oscillator topologies, producing many different waveforms. There are a handful of typical curves propably intuitively known to the reader, such as sine waves, rectangular waves (also with duty cycle different from 50 %), sawtooth waves and perhaps triangle waves. Of course, these are always abstractions since their frequency contents will deviate from the perfect distribution. The main question is: Does the waveform play an important role for oscillators in communication circuits? The answer is mostly no. Usually, the oscillator is used to drive a mixer (either for down- or upconversion), where abrupt switching of waveforms is desirable, in terms of noise (see [Raz12]). This means that the waveform of the oscillator itself shows a "switching characteristic" (similar to rectangular waves) or the local oscillator interface of the mixer is of a hard-switching nature. In both cases, the waveform should be stable in its frequency and phase, but the actual waveform is not of great importance. This also holds in phase-locked loops, which can be built entirely digital (all-digital PLL; of course the oscillator is still of analog nature). In this case, oscillators are followed by a buffer, which converts their intrinsic waveform into a rectangular type.

Together with different waveforms the term *purity* is not far. It is often quantified by *total harmonic distortion* (THD), which relates the power of harmonics to the power of the fundamental tone. Since the type of waveform is not of great interest in communication circuits, the THD is usually also not considered in design.

3.6.4. Noise

Do oscillators exhibit noise? Intuitively, the answer is yes. However, as will be shown further on, noise in oscillators is a quite complex process and still subject to many research studies. Noise in oscillators unfortunately can not be analyzed with the classical methods of linear superposition and frequency domain calculations. However, not surprisingly, it still plays a very important role in RF circuits and escpecially oscillators are a critical component for noise performance. Oscillators show their noise mainly in so-called *phase noise*. Since there are many aspects to this, the next section is dedicated to this.

3.7. Phase Noise

Phase noise is a phenomenon inherently present in every oscillator. Simply speaking, phase noise relates to a momentary frequency shift of the frequency of periodic signals. It is a random process, similar to voltage or current noise in an amplifier.

3.7.1. Phase noise in receivers and transmitters

Phase noise poses a problem in mixers. Here, a local oscillator is used as signal in order to perform the conversion process. If this oscillator shows significant noise skirts, interferers near the wanted signal can disturb the downconverted signal. While the interferer is actually converted into a band outside of the IF band, the folded noise components of the oscillator leak into the band of interest. This is especially severe since the interferer can be much larger in power, for example a transmitter which is located close to the receiver. Figure 3.12 shows this situation. Here, near to the wanted signal at f_{sig} there is a large interferer at f_{int}. Additionally, the local

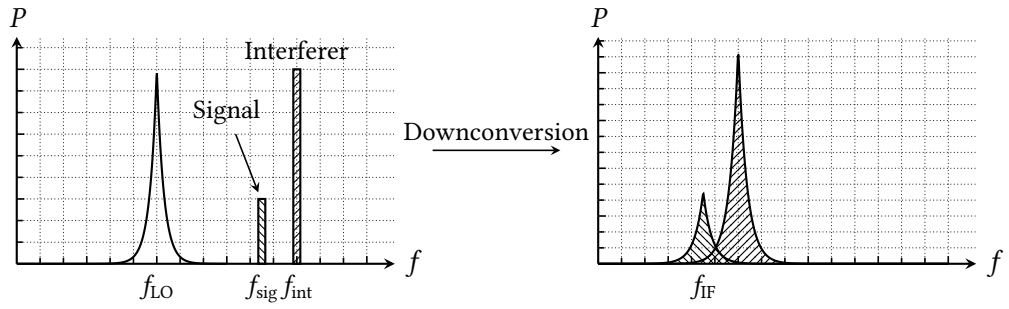

Figure 3.12. – Downconversion with noisy oscillators

oscillator signal located at f_{LO} shows significant noise skirts. Since a frequency translation like downconversion involves a convolution, the shape of the local oscillator also influences the shape of the downconverted signals. A convolution of two spectra *always* broadens the resulting

spectrum.[9] This is shown in the right image of figure 3.12 which shows the downconverted signals. The spectra of both the wanted signal and the interferer are broadened, which causes some part of the downconverted interferer spectrum to "leak" into the band-of-interest. This clearly corrupts the wanted signal, especially for interferer with high power.

Phase noise also poses a problem in transmitters. Here, a signal gets emitted, which is upconverted by a local oscillator, therefore having similar noise properties as the oscillator. Now consider a transmitter, which operates close to a receiver. If the received signal is in a channel close (but different) to the transmission channel, the noise skirts from the transmitted signal can leak into the reception channel, corrupting the possibly much smaller received signal. Note that this takes place before filtering or downconversion so that there is no possibility to differentiate between both signals. This is similar to the situation in the right image of figure 3.12, only that the center frequencies of the two signals are the respective channels, which are close to each other.

Together with wireless communication standards (such as GSM), this lays down strict requirements on the transceivers. For example, the phase noise of the local oscillator in a GSM-receiver must be below −113 dBc/Hz at an offset of 600 kHz (this example is taken from Razavi's book on RF microelectronics, see [Raz12, page 548 – 550]). Communication standards impose restrictions on transmitters in form of *transmission masks*, which are sets of power levels in certain frequency intervals, that are not to be exceeded.

3.7.2. Phase noise in oscillators

An ideal oscillator is a pure sinusoidal waveform $u(t) = a_0 \cos(\omega_0 t)$ with its spectrum (power spectral density) consisting of two delta impulses at $-\omega_0$ and ω_0, respectively. This notion of an ideal oscillator can be extended to a noise-free oscillator with harmonics[10], where the spectrum consists of delta impulses at integer multiples of the fundamental frequency. A typical (one-sided) spectrum of an ideal noise-free oscillator with harmonics can be seen in the left image of figure 3.13. As can be seen, the power of the individual impulses decreases with increasing frequency with the fundamental having the greates power.

To retrieve the power of the oscillator, the power spectral density has to be integrated from $-\infty$ to ∞, which is the same as the sum of the weights of the delta impulses. A real oscillator shows a similar behaviour, but here the power is not concentrated in the delta impules but peaks with finite width (see figure 3.13, right image). The spectrum shows some deviation (compared to the ideal spectrum) in form of so called *noise skirts*. Noise signals in the oscillator circuit disturb the phase of the signal and can be seen as momentary changes of the frequency of the oscillator, therefore there exist signals with a frequency different from ω_0. However, their power is lower than the "main" signal, so that the oscillator signal spends most the time at the center frequency.

[9] For real world signals. The convolution of a signal with a dirac impulse preserves the original spectrum.

[10] This depends on the application: As was shown, for typical RF applications, the waveform of the oscillator is not of great importance.

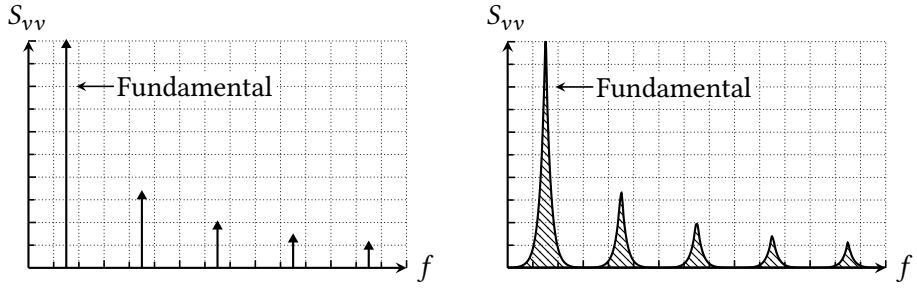

Figure 3.13. – Spectra of ideal and real oscillators

It is important to note that the noise sources do not add power to the oscillator. The integrated power spectral density of an ideal and a real oscillator yield the same result.[11] Noise sources in an oscillator lead to a broadening of the spectrum.

Now, why is phase noise called phase noise? What is the difference to amplitude noise? Consider the equation 3.4. The ideal waveform (represented by the cosine) gets perturbed in its amplitude and phase, respectively by $\alpha(t)$ and $\phi(t)$.

$$v(t) = \big(v_0 + \alpha(t)\big)\cos\big(\omega_0 t + \phi(t)\big) \tag{3.4}$$

The non-linear nature of the oscillator (needed for a steady amplitude) inherently rejects amplitude noise. Phase, on the other hand, has no restoring forces. There is no "reference phase", the phase is free-running. For this reason, any disturbance of the phase persists. This is consequently to the differential equations describing the oscillator: any phase-shifted version of a solution is a solution itself.

3.7.3. Effect of phase noise on long-term phase

In order to discuss the impact of disturbances within the oscillator on phase noise, first consider the trajectory of an oscillator in state-space depicted in figure 3.14. Here, two state variables x and y are present, which could for instance be the current through and the voltage across a capacitor. The dotted curve signifies the steady-state limit cycle of the oscillator. At some time t_0 the oscillator gets disturbed and the trajectory leaves the limit cycle. The amplitude stabilization mechanism will reestablish the steady-state amplitude of the oscillator. The phase, however, has no restoring forces, therefore a finite phase error θ remains indefinitely.

Now, consider an oscillator which is periodically disturbed by random values, which represent noise. Since the phase errors persist in time, the phase can *shift* over time. This is shown in figure 3.15 where the the effect of phase noise on the oscillator signal can be seen. Here, the signal gets a "noisy" shape (visible through the non-smooth curve), but more importantly, the zero crossings change significantly as compared to the ideal reference signal. This effect

[11] For the same oscillator with and without noise sources.

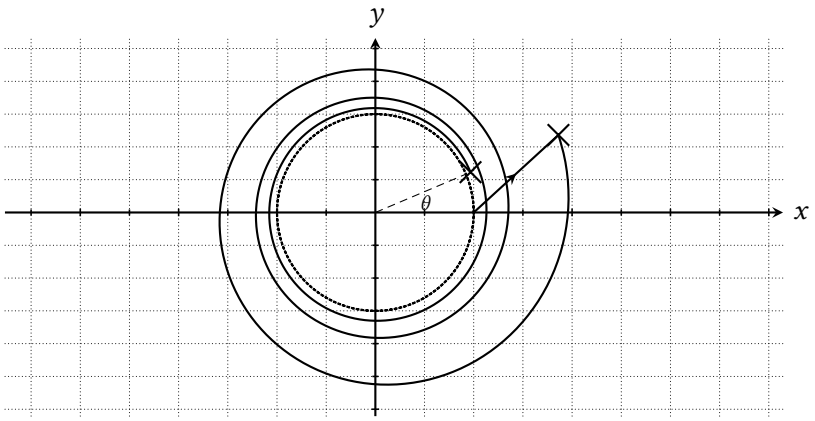

Figure 3.14. – A state-space trajectory of a free running oscillator disturbed by a single impulse

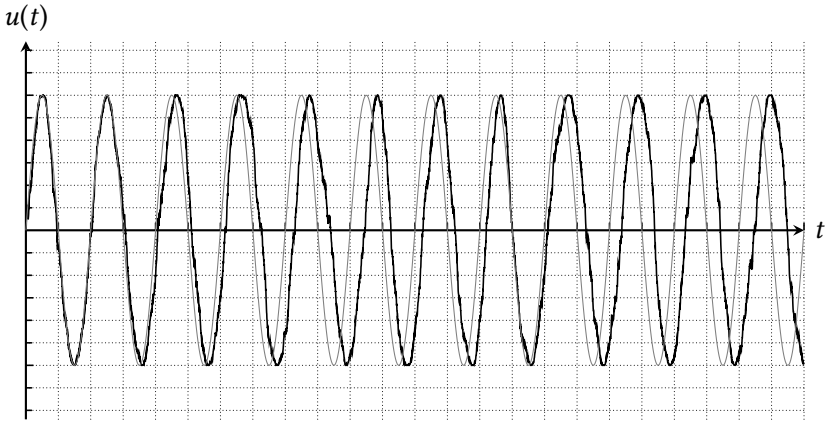

Figure 3.15. – Time-domain signals of real oscillators: Long-term effects of phase noise

increases in time, therefore also the variance of the zero crossings *increases in time*. If one waits for an infinite amount of time, the phase of the oscillator cannot be predicted.

In the following phase noise and its origins will be described further, as well as methods for calculation. For this, first an approach for measurements will be discussed, which also shows the properties of phase noise.

3.7.4. Phase noise characterization and measurements

Phase noise of periodic signals is measured through the means of a spectrum analyzer. Here, the power of the sidebands is measured in a bandwidth of 1 Hz and compared to the overall

power of the oscillator:

$$\mathscr{L} = 10 \log \left(\frac{P_{\mathrm{SB}}\left(\omega_0 + \Delta\omega\right)}{P_{\mathrm{osc}}} \right)$$

The unit used is dBc, which stands for decibel referenced to the **carrier**, so 0 dBc is exactly the power of the carrier. Therefore, the noise expressed in dBc will usually be negative.[12]

A spectrum analyzer filters the signal through a bandpass of a desired bandwidth and measures the power of the remaining signal. This yields a power in a certain bandwidth. This procedure is repeated across the whole band of interest with the power spectral density as result. Consider the left image of figure 3.16, which shows the power spectral density of an oscillator with a center frequency ω_0. Here, the power of the signal is filtered with a certain bandwidth at specific offset frequencies, which is shown by the grey areas. The position of the areas is the offset frequency, the width symbolyzes the bandwidth of the filter. Theoretically, the bandwidth of the filter should be 1 Hz, but this is hard to implement. Therefore, a higher bandwidth is used, which must be compensated for.

The power in a certain frequency intervall can be expressed by

$$P = \int_{f_1}^{f_2} S_{vv}\left(f\right) \mathrm{d}f$$

where S_{vv} is the *real* power spectral density of the signal. One must be cautious when speaking about measurements: Since it is hard to implement a measurement bandwith of 1 Hz, the power is measured in a larger bandwidth and must be *normalized* to a 1 Hz-bandwidth. The real power spectral density is assumed to be constant in a small frequency intervall, therefore:

$$P(\Delta f) = (f_1 - f_2) \cdot S_{vv}\left(\Delta f\right) = BW \cdot S_{vv}\left(\Delta f\right)$$
$$\mathscr{L} = \frac{P(\Delta f)}{BW} \cdot \frac{1}{P_{\mathrm{total}}}$$

The symbol $\mathscr{L}$ is used in different ways by different authors. The straight-forward measurement, that was described above (filtering and measuring power) yields the combined power spectral density of amplitude noise and phase noise. There are, however, also more sophisticated measurement methods which are able to truly separate phase and amplitude noise. This is done by quadrature mixing, which cancels out amplitude noise. Still, in many cases the symbol $\mathscr{L}$ is used only for phase noise.

The right image of figure 3.16 shows the resulting profile of the measured phase noise. Both

[12] Positive values are possible in theory, since this only means that the power of the oscillator in this bandwidth is higher than than the total power. All measurements are referenced to a 1 Hz-bandwidth, therefore the noise bandwidth in this example must be smaller.

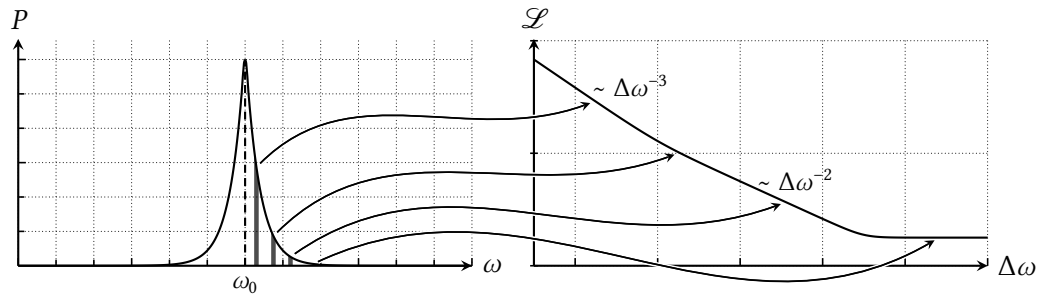

Figure 3.16. – Measurement of phase noise

axes are logarithmic axes[13], so that there are regions where the plot shows linear behaviour. Here, three main regions are visible: One constant region and two negative-slope regions with different exponents.

The probably best-known equation describing the characteristica of phase noise in oscillators is the so-called "Leeson-Cutler" model. It is based on empirical examinations of oscillators but not theoretically founded. Still, it provides a description of actual phase noise profiles.

$$\mathscr{L}(\Delta\omega) = 10\log\left(\frac{2FkT}{P_{\text{tot}}}\cdot\left(1+\left(\frac{\omega_0}{2Q\Delta\omega}\right)^2\right)\cdot\left(1+\frac{\omega_{1/f}}{\Delta\omega}\right)\right) \tag{3.5}$$

In equation 3.5, the first fraction consists of the total power of the oscillator (P_{tot}) and the device excess noise (F), which is an empirical parameter ([Lee66]). Furthermore, two important frequencies appear in the expression, the center frequency of the oscillator ω_0 and the corner frequency of device flicker noise. Note that in this model it is assumend that the device flicker noise corner frequency matches the corner frequency of the oscillator flicker noise, which is not true in general (see [HL98]). Lastly, the quality factor of the oscillator influences only the ω^{-2}-region, not the region of flicker noise. For high frequencies, equation 3.5 reduces to

$$\mathscr{L}(\Delta\omega) = 10\log\left(\frac{2FkT}{P_{\text{tot}}}\right)$$

and the phase noise becomes constant.

The Leeson-Cutler model gives straight-forward recommendations for reducing phase noise, which all are quite intuitive: The total power should be maximized (phase noise is measured with respect to the carrier, so a carrier with higher power shows less relative phase noise), the device noise, both flicker and white, should be minimized. These recommendations are what one would intuitively expect.

[13]The y-axis is measured in dBc/Hz, so the axis is actually linear, but it has the same effect.

Figure 3.17 shows a simple model to explain the different regions of phase noise. The left inverter, together with the resonator, builds a simple oscillator, the right inverter is the output buffer. Both inverters are noisy and therefore contributing to phase noise.

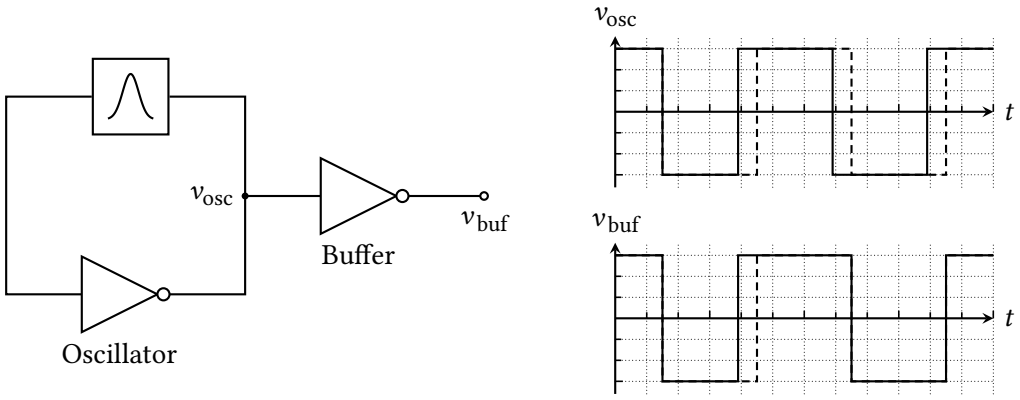

Figure 3.17. – Oscillator with output buffer generating different kinds of phase noise

First, consider only the oscillator. Around the signal edges the signal is small, so the noise of the inverter (which acts as comparator) moves the edge forward or backward in time. This is because its switching threshold is changed by the noise. Now the signal is phase-shifted by the resonator and again fed to the inverter. If the inverter is suddenly noise-free, the phase error introduced before is persistent. Any future phase error is *added* to the previous errors so that the total error accumulates. This is the behaviour of an integrator, therefore the generated phase noise shows the same frequency profile, which is $\propto \omega^{-2}$.

Now have a look at the buffer: Here, the noise of the inverter also changes the phase of signal by moving the edge in time, but now it is *driven* by a signal, not free running. Since the buffer has no influence on its input signal, phase errors can not accumulate as in the oscillator. Any change is momentary and not correlated to previous values. This is the definition of white noise, so that the phase noise generated by the buffer has a flat spectrum.

This explains the flat and the negative-slope regions of the phase noise profile, but does not consider flicker noise. Intuitively, if the inverters have flicker noise, this will show itself also in the phase noise profile, therefore creating a ω^{-3}. But how is the flicker noise corner frequency constituted? As was already mentioned, it does not generally match the device flicker noise corner frequency. Apparently, there is more to the picture, which will be investigated in the following section.

3.7.5. Relation to jitter

There is another measure of phase instability, which is called *jitter*. It describes the deviation of the timing of edges in signals. A perfect square wave, for example, will have its edges always at the same times (shifted by the period of the signal, of course). If the period and the time of

an edge is known, all previous and next edges can be predicted. With jitter, the timing varies around the ideal value. This can be expressed by shifting a periodic signal in time by a random process ([Kun12]):

$$y_N(t) = y(t + t_j(t))$$

Here, $t_j(t)$ is a random process with a zero mean. This can be transformed into a phase noise description using the period of the signal:

$$y_N(t) = y\left(t + \frac{\phi(t)T_0}{2\pi}\right)$$

Since jitter describes timing instabilities of signal edges and phase noise phase errors of the signal the question arises how the two are related. Seemingly, they describe the same phenomena, which in fact is true. Both are different *perspectives* on phase instabilities. Jitter is the time-domain representation of the frequency-domain phase noise.

How is jitter measured? First, one has to define exactly what jitter describes. Since jitter is about timings of edges or zero crossings, there must be a reference. Here, the following measures are considered: Absolute jitter, which is the time difference of the ideal time of the edge and its actual occurence. This is referred to an arbitrary start edge. Absolute jitter (sometimes also called long-term jitter) free-running systems increases indefinitly in time and is therefore not a useful measure. For driven system with a perfect periodic input (for example the buffer in figure 3.17) on the other hand, absolute jitter does not increase, however, this configuration is hardly realistic.

Different authors use different definitions of absolute jitter: See for example the article of Rick Poore [Poo01], where absolute jitter is defined as the sum of the variation in the length of periods (equation 3.7). Kundert, on the other hand, uses a similar measure but calls it *k-cycle*-jitter. Here, the timings of two edges seperated by k cycles are compared and the standard deviation is calculated (equation 3.6).

$$J_k(n) = \sqrt{\mathrm{var}\left(t_{n+k} - t_n\right)} \qquad \text{(Kundert)} \tag{3.6}$$

$$\sigma_{\mathrm{abs}}(N) = \sum_{n=1}^{N}\left(T_n - T_{\mathrm{avg}}\right) \qquad \text{(Poore)} \tag{3.7}$$

Here, N denotes the Nth edge, T_n is the nth period (as time) and T_{avg} is the average period.

A more useful measure for non-driven systems is *cycle-to-cycle*-jitter. Here, the length of the current period is compared to the length of the previous period. Since it is always referenced to the same edge (relative), cycle-to-cycle jitter does *not* increase in time.

$$J_{\mathrm{cc}}(N) = \sqrt{\mathrm{var}\left(T_{N+1} - T_N\right)}$$

Figure 3.18 shows the described jitter characterizations. The dashed line indicates the ideal,

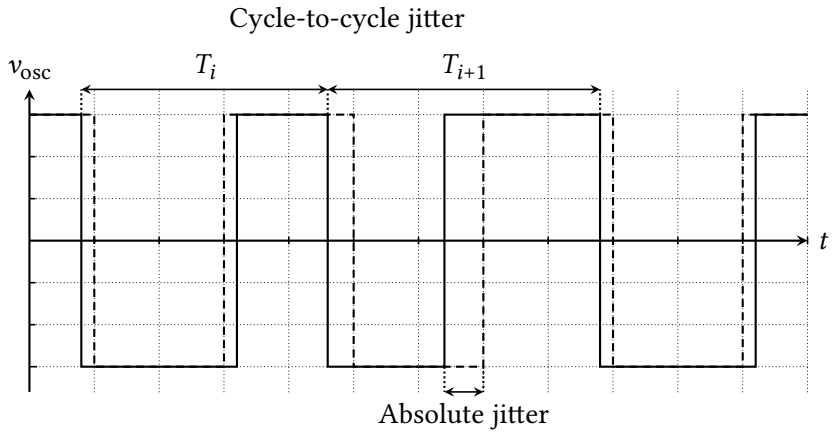

Figure 3.18. – Different characterizations of jitter

noise-free signal, the solid line shows the signal corrupted by noise. The length of the periods are measured from edge to edge (rising or falling), the absolute jitter is the deviation from the theoretical time.

How is phase noise related to jitter? As already mentioned, both describe the same phenomenom, so one must be able to be calculated from the other. Kundert calculates this relation and it is given here without proof (see [Kun12, section 10.1]):

$$J = \sqrt{cT_0} = \sqrt{\frac{2\pi c}{\omega_0}}$$

with

$$c = \mathscr{L}(\Delta\omega)\frac{\Delta\omega^2}{\omega_0^2}$$

Here, J denotes the period jitter, which is $J_{cc}(1)$. It stands for the standard deviation of the length of one period.

3.7.6. The impulse sensitivity function

A method providing great insight into the mechanisms of frequency folding of phase noise is proposed by Hajimiri et al. ([HL98]). They introduce a function called *impulse sensitivity function (ISF)*, which is denoted by the symbol Γ. This function is a measure of how much the phase of the oscillator is disturbed depending on the injection time of noise/unwanted[14] signals.

[14]The ISF is used for noise calculations, but not limited to it.

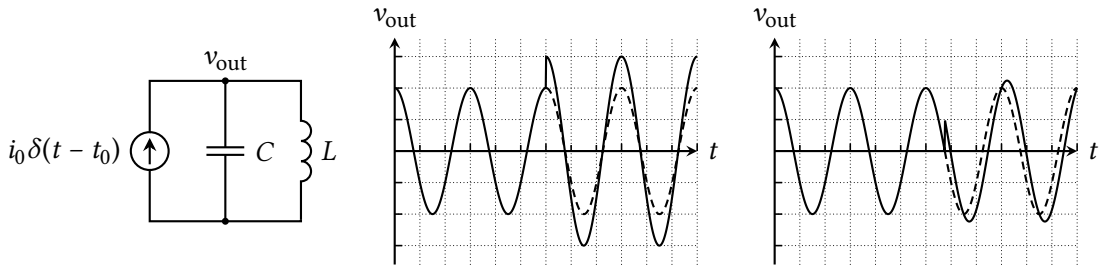

Figure 3.19. – Injection of charge in an ideal oscillater

Imagine a current impulse, that injects an amount of charge at some specific time into the oscillator[15] of figure 3.19. The current is absorbed entirely by the capacitor, since the inductor presents a high impedance to fast signals (this can be shown). If the impulse occurs at the peaks of the waveform, it changes the amplitude, but not the phase of the oscillator signal (middle image of figure 3.19). The opposite happens if the impulse occurs at the zero crossing of the waveform. Here, the phase changes (right image of figure 3.19).[16]

The produced phase change due to the current impulse persists, which implies that the impulse response of *excess phase* is a step function. This matches the discussion on phase noise profiles in oscillators above, where a integrator-like behaviour was shown. The integral of an impulse is a step. The height of the step varyies with the time of injection of the impulse, it is therefore *time-variant*. This time-variance is not arbitrary but periodic. It does not matter at which cycle the impulse is injected. The time relative to this period is important, not its absolute time. Therefore, the variation of the height of the impulse response of the oscillator has the same periodicity as the oscillator waveform. For this, the impulse response can be described as (with $\sigma(t)$ being the step function)

$$h(t, t_0) = k \cdot \Gamma(\omega_0 t_0)\sigma(t - t_0)$$

Here, Γ denotes the periodic variation of the height of the impulse response with the time of injection t_0. Is called the *impulse sensitivity function (ISF)* and is a measure for the amount of phase change through injection in dependence of time. What is the meaning of k? For this, the linearity of the system needs to be evaluated.

Until now, it was assumed that the height of the impulse response varies with time, but does depend on the amount of injection. This is the linearity property for systems. Is this system linear? Hajimir et al. check for this empirically: They use two different oscillators (LC colpitts

[15] Recall the above discussion on what is to be called an oscillator. This "oscillator" has no amplitude-restoring mechanisms, which disqualify it of its name. Since the poles are always located on the imaginary axis, there occur no damping actions for amplitudes that exceed the "stable" amplitude.

[16] To be precise: the opposite would mean that there are only changes in phase, not in amplitude. This is not true, although it is often portrayed like that in literature, even in the original paper. For simple cases like the presented one, the problem can be analyzed by solving the differential equation, which shows that there is an amplitude change occuring at injection at the zero crossings. There is, however, a point where no amplitude change occurs, but this is not relevant for this discussion. See appendix A.2.3 for a calculation of this point.

and a ring oscillator) and inject charge at some nodes. For small amounts of charge the oscillators can empirically shown to be linear systems (regarding these nodes as input and the phase change as output). See [HL98, section III and figures 5 and 6]. This leads to the proportionality factor k in the above equation being expressed through the maximum stored charge at the respective node $q_{\max}$.

$$h(t, t_0) = \frac{\Gamma(\omega_0 t_0)}{q_{\max}} \sigma(t - t_0)$$

In order to arrive at the excess phase $\Delta\phi$ for a given injection signal, the convolution integral $i(t)$ for time-variant systems need to be solved:

$$\begin{aligned}\Delta\phi(t) &= \int_{-\infty}^{\infty} h(t, \tau) i(\tau)\, \mathrm{d}\tau \\ &= \frac{1}{q_{\max}} \int_{-\infty}^{t} \Gamma(\omega_0 \tau) i(\tau)\, \mathrm{d}\tau\end{aligned}$$

Since the impulse sensitivity function is dimensionless, the whole expression will be dimensionless as well, since the integral of a current is charge, which gets divided by the maximum stored charge. This also motivates the choice of the proportionality constant in the impulse response.

Now the excess phase is known and can be calculated for some special signals: For this, signals that are periodic and have a frequency that is a integer multiple of the oscillator frequency will be considered. For this discussion, the periodic nature of the ISF is used to express it as a fourier series (the general form of a fourier series is a bit more complex, it contains for example a phase shift for every signal. However, this discussion is qualitive and therefore these details are not important):

$$\Gamma(\omega_0 t_0) = \sum_{n=0}^{\infty} c_n \cos\Big(n\omega_0 t_0\Big)$$

This function is now inserted into the convolution integral in order to calculate the phase shift:

$$\Delta\phi(t) = \frac{1}{q_{\max}} \int_{\infty}^{t} i(\tau) \sum_{n=0}^{\infty} c_n \cos\Big(\frac{2\pi n\phi}{P}\Big)\, \mathrm{d}\tau = \frac{1}{q_{\max}} \sum_{n=0}^{\infty} c_n \int_{\infty}^{t} i(\tau) \cos\Big(\frac{2\pi n\phi}{P}\Big)\, \mathrm{d}\tau$$

The described injection signals have the following form:

$$i_{\mathrm{inj,n}}(t) = I_n \cos\Big(n\omega_0 + \Delta\omega\Big)$$

For this discussion, they have not exactly the same frequency as the oscillator waveform (or

a integer multiple, including 0) but deviate by a small frequency $\Delta\omega$. This frequency is much smaller than ω_0.

The multiplication of the injection signal with the components of the ISF yields several frequencies with the sum or the diffference of the individual frequencies. Only the component "matching" the frequency of the injection signal will generate a signal which is near DC (only $\Delta\omega$ left). Hajimir et al. argue that, due to the averaging nature of the integral, all other components are negligible, with only the slow, near-DC signal remaining. This is not a rigorous approach and needs further evaluation. However, it does provide some inside and the resulting analyzation seem to are valid. Using this approach, the excess phase due to a periodic injection signal at the frequency $n\omega_0 + \Delta\omega$ is calculated to

$$\Delta\phi(t) \approx \frac{I_n c_n \sin(\Delta\omega t)}{2 q_{\max} \Delta\omega}$$

Interestingly, all injection signals generate a excess phase, which is slowly varying with $\Delta\omega$, but no higher frequency components. Therefore, all injection signals get folded to the same frequency region.

Now that the excess phase is known, the influence on the oscillator can be determined. For this, the output voltage of the oscillator is of interest. The power spectral density S can then be calculated. Since the oscillator output voltage is of the form

$$v_{\text{out}}(t) = v_0 \cos(\omega_0 t + \phi(t))$$

the excess phase due to current injection amounts to a phase modulation. Since noise usually is small, the narrow bandwidth approximation can be used and the spectrum exhibits two sidebands left and right to the carrier with a frequency of $\omega_0 \pm \Delta\omega$. Hajimiri et al. calculate the single-sided power spectral density to ([HL98, page 183, equation (18)]):

$$P_{\text{SBC}}(\Delta\omega) = 10 \log\left(\frac{I_n c_n}{4 q_{\max} \Delta\omega}\right)$$

The above discussion shows how injection signals *far* from the carrier (at $n\omega_0 + \Delta\omega$, with $n \neq 0$) create phase noise *near* the carrier (at an offset frequency $\Delta\omega$). This also explains the occurence of device flicker noise in phase noise: The respective noise gets upconverted to the carrier frequency, where it adds to the noise skirts.

Figure 3.20 shows this process: The left image shows the power spectral density of a noise source, where a constant (white) and a flicker noise region can be seen. The noise at integer multiples of the oscillator frequency gets up- and downconverted (upconversion for components with $\omega < \omega_0$, downconversion for $\omega > \omega_0$), so that it now lies around the fundamental tone of the oscillator (which also happens at the harmonics). The low frequency (in this case flicker) noise gets weighted by the DC value of the ISF, c_0. Noise around the carrier gets weighted by c_1 and so on. Since the ISF has (usually, this can differ) the same period as the oscillator waveform, c_1 is of the largest value. Therefore, noise in the vicinity of the carrier frequency has the biggest

influence on oscillator phase noise (but the sum of all other components could outweigh this).

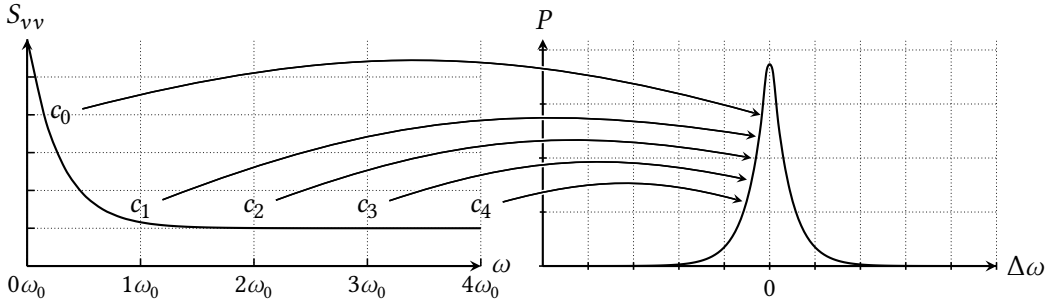

Figure 3.20. – Noise frequency translations, weighted by fourier coefficients of the ISF

Since device flicker noise (with a corner frequency of f_c) gets weighted by the DC value of the ISF (c_0), it can become very small and insignificant for phase noise for symmetrical ISFs. This also changes the flicker noise corner frequency in phase noise. Here, only the result of the investigation made by Hajimiri et al. is given. See [HL98, page 185] for details.

$$f_{1/f^3} = f_c \frac{c_0^2}{2\Gamma_{\text{rms}}^2} \approx f_c \left(\frac{c_0}{c_1}\right)^2$$

The corner frequency changed by the quotient of the DC value and the RMS value of the ISF. Since usually c_1 has the biggest influence on the RMS value, an approximation can be used.

Interestingly, in some oscillators flicker noise is of no importance. If the ISF is perfectly symmetric, c_0 becomes zero, which shifts the corner frequency of the $1/f^3$-region of phase noise to zero, therefore suppressing flicker noise. The symmetry of the ISF is highly dependent on the oscillator waveform and its non-linearities.

While the impulse sensitivity function theory delivers a nice approach in explaining the conversion mechanisms for noise into phase noise, it is unfortunately unhandy and hard to calculate. Hajimir et al. propose techniques for computation, but this almost always involves a simulator, so that the question arises whether or not the phase noise should be simulated directly. There are some publications on finding methods for simpler computation of the ISF, such as a paper by Levantino et al. ([Lev+12]).

For the simple LC tank, the answer to a current impulse injected at an arbitrary time can be calculated analytically. The result is presented here for completeness, see appendix A.2 for a detailed derivation. Equation 3.8 shows the result.

$$v = v_0 \cos(\omega_0 t) + \sigma(t - t_0) \cdot \Delta v \cos\big(\omega_0 (t - t_0)\big) \tag{3.8}$$

This result can be used to calculate the impulse sensitivity function, which, even in this simple case, is tedious.

3.7.7. Amplitude noise

Up to here, only phase noise was considered. The question of what amplitude noise is and if it exists may arise. In fact, amplitude noise is present in oscillators, but often not considered. This is because of the amplitude restoring mechanism in an oscillator. However, since this mechanism is of negative-feedback type, it also exhibits a certain bandwidth. For perturbations larger in frequency, the restoring forces have no control any more, so that the disturbance persists. This is true for large offset frequencies

3.8. Oscillator Topologies

In this section, a short overview of the most important oscillator topologies will be given. This is as introduction for the reader, what typical oscillator structures exist and what their main characterstics are.

3.8.1. LC Oscillators

LC oscillators play an important rule in modern RF electronics. Their sinusoidal waveform and, foremost, their excellent phase noise performance set them apart from other oscillators. LC oscillators are very well analyzed and subject to much research and many improvements.

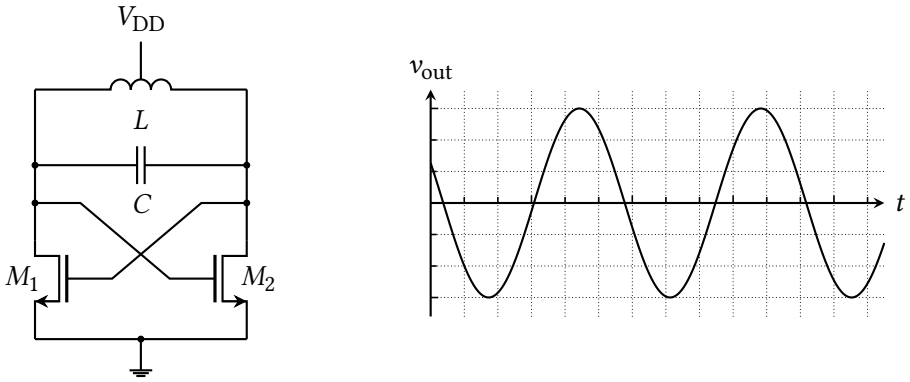

Figure 3.21. – The classical LC oscillator used in RF circuits

Typical variations include a current source at the bottom or the top, a pmos-implementation or a complementary implementation (using cross-coupled pairs made from nmos- as well as pmos-transistors). They can be built in any standard technology with the inductor made of special arrangements of the metal wiring. For tuning most implementations used either variable capacitors (varactors) or capacitor arrays with switches. LC oscillators offer a sine wave of high purity, but this is often not important, since usually a digital buffer directly follows the oscillator.

3.8.2. Ring Oscillators

Ring oscillators are often used as clock generators. They achieve considerable low phase noise but need a lot of power. They are made of a chain of inverters, which drive each other. Because of the delay introduced by the single stages, this chain can oscillate. Figure 3.22 shows a block diagram (left image) and corresponding waveforms (right image). The different line types of the curves denote the outputs of the individual inverters. These curves show "digital" curves, where also, depending on frequency, also more "analog" waveforms are possible. How many

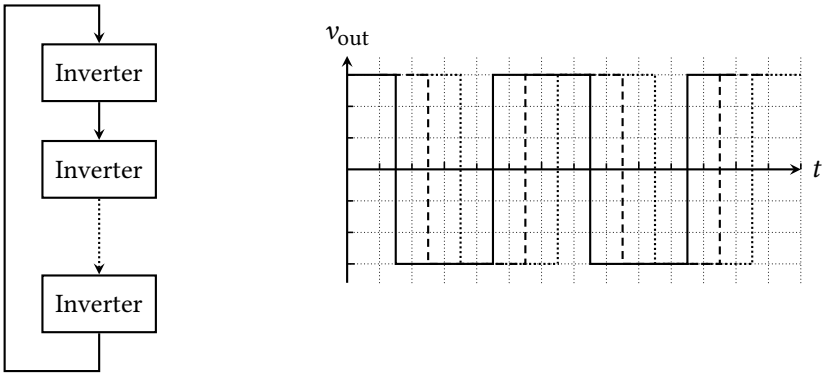

Figure 3.22. – Structure of a ringoscillator

inverters are needed in order to build an oscillator? For this, single-pole inverters are assumed, providing a maximum phase shift of of 90°. An odd number of inverters (say: three) produce on total one inversion (the others cancel out each other), therefore adding another 180° phase shift. That means a three-inverter chain can oscillate, where each stage adds a phase shift of 60°. This implies that two inverters are enough for stable oscillations (phase shift of 360°), but recall that the maximum phase shift of 90° per inverter is only reached for $\omega \longrightarrow \infty$, where only a gain smaller than 1 is provided. This violates the barkhausen criteria, so that two one-pole systems can not oscillate.

3.8.3. Relaxation Oscillators

A relaxation oscillator is a two-phase oscillator, where some kind of energy storage gets filled until it reaches a threshold. After this, the stored energy quickly gets released and the oscillator returns to its uncharged state (or a state of opposite charge). Now the storing process stars again, and so on. Usually, this energy storage is a capacitor, which gets charged by a constant current.

Figure 3.23 shows the system structure and a typical waveform of a relaxation oscillator. In this "implementation", the charge time is much bigger than the discharge time, which leads to an assymetric waveform. There are many different implementations of relaxation oscillators, where this behaviour is different. For example, the output of the comparator is a rectangular waveform, its duty cycle depends on the relation of the rise and the fall time of the oscillator

signal. This property can be used to adjust the duty cycle to the application, even make it controllable.

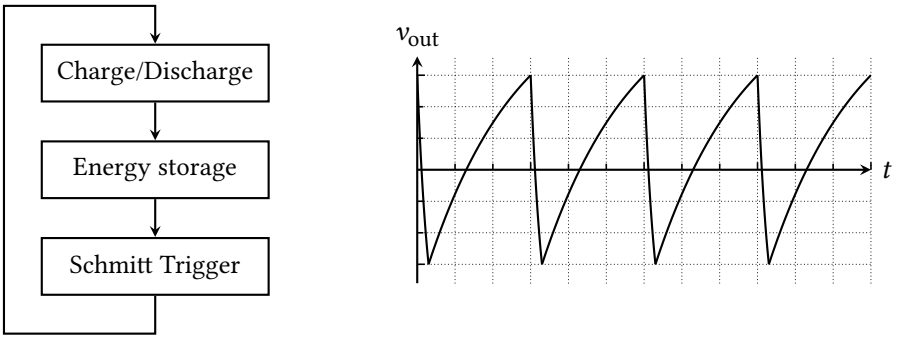

Figure 3.23. – Structure of a relaxation oscillator

There are many different implementations of relaxation oscillators, both in discrete and integrated electronics. They can be built by incorporating full operational amplifiers and comparators or simply by using current sources and capacitors as integrators and cross-coupled pairs as comparators (a circuit very similar-looking to the circuit in figure 3.21). Relaxation oscillators are maybe the most sold oscillators of all time, in form of the well-known 555 timer IC.

3.8.4. Quartz Oscillators

Quartz oscillators cannot be fully implemented on-chip, due to the needed quartz crystal, which is very big. They do, however play an important role as reference oscillators for phase-locked-loops, since their phase noise performance is unmet by other oscillator types.

A quartz oscillator uses a mechanical resonating crystal made of piezoelectrical materials. The oscillator can be built with few parts, consisting of an fed-back inverter and capacitances for tuning. The crystal also allows operation at higher frequencies using resonance at higher harmonics. To acchieve this, the unwanted harmonics must be made unstable (stable in a oscillatory sense, where “unstable” means damped). The usual frequency ranges of quartz crystals are of the order kHz to hundreds of MHz.

3.8.5. Other Topologies

There are many other topologies, many of them exploiting special techniques and phenomena like stripline resonantors or surface acoustic wave (SAW) oscillators. However, they usually need special technologies and therefore can’t be realized in standard CMOS. Because of this, these kind of topologies will not be further investigated in this work.

3.9. Figure of merits

In order to compare different oscillators, a "fair" measure is needed. For this, a so called *figure of merit (FoM)* is used. Unfortunately, there are varying definitions of this FoM. The most basic variant solely compares phase noise performance at a certain offset frequency and the power consumption. Also included in the definition is the oscillator center frequency, which compensates for harder-to-reach phase noise in high frequency oscillators:

$$\mathrm{FoM} = \mathscr{L}(\Delta\omega) - 20\log\left(\frac{\omega_0}{\Delta\omega}\right) + 10\log\left(\frac{P_{\mathrm{tot}}}{1\,\mathrm{mW}}\right) \quad \text{(dBc/Hz)}$$

The first part is the measured phase noise at a certain offset frequency, the second part is a consequence of Leeson's equation in the ω^{-2} region. There, an increase in oscillation frequency *increases* phase noise. In order to compare low- with high-frequency oscillators, this phenomenom is compensated. The third part introduces the power of the oscillator, the less the better. In total, this leads to a FoM where smaller values are *better*.[17]

In general, having a higher tuning range in a VCO increases phase noise (see [SOM11]), so the tuning range often is integrated into the figure of merit to have a fair comparison of oscillators with highly different tuning ranges (TR):

$$\mathrm{FoM}_T = \mathscr{L}(\Delta\omega) - 20\log\left(\frac{\omega_0}{\Delta\omega}\cdot\frac{TR}{10}\right) + 10\log\left(\frac{P_{\mathrm{tot}}}{1\,\mathrm{mW}}\right) \quad \text{(dBc/Hz)}$$

where the tuning range is defined by ([Ito+06])

$$TR = \frac{f_{\max} - f_{\min}}{f_0}$$

The motivation for the factor of 0.1 in the definition of the above figure of merit is unclear. It is presented and used like this in publications. Obviously, it is used as a scaling factor. Here, this factor will be omitted.

When comparing oscillators one must be cautious: The shown figures of merit do not compensate all effects, which means that, most propably, there will be a best and a worst case FoM for any oscillator. Not always is the worst case used for calculations, which has to be considered.

[17] There are definitions where all signs are inverted to get a positive, higher-is-better FoM. However, most of the publications seem to use the here presented definition.

Chapter 4.

Active inductors

Since passive inductors can be implemented in standard CMOS, the cross-coupled LC oscillator is the preferred on-chip oscillator for many applications. It provides an excellent phase noise performance as well as low harmonic distortion and low power consumption. As was shown in the introduction, the passive inductors, however, occupy a lot of space. In a typical oscillator, the inductor can easily make up for half the space, having in total some area consumption of 300 µm × 300 µm. Therefore it would be interesting to investigate some alternatives to oscillators without passive inductors. For this, active implementations of passive inductors are presented in this chapter, after a short introduction to passive on-chip inductors.

4.1. Passive Inductors

In this section a short overview of the most important properties of passive inductors, especially on-chip inductors, will be given.

4.1.1. On-chip inductor shapes

A passive on-chip inductor usually consists of metal lines shaped in a manner that enhance the parasitic inductance of the interconnections by coupling magnetic fields from one line to another. For this, inductors are made of wires running close to each other.

Lumped inductors can be implemented on-chip, preferable by means of spiral inductors. Inductances in around 1 nH can be built reasonable. The major disadvantage of this approach is the occupied space: an oscillator using a passive inductor can easily need 0.5 mm^2, with the inductor occupying one third of the total area. Figure 4.1 shows a die photograph of a LC oscillator with a center frequency around 50 GHz. Inductors tend to be built smaller for larger frequencies, as can be seen here. The diameter of the coil only is 44 µm, but it is still clearly visible on the photograph and much bigger than the rest of the oscillator

Another problem of passive on-chip inductors is that they are susceptible to electromagnetic fields. Phenomena like injection lock, which cause oscillators to shift in frequency due to

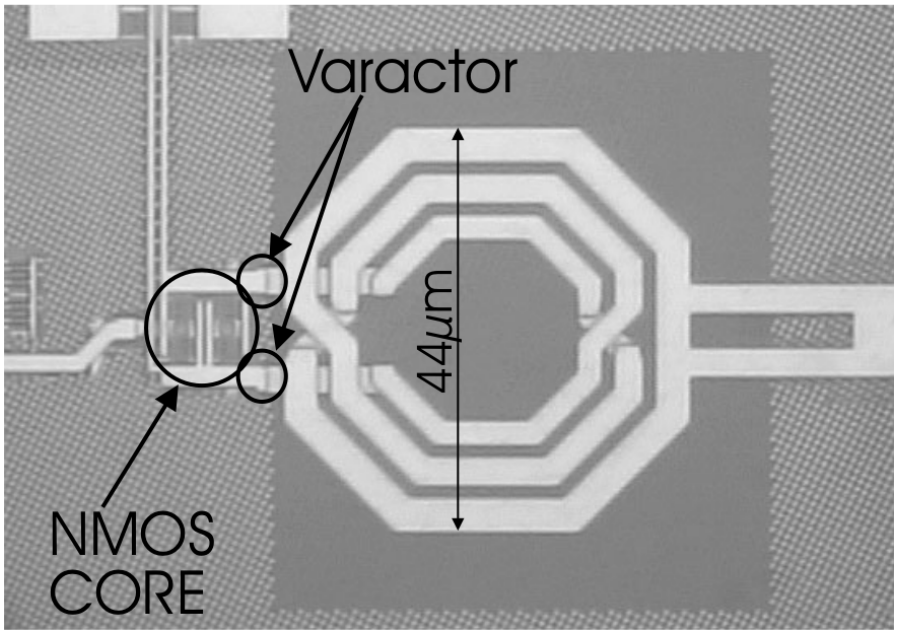

Figure 4.1. – A schematic view of a typical chip layout with an on-chip LC oscillator [Tie06]

another periodic signal can occur because of the coupling of fields into the oscillator through the inductor. This is a major problem and devices need to be shielded appropriately.

On-chip inductors can be built in differential configuration, which has two advantages: First, electromagnetic forces common to both sides of the inductor cancel out. Second, the inductance increases. On the other hand, of course the area increases as well. Therefore, the choice of the configuration depends on the application.

4.1.2. Parasitic elements and small signal model

A passive on-chip inductor shows many parasitic effects, not only due to parasitic capacitances and resistances. Also, as was already mentioned, electromagnetic coupling can occur, not only externally but also on-chip. This disturbs neighboring conductors as well as it can create eddy currents in the chip substrate (see [Tie06, page 42 – 44]).

Figure 4.2 shows an equivalent circuit of an on-chip inductor. Here, the non-idealities (parasitics) are modeled as three lumped devices: a parallel and a series resistance and a parallel capacitance. For large frequencies, the impedance is dominated by C_p, since its impedance is small. Therefore, the inductor shows capacitive behavior for fast signals. Furthermore, for very low frequencies, the ohmic losses dominate the overall performance. In these regions, the inductor shows resistive behavior, which in turn is dominated by either R_s or R_p. For a set of distinct frequencies, the inductor shows the expected inductive behavior with the magnitude of impedance increasing with frequency and a phase shift of (ideally) 90°.

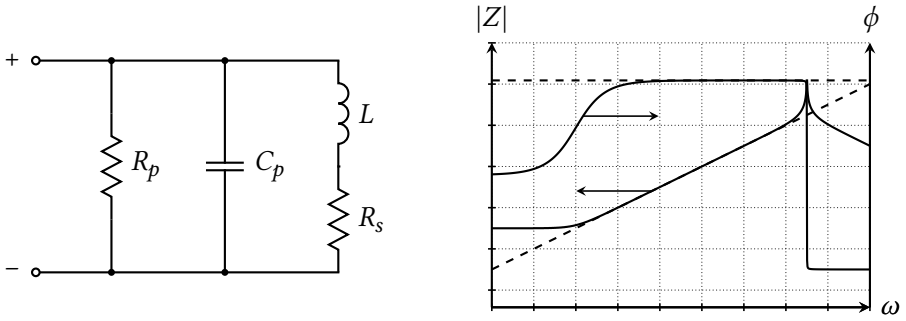

Figure 4.2. – Equivalent circuit model of an on-chip inductor

The overall impedance of the inductor is

$$\begin{aligned} Y(\omega) &= \frac{1}{R_p} + sC_p + \frac{1}{R_s + sL} \\ \Longleftrightarrow Z(\omega) &= \frac{1}{\frac{1}{R_p} + sC_p + \frac{1}{R_s+sL}} \\ &= \frac{R_p \cdot \left(R_s + sL\right)}{R_p + R_s + s\left(\left(R_p + R_s\right)C_p + L\right) + s^2 C_p L} \end{aligned}$$

Since the inductor shows both an inductive and a capacitive region (neglecting the resistive region), a self-resonance frequency, similar as in a conventional LC-tank is to be expected. However, in practical applications the self-resonance frequency is not of great interest, since it is usually much higher than the desired operating frequency of the inductor.

The above model can also be used for resonators consisting of an inductor and a capacitor, where the capacitor is a lumped device, not a parasitic. A series resistor for the capacitor could also be included, but the series loss of the inductor is usually more significant. The resonance frequency of the resonator occurs at the maximum of the magnitude of its impedance. For convenience, the squared magnitude is used for calculation:

$$Z(s) = \frac{1}{\frac{1}{R_p} + \frac{1}{R_s+sL} + sC} = \frac{R_p R_s + sR_p L}{R_p + R_s + s(L + R_p R_s C) + s^2 C R_p L}$$

$$\left|Z(j\omega)\right|^2 = \frac{(R_p R_s)^2 + (\omega R_p L)^2}{(R_p + R_s - \omega^2 R_p C L)^2 + \left(\omega(L + R_p R_s C)\right)^2}$$

$$
\begin{aligned}
&\frac{\partial}{\partial\omega}\left|Z(j\omega)\right|^2 \stackrel{!}{=} 0 \\
&\quad\Leftrightarrow 0 = 2\omega R_p^2 L^2 \cdot \left(R_p^2(1+\frac{R_s}{R_p}-\omega^2 CL)^2 + \omega^2(L+R_pR_sC)^2\right) \\
&\qquad - \left(\omega^2 R_p^2 L^2 + R_p^2 R_s^2\right) \cdot \left(-4\omega LCR_p^2(1+\frac{R_s}{R_p}-\omega^2 CL) + 2\omega(L+R_pR_sC)^2\right) \\
&\quad\Leftrightarrow 0 = 2\omega R_p^2 L^2 \cdot \left(R_p^2(1+\frac{R_s}{R_p}-\omega^2 CL)^2\right) - \omega^2 R_p^2 L^2 \cdot \left(-4\omega LCR_p^2(1+\frac{R_s}{R_p}-\omega^2 CL)\right) \\
&\qquad - R_p^2 R_s^2 \cdot \left(-4\omega LCR_p^2(1+\frac{R_s}{R_p}-\omega^2 CL) + 2\omega(L+R_pR_sC)^2\right) \\
&\quad\Leftrightarrow 0 = \left(1+\frac{R_s}{R_p}-\omega^2 LC\right)\left(1+\frac{R_s}{R_p}+\omega^2 LC\right) + R_s^2\left(2\frac{C}{L}(1-\omega^2 LC) - \frac{1}{R_p^2} - R_s^2\frac{C^2}{L^2}\right)
\end{aligned}
$$

The resonance frequency can be calculated as

$$
\omega_0 = \sqrt{\frac{\sqrt{1+2R_s\left(\frac{C}{L}R_s+\frac{1}{R_p}\right)} - R_s^2\frac{C}{L}}{LC}} \approx \sqrt{\frac{1+R_s\left(\frac{C}{L}R_s+\frac{1}{R_p}\right) - R_s^2\frac{C}{L}}{LC}} = \sqrt{\frac{1+\frac{R_s}{R_p}}{LC}}
$$

The last expression incorporates all devices of the small signal model and is quite accurate. However, usually R_s is much smaller than R_p, therefore the quotient of the two is much smaller than 1. With this, the resonance frequency reduces to the well-known form:

$$
\omega_0 = \frac{1}{\sqrt{LC}}
$$

4.1.3. Noise

The total noise of the inductor (in this model) is contributed by R_p and R_s. Here it is assumed that both resistors contribute only white noise with a power spectral density of

$$
\overline{i_N^2} = 4kTR
$$

Note that this is the one-sided power spectral density for frequencies above 0, so a factor of 4 instead of 2 is used.

4.1.4. Quality factor

Since inductors are used for oscillator design, their quality factor is of interest. The quality factor Q is a measure for how good the device shows the desired behavior. For an inductor

with a series or parallel resistance (neglecting other parasitic effects), the quality factor can be expressed as

$$Q = \frac{\omega L}{R_s} \quad \text{(series)}$$
$$Q = \frac{R_p}{\omega L} \quad \text{(parallel)}$$

For a given inductance and frequency, the series resistor should be minimized while the parallel resistor should be maximized, which is intuitively understood.

Typical on-chip inductors reach quality factors of a few tenths, for example 30.

Together with the parallel capacitor, the resonator has a total quality factor, which can be calculated from the individual quality factors of its devices:

$$\frac{1}{Q_{\text{tot}}} = \frac{1}{Q_L} + \frac{1}{Q_C}$$

Since the quality factor of on-chip capacitors can easily reach values above hundred, the resonator Q is usually dominated by the Q of the inductor. There are techniques for raising the quality factor of on-chip inductors, however, there are no significant improvements. In order to come near the capacitor quality, another approach has to be taken. This can be made in form of active inductors, which can be built by using a device called *gyrator*.

4.2. The gyrator

A gyrator is an ideal two-port network building block which can be used – besides others – to build virtual inductances. It was proposed 1948 by Tellegen [Tel48] as addition to the existing linear circuit elements (resistor, capacitor, inductor and transformer). The gyrator forms the counterpart to the transformer in a sense that it cross-couples voltage from one port to current on the other port. The ideal transformer couples voltage to voltage and current to current.

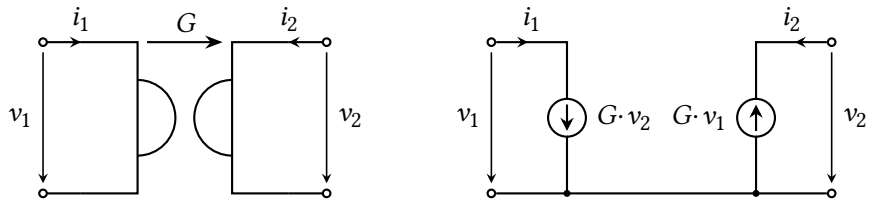

Figure 4.3. – Symbolic representation of a gyrator and its circuit equivalent

The ideal gyrator is described by its voltage-to-current transfer functions:

$$\begin{pmatrix} i_1 \\ i_2 \end{pmatrix} = \begin{pmatrix} 0 & G \\ -G & 0 \end{pmatrix} \cdot \begin{pmatrix} v_1 \\ v_2 \end{pmatrix} = \begin{pmatrix} G \cdot v_2 \\ -G \cdot v_1 \end{pmatrix}$$

With this, the gyrator can be represented by the circuit in the right image in figure 4.3, with its symbol shown in the left image.

The cross-coupling action of a gyrator leads to an inversion of the voltage-current characteristic of an electrical device. Consider the circuits in figure 4.4. Here, a generic impedance Z is attached to the gyrator. Note that both circuits are equivalent, the input of the gyrator can be any of the two ports.

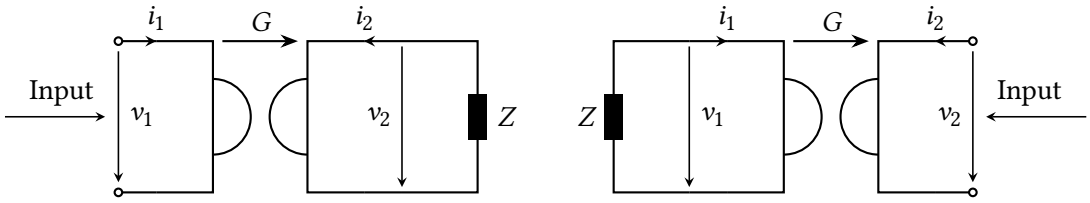

Figure 4.4. – Gyrator attached with generic impedance Z

The calculation of the equivalent input impedance of the gyrator yields[1]:

$$\begin{aligned} i_{in} &= i_1 = G \cdot v_2 & \qquad i_{in} &= i_2 = -G \cdot v_1 \\ v_2 &= -Z \cdot i_2 = -Z \cdot (-G) \cdot v_1 & \qquad v_1 &= -Z \cdot i_1 = -Z \cdot G \cdot v_2 \end{aligned}$$

$$\begin{aligned} &\Longleftrightarrow && i_{in} = G^2 \cdot Z \cdot v_{in} \\ &\Longleftrightarrow && Z_{in} = \frac{v_{in}}{i_{in}} = \frac{1}{G^2 \cdot Z} \end{aligned}$$

If Z is replaced by a capacitor with the impedance $(sC)^{-1}$, the input impedance of the gyrator becomes

$$Z_{in} = \frac{sC}{G^2}$$

which shows inductive behavior:

$$\begin{aligned} Z_{in} &= sL_{eq} \\ \text{with} \quad L_{eq} &= \frac{C}{G^2} \end{aligned}$$

[1] Note that both cases show the same result.

In order to build a gyrator, the above circuit is restructured and the controlled current sources are replaced by ideal transconductance amplifiers. Figure 4.5 shows the restructured circuit on the left, the replacement circuit on the right. Here, two OTAs are used in a back-to-back

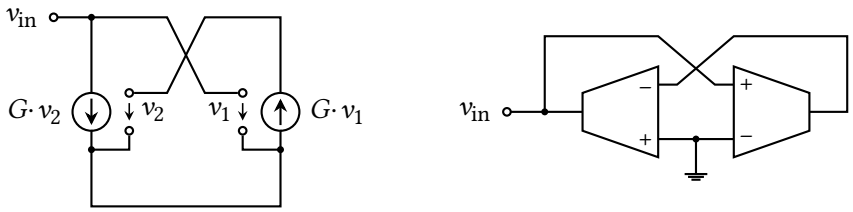

Figure 4.5. – Gyrator circuit redrawn

configuration (note the sign inversion in one of the OTAs). Again, the choice where the input lies is arbitrary. The shown structure also enables easy fully-differential implementation, suitable for high-performance circuits. Here, only the single-ended OTAs are exchanged for fully-differentially amplifiers, with the lower inputs in figure 4.5 connected to the inverting outputs.

4.2.1. Small signal behavior

Since the gyrator consists of two voltage-controlled current sources, it can be implemented by the means of two operational transconductance amplifiers (OTA). In this section, the small signal behavior of the active inductor will be analyzed, using the OTA model shown in figure 4.6. In this model, the OTA is composed of a transconductance g_m, an input capacitance C_{in}, an output resistance r_{out} and a feed-forward capacitance C_{ff}. An output pole of the OTAs is not included in the model (an output capacitance together with the output resistance), since the OTAs drive large capacitive loads.

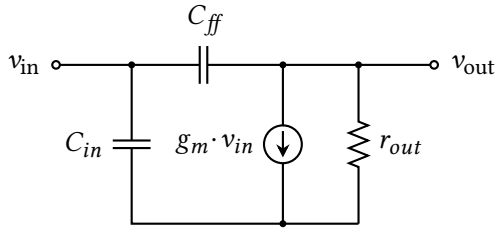

Figure 4.6. – Operational transconductance amplifier with its parasitic elements

Figure 4.7 shows the small signal model of the active inductor using non-ideal OTAs. For simpler analysis, both OTAs are assumed to be identical. Additionally, the resonator capacitance C_T is also shown. It will be used in further discussions. Since the input capacitances are in parallel with C_T and C_L, respectively, they can safely be neglected. Therefore, only C_T, C_L and C_{ff} need

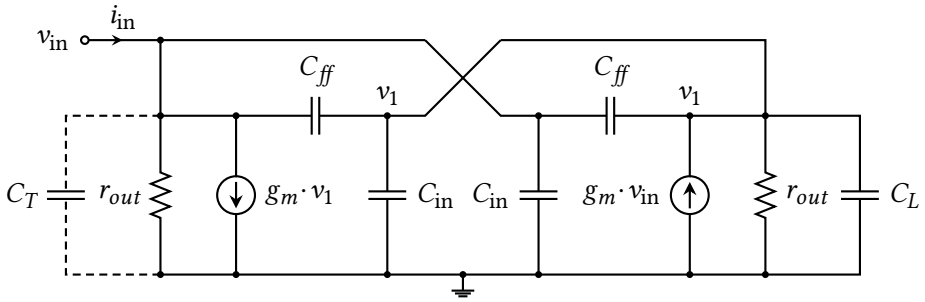

Figure 4.7. – Small signal model of the active inductor

to be considered.

$$(v_{\text{in}} - v_1)sC_{ff} + v_{\text{in}}g_m = \frac{v_1}{r_{\text{out}}} + v_1 sC_L + (v_{\text{in}} - v_1)sC_{ff}$$

$$i_{\text{in}} = v_{\text{in}}sC_T + \frac{v_{\text{in}}}{r_{\text{out}}} + g_m v_1 + 2(v_{\text{in}} - v_1)sC_{ff}$$

$$Z_{\text{in}} = \frac{r_{\text{out}} + sr_{out}^2\big(C_L + 2C_{ff}\big)}{s^2 r_{out}^2\Big(C_L C_T + 2C_{ff}\big(C_L + C_T\big)\Big) + sr_{\text{out}}\big(C_L + C_T + 4C_{ff}\big) + g_m^2 r_{out}^2 + 1}$$

The input impedance can be greatly simplified by using the restructuring the small signal model similar to passive inductors. See the circuit in figure 4.2.

$$Y_{in} = \frac{1}{R_p} + \frac{1}{C_p} + \frac{1}{R_s + sL_{eq}}$$

$$R_p \approx r_{out} \qquad C_p \approx C_T + 2C_{ff}\left(1 + \frac{C_T}{C_L}\right)$$

$$R_s \approx \frac{1}{g_m^2 r_{out}} \qquad L_{\text{eq}} \approx \frac{C_L + 2C_{ff}}{g_m^2}$$

As expected, the parasitic capacitor C_{ff} changes the parallel capacitance and the equivalent inductance of the resonator, but not the resistors. Furthermore, it does *not* introduce any additional zeros or poles, therefore it has no important influence on the frequency behavior of the resonator.

The resonance frequency of the tank is at

$$\omega_0 = \frac{1}{\sqrt{C_p L_{\text{eq}}}} \approx \frac{g_m}{\sqrt{C_L C_T}}$$

If non-identical transconductors g_{m1} and g_{m2} are assumed, then the resonance frequency

becomes

$$\omega_0 \approx \sqrt{\frac{g_{m1} g_{m2}}{C_L C_T}} = \sqrt{\omega_{u1} \omega_{u2}}$$

which is the geometrical mean of the unity-gain frequencies of the transconductors, presumed that the two capacitances C_L and C_T mainly determine the respective gain-bandwidth product. This is a good starting point for gyrator designs, since it defines the minimum needed transconductance.

R_s can be transformed to a parallel resistor for easier handling and better comparison with R_p. This is an approximation, which works well for frequencies near the resonance frequency. For very small signals, this is obviously not correct, since otherwise the resonator would be a short circuit for DC values (the inductor has no resistance). For the transformation of the series resistor, the corresponding quality factor of the inductor together with the series resistor is needed (see [Raz12] for the impedance transformation):

$$\begin{aligned}
\tilde{R}_s &= R_s\left(Q^2 + 1\right) \\
Q &= \frac{\omega_0 L_{eq}}{R_s} \\
\tilde{R}_s &= R_s\left(\frac{\omega_0^2 L_{eq}^2}{R_s^2} + 1\right) \approx \frac{\left(\omega_0^2 L_{eq}\right)^2}{R_s} \\
&= g_m^2 r_{\text{out}} \left(\omega_0 \frac{C_L}{g_m^2}\right)^2 = \frac{r_{\text{out}}}{g_m^2} \left(\omega_0 C_L\right)^2 = r_{\text{out}} \frac{C_L}{C_T}
\end{aligned}$$

The total parallel resistance of the tank near resonance can now be calculated from the parallel combination of R_p and $\tilde{R}_s$ using the relation above:

$$\begin{aligned}
R_{\text{tot}} &= R_p \parallel \tilde{R}_s = r_{\text{out}} \parallel r_{\text{out}} \frac{C_L}{C_T} \\
&= r_{\text{out}} \frac{C_L}{C_L + C_T}
\end{aligned}$$

In order to maximize the quality factor Q of the tank, R_{tot} should be maximized.

The obvious way to do this is to minimize C_T, but this also changes the resonance frequency ω_0. If ω_0 should stay constant, C_L has to vary accordingly to C_T:

$$\omega_0 = \frac{g_m}{\sqrt{C_L C_T}} = \frac{g_m}{C_0} \qquad \text{with} \quad C_0 = \sqrt{C_L C_T}$$

with

$$C_L = \alpha C_0 \quad \text{and} \quad C_T = \frac{1}{\alpha} C_0$$

With this definition, ω_0 is independent of α and R_{tot} becomes

$$R_{\text{tot}} = R_p \cdot \frac{\alpha^2}{1+\alpha^2} \tag{4.1}$$

This fraction is big for big values of α. Therefore (since $C_L = \alpha C_0$), equation 4.1 suggests that C_L should be big compared to C_T. However, a symmetrical design will show itself advantageous for phase noise performance.

With the above definitions the total resonator impedance can be expressed similar to passive inductors:

$$\begin{aligned} Z_{\text{tank}} &= \frac{1}{\frac{1}{R_p} + sC_p + \frac{1}{R_s+sL_{\text{eq}}}} = \frac{R_p\big(R_s+sL_{\text{eq}}\big)}{R_s + sL_{\text{eq}} + R_p + sR_pC_p\big(R_s+sL_{\text{eq}}\big)} \\ &= \frac{R_pR_s + sR_pL_{\text{eq}}}{s^2R_pL_{\text{eq}}C_p + s\big(L_{\text{eq}} + R_pC_pR_s\big) + R_s + R_p} \end{aligned}$$

which reduces to

$$Z_{\text{tank}} \approx \frac{sR_{\text{tot}}L_{\text{eq}}}{s^2R_{\text{tot}}L_{\text{eq}}C_p + sL_{\text{eq}} + R_{\text{tot}}}$$

4.2.2. Large signal effects

Until now, only a small signal model of the active inductor has been derived. However, due to the significant non-linear nature of the devices used to build gyrators (OTAs, transistors), the active inductor also has great dependencies on signal level. In this section the importance of this will be evaluated. Note that passive inductors also show non-linear behavior due to magnetic saturation effects. For typical on-chip signals however, this plays no role.

The large signal effects of active inductors can be best evaluated with a harmonic analysis. It is of foremost importance that the inductance is still correctly synthesized for large excitation. While a rigorous evaluation of this seems to be missing, it does not appear to have an influence on the functioning of the device as inductor (see for example [LHL06]). However, the large signal non-idealities should be taken into account in the design process. A gyrator consisting of two OTAs needs to deliver quite large currents: An oscillator with an intrinsic frequency of 5 GHz, an amplitude of 1 V and an inductor of 1 nH exhibits a reactive current through the inductor of around 30 mA. If an OTA has to supply this large currents, it will need a lot of power and chip area. Important is the fact that the current through the individual branches of the oscillator resonator is quite large, the total however is small (at resonance). Here, the tank impedance is high and the relevant current only passes through the resistance of the tank. Therefore, it is of great interest to implement not only the active inductor but *the whole resonator*. For this, the tank capacitor should be included in designing the active inductor.

The tank impedance at resonance takes the following form:

$$|Z|^2 = \frac{\omega_0^2 R^2 L^2}{(R - \omega_0^2 LRC)^2 + \omega^2 L^2} = \frac{\omega_0^2 R^2 L^2}{(R - R)^2 + \omega_0^2 L^2} = R^2$$

This is usually a large impedance, therefore the total current is small. Since the oscillator operates at the resonance frequency of the tank, this also dictates the maximum output current the internal OTAs need to provide. The parallel resistor R depends on the losses so that loss-less OTAs need no output current capabilities in theory.

4.2.3. Stability

Since gyrators are negative feedback systems, stability is an issue which needs investigation. For this, the locations of the poles of the input impedance are investigated, which have to reside in the left half-plane. There is some older work on gyrator stability (see for example [Rao70]), but it does not seem as big of an issue, since it is not mentioned in most recent publications. Some basic introductory information on stability in gyrators can be found on course slides by Yuan ([Yua15]).

The poles of the active resonator reside at

$$Z_{\text{in}} = \frac{r_{\text{out}} + s r_{out}^2 \left(C_L + 2C_{ff}\right)}{s^2 r_{out}^2 \Big(C_L C_T + 2C_{ff}\left(C_L + C_T\right)\Big) + s r_{\text{out}}\left(C_L + C_T + 4C_{ff}\right) + g_m^2 r_{out}^2 + 1}$$

$$s_p = \frac{-\left(C_L + C_T + 4C_{ff}\right) \pm \sqrt{\left(C_L + C_T + 4C_{ff}\right)^2 - 4\Big(C_L C_T + 2C_{ff}\left(C_L + C_T\right)\Big)\left(g_m^2 r_{out}^2 + 1\right)}}{r_{out}\Big(C_L C_T + 2C_{ff}\left(C_L + C_T\right)\Big)}$$

Can this system become unstable? If the term beneath the square root is negative, there are two complex-conjugate poles with a negative real part. If the square root becomes real, it must compensate the negative real part, therefore:

$$\sqrt{\left(C_L + C_T + 4C_{ff}\right)^2 - 4\Big(C_L C_T + 2C_{ff}\left(C_L + C_T\right)\Big)\left(g_m^2 r_{out}^2 + 1\right)} > \left(C_L + C_T + 4C_{ff}\right)$$

Since the second term beneath the square root is always negative, the above relation will never be true, making this a always stable system.

4.3. Implementation of active inductors

There are many very different implementation of active inductors, some using the conventional approach with OTAs, other using as little as one transistor and a phase-shifting network. Some approaches will be briefly shown here, it is however beyond the scope of this work to present

all the details. The reader is referred to a book on active inductors ([Yua08]) and the habilitation thesis of Ulrich Rohde ([Roh11]).

As was showed above, a gyrator can be built by using two operational transconductance amplifiers. However, there are simpler approaches. All that is needed is a non-inverting and an inverting transconductor. For these, simple circuits such as a common-drain and a common-source are used. The approach is shown in figure 4.8. This configuration suffers from the

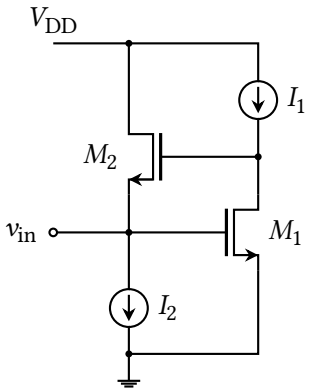

Figure 4.8. – A simple gyrator based on non-inverting and inverting transconductors

low output resistances of the transistors, which gets especially severe in newer technologies. There are numerous methods for enhancement, which involve the use of cascodes and negative resistances at the output of the transconductors. The two mentioned publications give a good overview of the use of these techniques in active inductors, which yields many different topologies with interesting names. However, most of these configurations are single-ended.

Differential active inductors are usually built by using a the classic approach with two operational transconductance amplifiers, but are not limited to it. Again, many approaches are taken to boost the gain of the transconductors. A good representative of this is the topology by Grözing (see [GPB01]), who places a cross-coupled pair at the outputs of both transconductors. Figure 4.9 shows a system structure of this gyrator. The negative resistance of the cross-coupled pairs can be tuned by varying the current source. With this, the compensation can be made quite well, yielding high quality factors. Note that this differential active inductor needs a common-mode stabilization mechanism (common-mode feedback).

Lastly, an active inductor made with only one transistor is presented. For this, a phase-shifting network is needed, which guarantees that the input shows inductive behavior (appropriate phase shift between input voltage and input current):

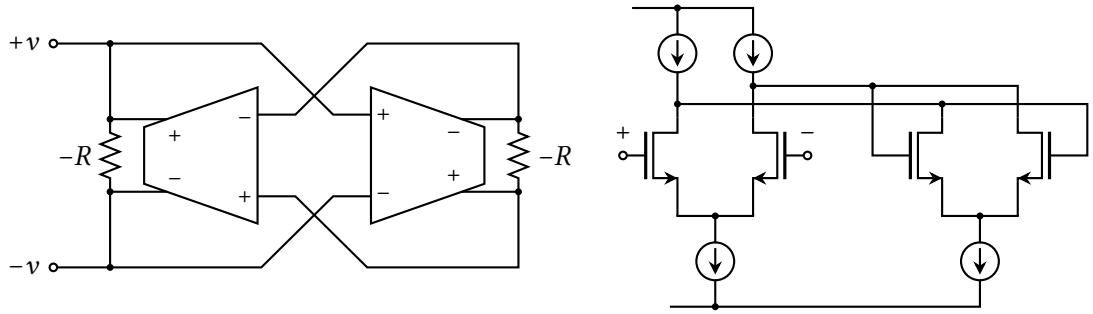

Figure 4.9. – A differential gyrator based on operational transconductance amplifiers with boosted output resistances. The negative compensation resistors are implemented as cross-coupled pairs.

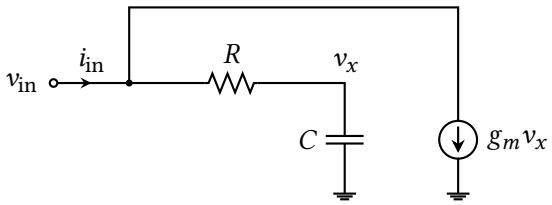

Figure 4.10. – A gyrator built from one transistor and a phase-shifting network.

$$
\begin{aligned}
i_{\text{in}} &= \frac{v_{\text{in}} - v_x}{R} + g_m v_x \\
v_x &= v_{\text{in}} \frac{1}{1 + sRC} \\
\iff i_{\text{in}} &= v_{\text{in}} \left(\frac{1}{R} + \frac{1}{1 + sRC} \left(g_m - \frac{1}{R} \right) \right) \\
\iff Z_{\text{in}} &= \frac{R\left(1 + sRC\right)}{1 + sRC + R\left(g_m - \frac{1}{R}\right)} = \frac{1 + sRC}{g_m + sC}
\end{aligned}
$$

which has an inductive region for $g_m > R^{-1}$.

The above circuit is shown by Pantoli et al. (see [PSL15]), where a class AB active inductor is built. This maximized possible voltage swing.

All in all, there are many different implementations of active inductors. Which one serves the best needs to be evaluated further.

Chapter 5.

Oscillators with Active Inductors

In this chapter, oscillators based on active inductors are presented. For this, the basic concepts of active inductors derived in the last chapter are used and expanded for analysis of oscillators.

A LC oscillator will be taken as reference design, which has an operation frequency of 5 GHz and achieves a phase noise performance of approximately −120 dBc/Hz. While this is also the goal for the oscillator to be implemented, it is only to be seen as orientation.

5.1. General considerations

In order to build oscillators with active inductors, the topology will be borrowed from the regular LC oscillator circuit. Here, a resonator determines the oscillation frequency and an active element compensates the losses of the tank. Figure 5.1 shows this principle. Since the

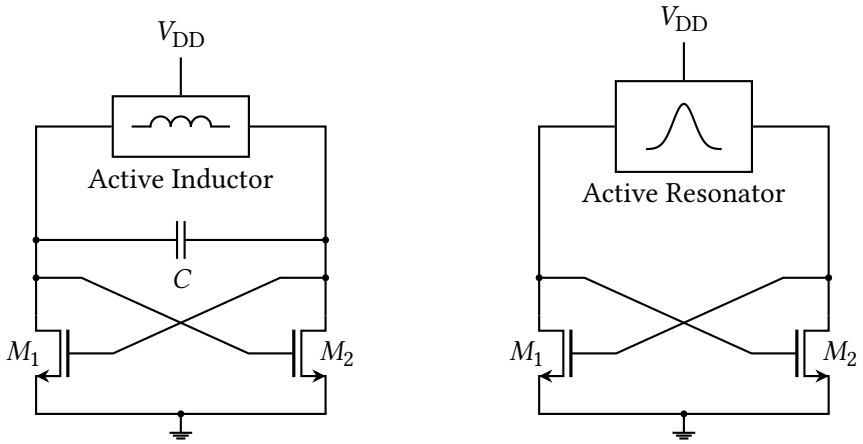

Figure 5.1. – An oscillator using an active inductor

structure of the oscillator is basically identical to the classical LC oscillator, it seems natural to use the same design methodologies for both topologies. Therefore, many known enhancements can also be used for the proposed approach, including filtering techniques (see [HSA01]) and tail current-shaping (see [SK06]). Furthermore, one can employ conventional tuning techniques,

as capacitor arrays. Interestingly, since the inductance of an active inductor depends on a capacitance, there is an additional tuning dimension using capacitor arrays also for the inductor.

The straight-forward implementation (as shown in the previous chapter) using two operational transconductance amplifiers is feasible, but it is possible to build active inductors with fewer transistors, even down to only one (see [PSL14]). Especially for differential architectures, the OTA approach has some disadvantages, since additionally to stability of the circuit the common-mode stability must be considered. There exist topologies, that circumvent this problem.

Lu et al. ([LHL06]) propose the oscillator structure shown in figure 5.2. Transistors M1 – M3 form the active inductor, which in turn, together with C forms the resonantor. The losses are compensated by the classical cross-coupled pair. Note that no current source is used in order to maximize voltage swing.

The transistors M1 and M2, together with their gate-source capacitances, perform the gyration action. The transistor M3 is mostly used in triode region and so behaves like a resistor. As will be shown below, this can be used to tune the inductance. In the original design, this property is used for the tuning of the oscillator, additionally to the use of a varactor. Therefore, the gate voltage of the two triode transistors sets the corresponding resistances. By decreasing the gate-source voltage (by increasing v_{ctrl}), the resistance also increases. At some point, the devices enter the saturation region, where the resistance will be very high, compared to the triode region. Both operating regions are suitable for this oscillator, but influence the operation frequency.

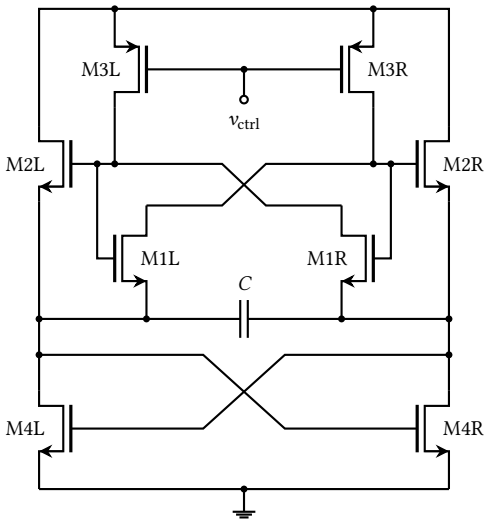

Figure 5.2. – An oscillator using a differential active inductor ([LHL06])

In this implementation of the active inductor, no lumped capacitors are used in order to set the inductance. Here, the parasitic capacitances are used, indeed the gate-source capacitors of M1

and M2 are used in the small signal model for determination of the inductance. This has the advantage of reaching higher frequencies and the lack of additional capacitors.

5.2. Small Signal Analysis

To derive the AC response of the active inductor, the a small signal model will be used. A straightforward representation of the circuit yields the model in shown in figure 5.3, here the transistors are represented by their transconductances. Additionally, the gate-source capacitances of M1 and M2 are included as C_{12} ($C_{gs1} + C_{gs2}$ since they are in parallel) as well as the gate-drain capacitance of M1. For this calculation, a differential excitation will be assumed, therefore it is sufficient to calculate the repsonse of one half of the circuit. The current law at node 1 and 2 yield the following equations:

$$i_{in} = -v_x \cdot g_{m1} + -v_x \cdot g_{m2} - s v_x C_{12} \qquad \text{Node 1}$$

$$v_x \cdot g_{m1} = \left(v_x + \frac{v_{\text{in}}}{2}\right) \cdot \left(g_{ds3} + sC_{23}\right) + s v_x C_{12} + 2s\left(2v_x + v_{\text{in}}\right) \cdot C_{gd1} \qquad \text{Node 2}$$

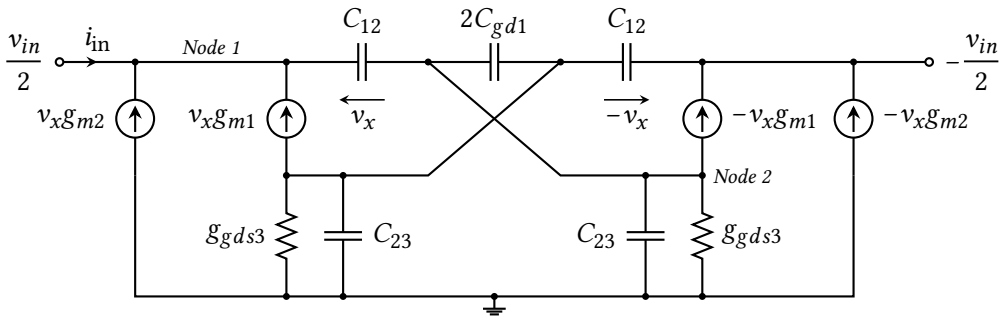

Figure 5.3. – Small signal model of the active inductor

The above equations lead to the following input impedance:

$$v_x = -v_{\text{in}} \frac{\frac{1}{2}\left(g_{ds3} + sC_{23}\right) + 2sC_{gd1}}{g_{gd3} - g_{m1} + s\left(C_{12} + C_{23} + 4C_{gd1}\right)}$$

$$i_{\text{in}} = v_{\text{in}} \frac{\frac{1}{2}\left(g_{ds3} + sC_{23}\right) + 2sC_{gd1}}{g_{gd3} - g_{m1} + s\left(C_{12} + C_{23} + 4C_{gd1}\right)} \left(g_{m1} + g_{m2} + sC_{12}\right)$$

$$Z(s) = 2 \frac{g_{ds3} - g_{m1} + s\left(C_{12} + C_{23} + 4C_{gd1}\right)}{s^2 C_{12}\left(C_{23} + 4C_{gd}\right) + s\left(g_{ds3} C_{12} + \left(C_{23} + 4C_{gd1}\right)\left(g_{m1} + g_{m2}\right)\right) + g_{ds3}\left(g_{m1} + g_{m2}\right)}$$

Again, the four-devices small signal equivalent circuit will be used to characterize the resonator:

$$L_{\text{eq}} = 2\frac{\left(C_{12}+C_{23}+4C_{gd1}\right)^3}{\left(C_{12}g_{ds3}+\left(C_{23}+4C_{gd1}\right)g_{m1}\right)\left(C_{12}\left(2g_{m1}+g_{m2}-g_{ds3}\right)+\left(C_{23}+4C_{gd1}\right)\left(g_{m1}+g_{m2}\right)\right)}$$

$$C_p = \frac{C_{12}(C_{23}+4C_{gd1})}{2(C_{12}+C_{23}+4C_{gd1})}$$

$$R_p = \frac{2(C_{12}+C_{23}+4C_{gd1})^2}{C_{12}^2 g_{ds3}+(C_{23}^2+16C_{gd1}^2+8C_{23}C_{gd1})(g_{m1}+g_{m2})+C_{12}(C_{23}+4C_{gd1})(2g_{m1}+g_{m2})}$$

$$R_s = 2\frac{\left(C_{12}+C_{23}+4C_{gd1}\right)^2\left(g_{ds3}-g_{m1}\right)}{\left(C_{12}g_{ds3}+\left(C_{23}+4C_{gd1}\right)g_{m1}\right)\left(C_{12}\left(2g_{m1}+g_{m2}-g_{ds3}\right)+\left(C_{23}+4C_{gd1}\right)\left(g_{m1}+g_{m2}\right)\right)}$$

This expression are rather complicated and not very practical. Although a different structure for the implementation of the active inductor is used, the basic properties and relations are still visible. The inductance of the resonator is a quotient of capacitances and transconductances, the tank capacitor depends in a simple manner on the involved capacitors.

More interesting is the usuable frequency range. The active inductor should have a preferably large inductive frequency range, that is a region where the magnitude of the impedace increases with frequency. This is influenced by the location of the poles and the zeros of the impedance:[1] The corresponding positions are

$$s_z = -\frac{g_{ds3}-g_{m1}}{C_{12}+C_{23}+4C_{gd1}}$$

$$s_{p1} = -\frac{g_{m1}+g_{m2}}{C_{12}}$$

$$s_{p2} = -\frac{g_{ds3}}{C_{23}+4C_{gd1}}$$

The active inductors presented above has one zero, which shows the inductive behaviour. Because of parasitic capacitances, two poles are also present, which must be higher in frequency than the zero. Note that one pole is always present in this topology, even in the ideal case. Since the zero contains a difference of two transconductances, it can be very low in frequency. This corresponds to the series resistor (in the inductor branch) of the small signal model to become very low. The poles are always negative, so this configuration is always stable.

A zero always increases the impedance with increasing frequency, but the phase shift depends on its sign. A zero situated in right half-plane produces phase shifts similar to capacitors, only a left half-plane zero shows the correct (inductive) behaviour. It is therefore necessary that the

[1] Usually, the term poles and zeros is used for systems with a transfer function, but this does not prevent the analysis discussed here.

zero of the active inductor is located at frequencies below zero:

$$s_z < 0$$
$$\iff g_{ds3} > g_{m1}$$

Furthermore, the magnitude of the zero must be smaller than that of the poles or the inductive region will be "overwritten" by capacitive behaviour. Therefore:

$$\frac{g_{ds3} - g_{m1}}{C_{12} + C_{23} + 4C_{gd1}} < \frac{g_{m1} + g_{m2}}{C_{12}} \iff g_{ds3} < \left(g_{m1} + g_{m2}\right)\frac{C_{12} + C_{23} + 4C_{gd1}}{C_{12}} + g_{m1} \quad (5.1)$$

$$\frac{g_{ds3} - g_{m1}}{C_{12} + C_{23} + 4C_{gd1}} < \frac{g_{ds3}}{4C_{gd1}} \iff g_{ds3} > -4\frac{C_{gd1}}{C_{12} + C_{23}}g_{m1} \quad (5.2)$$

Relation 5.1 has a dependence on the capacitances, but the fraction will never be smaller than 1 ($C_{12} \longrightarrow \infty$). Relation 5.2 is always true, since all circuit parameters will be always positive. Therefore, the transconductances must fulfill the following constraints:

$$g_{m1} < g_{ds3} < 2g_{m1} + g_{m2}$$

In order to minimize R_s, g_{ds3} is chosen to be of the same magnitude as g_{m1} (but slightly bigger): $g_{ds3} \approx g_{m3}$. Considering g_{m2}: Figure 5.2 shows that M1 and M2 operate at the same gate-source voltage and therefore have the same operating point. The slight difference of the drain voltages can be neglected. With this, g_{m1} is defined to be a linearly scaled version of g_{m2}.

$$g_{m1} = \alpha \cdot g_{m2}$$
$$g_{ds3} = \alpha \cdot g_{m2}$$

With this, L_{eq} becomes:

$$L_{eq} = 2\frac{\left(C_{12} + C_{23} + 4C_{gd1}\right)^3}{\alpha g_{m2}\left(C_{12} + C_{23} + 4C_{gd1}\right)(\alpha + 1)g_{m2}\left(C_{12} + C_{23} + 4C_{gd1}\right)} = \frac{C_{12} + C_{23} + 4C_{gd1}}{\alpha(\alpha + 1)g_{m2}^2}$$

In order to minimize dependence on parasitic transistor capacitances, C_{gs1} and C_{gs2} will be replaced by a big lumped capacitor C_{ind}. This allows better control of the oscillation frequency with varying supply voltage and of course process corners. Furthermore, this allows quite exact hand calculations: A minimum value for the equivalent inductor will be chosen in order to maximize the frequency range of the oscillator. A parallel tank capacitor of 1 pF will be used for the following calculations. This value is sensible to integrate and allows relativly high

frequencies. With this, the sum of the capacitances C_{12}, C_{23} and C_{gd1} is simplified as C_{ind}:

$$f_0 = \frac{1}{2\pi\sqrt{LC}} \stackrel{!}{=} 5\,\text{GHz}$$
$$L_{eq} = \frac{1}{\left(2\pi f_0\right)^2 C_{\text{tank}}} = \frac{C_{12} + C_{23} + 4C_{gd1}}{\alpha(\alpha+1)g_{m2}^2} \approx \frac{C_{\text{ind}}}{\alpha(\alpha+1)g_{m2}^2}$$
$$\Longleftrightarrow g_{m2} \approx 2\pi f_0 \sqrt{\frac{C_{\text{ind}} C_{\text{tank}}}{\alpha(\alpha+1)}}$$

With values of 1 pF for the capacitors and an oscillator frequency of 5 GHz the following g_{m2} is needed:

$$g_{m2} \approx \frac{31.4\,\text{mS}}{\sqrt{\alpha(\alpha+1)}}$$

The easiest approach is to set α to one in order to make g_{m1} and g_{m2} equal, then the maximum g_{ds3} can be calculated, obeying the above stated constraints.

With the loss known from the small signal model containing R_s and R_p, the minimum needed transconductance of the cross-coupled pair for stable oscillation can be calculated.

5.3. Noise Analysis

The discussion above on transistor sizes, transconductances and capacitor sizing may suggest to size the capacitors equally. This also corresponds to the investigation on output currents of OTAs in classical gyrators, where the findings suggested building the whole tank, not only the active inductor. In fact in can be shown that equal sizing of the capacitors yields minimum phase noise. Therefore, the inductor capacitance C_L and the tank capacitor C_T are made equal, both 1 pF.

Lu et al. perform a classical small-signal noise calculation of the input-referred noise current of the LC tank (see [LHL06, section E]) and state that with that result and the corresponding impulse sensitivity function the total phase noise can be found. They do not, however, propose any further calculation and observations so that there is no prediction of phase noise. This also applies for this work. However, some simulations have been done in order to determine the dependence of the phase noise on several circuit parameters. The findings are summarized in the next section.

5.4. Circuit improvements

In the original paper, Lu et al. place a capacitor (a varactor) parallel to the active inductor in order to obtain a resonator to be used in an oscillator. However, they do not use extra capacitances in order to set the inductance of the active inductor. For this, only the intrinsic parasitic capacitances of the transistors are used, in the model predominantly C_{gs1} and C_{gs2}. However, the these transistor capacitances are highly non-linear with varying voltage across them, which deteriorates the performance of the oscillator. In this work it was found that using additional capacitances in order to set the inductance helps the phase noise performance of the oscillator. Since the oscillator frequency decreases with increasing inductance, and the inductance increases with increasing capacitances, this has to be compensated for with a higher transconductance of the transistors M1 and M2 for constant oscillator frequency.

Additionally, the transistors don't use the whole allowed voltage swing while using a power supply with the maximum allowed voltage (in this case 1.2 V). Besides, no transistor exhibits the total voltage swing whithin the oscillator. Therefore, it is possible to raise the operating voltage and maximize the waveform amplitude. This also improves the phase noise performace. In this case, a supply voltage of 1.8 V was used. In production, the reliability has to be checked. A high voltage could pose enhanced stress on the individual transistors, decreasing their lifetime.

In this work, simulations across different operating regions of the oscillators where performed, showing no problems concerning high voltage across devices. Still, the used voltages are near forbidden regions and an extensive investigation in practical designs is necessary.

Noise simulations can show the individual contributions of the devices to the total noise. Here, it was revealed that the transistors M3L and M3R add significant amounts of noise. White noise of the value $4kT\gamma g_m$ can't be avoided, but also flicker noise plays an important role. Therefore, the area of these devices should be maximized, which in turn leads to very large devices for the small resistances needed. Therefore, it may be preferable to exchange the transistors with real resistors, which can be implemented fairly easy on chip.

The described methods of reducing noise make a big impact on the total phase noise performance. Here, it was possible to reduce the noise by nearly 20 dB from −80 dBc/Hz to −100 dBc/Hz at on offset frequency of 1 MHz, while having a constant oscillator frequency.

Chapter 6.

Experimental Results

In this chapter, simulation results for the oscillator in figure 5.2 are presented and discussed. These results are to be seen as proof-of-concept, since the oscillator was not fabricated and no layout or corner simulation were performed. However, they show what can be done and serve as starting point for circuit optimizations.

Figure 6.1 shows the tuning characteristic (left image) and the phase noise at highest and lowest frequency (right image) of the oscillator. Since both axes of the left image are logarithmic, one can see that the tuning characteristic of the oscillator is highly nonlinear. However, if linearity is important, the tuning resistances dependence on the control voltage (or word) can be made the inverse of the tuning characteristic and therefore have a linearizing effect.

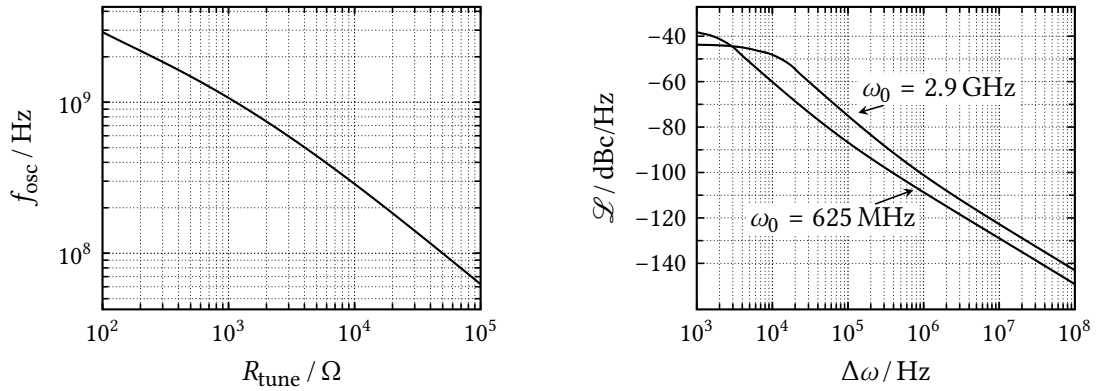

Figure 6.1. – Tuning and phase noise of the oscillator

As expected, the phase noise is lower for the slower oscillation, and the linewidth of the oscillator at the lower tuning setting is more narrow. This can be seen from the flat region of the phase noise.

Figure 6.2 shows the waveform of the oscillator at both the highest (left image) and the lowest (right image) frequency setting. As can be seen the purity of the oscillation degrades at lower frequencies. The oscillation amplitude, however, does not vary much (see also figure 6.4 for a comparison).

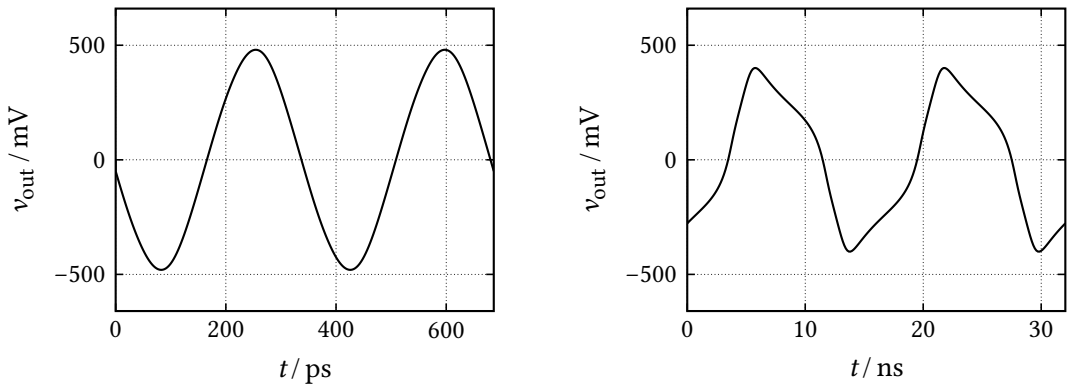

Figure 6.2. – Time-domain waveform of the oscillator at the highest (left) and the lowest (right) tuning setting. Note the change of the scaling of the x-axis.

Figure 6.3 shows the corresponding spectra of the two oscillator signals (highest setting left, lowest setting right). Again, the higher purity of the high-frequency signal is clearly visible, since the peak of the harmonics decreases more rapidly in the left image. Additionally, the absense (or low magnitude) of even-order harmonics reveals the differential design of the oscillator, which suppresses even-order nonlinearity.

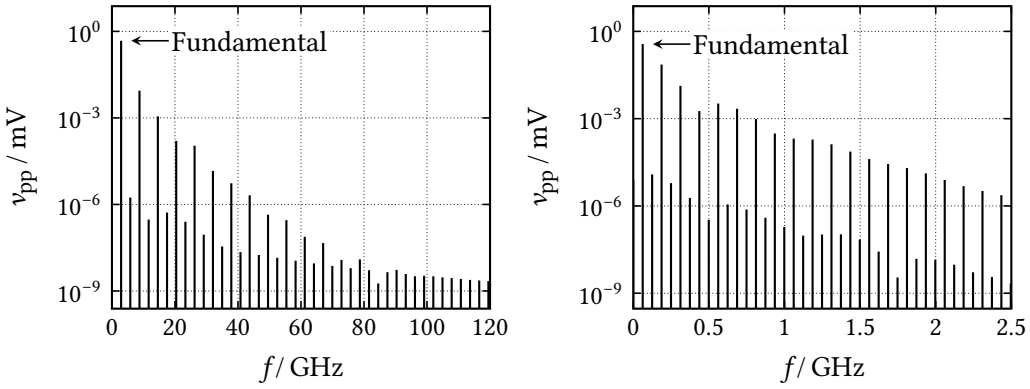

Figure 6.3. – Spectrum of the oscillator waveform at the highest (left) and the lowest (right) tuning setting. Note the change of the scaling of the x-axis

The variation of amplitude across the tuning range can be seen in the left image of figure 6.4. The amplitude is prone to some variation, but limited to about 20 %. The amplitude rises with increasing frequencies and reaches a maximum around 2 GHz. After that, it starts to decrease with a higher slope, indicating the maximum operating frequency of the oscillator. While the purity of the oscillator waveform is often not of great importance (since an output buffer is used), it does deteriorate the figure of merit and therefore the power effieciency of the oscillator. This connection of total harmonic distortion and the figure of merit can be seen in the right image of 6.4.

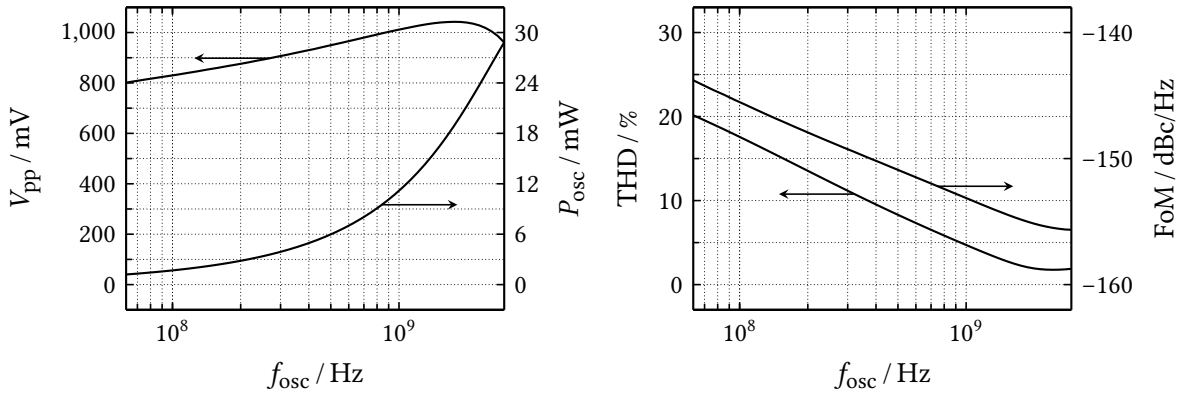

Figure 6.4. – Amplitude and total harmonic distortion (THD) across the tuning range.

Chapter 7.

Conclusions and prospects

As was shown, it is possible to build reasonable low-noise oscillator based on active inductors. However, the question arises whether it is sensible to use this topology. In the following section, the topology used in this work will be compared to other typical oscillator topologies without an inductor such as ring oscillators and relaxation oscillators.

7.1. Theoretical noise minimum of oscillators based on active inductors

An important question is the theoretically minimum achievable phase noise of an oscillator. It was shown that relaxation oscillators can't get better than a certain figure of merit (see [NLD05]). So what is the best performance an oscillator based on active inductors can achieve?

To answer this question, a linear model of the resonantor is considered. Here, the conventional approach using two OTAs is used. An OTA can be modeled by its transconductance, its output resistance and (associated with a pole) a capacitor.[1] The corresponding model can be seen in

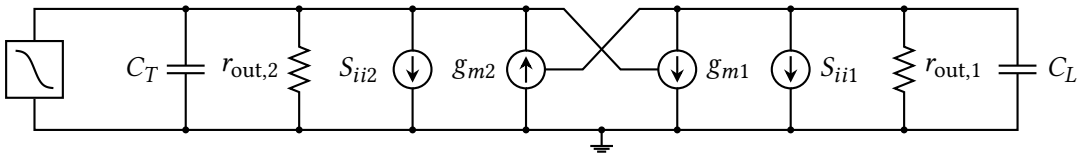

Figure 7.1. – Linear active resonantor model with non-linear energy restoring element to study phase noise behaviour

figure 7.1, where a non-linear, energy-restoring element is added in order to build a proper oscillator. Note that the rest of the model is truly linear. This circuit is simulated in cadence with varying outpout resistances.

Figure 7.2 (left image) shows the simulation result. The phase noise decreases with increasing output resistance, which is reasonable. An increase in output resistance improves the quality

[1] Here only single-pole systems are assumed.

factor of the resonator. For an infinitive output resistance the phase noise reaches 0 ($-\infty$ dBc/Hz).

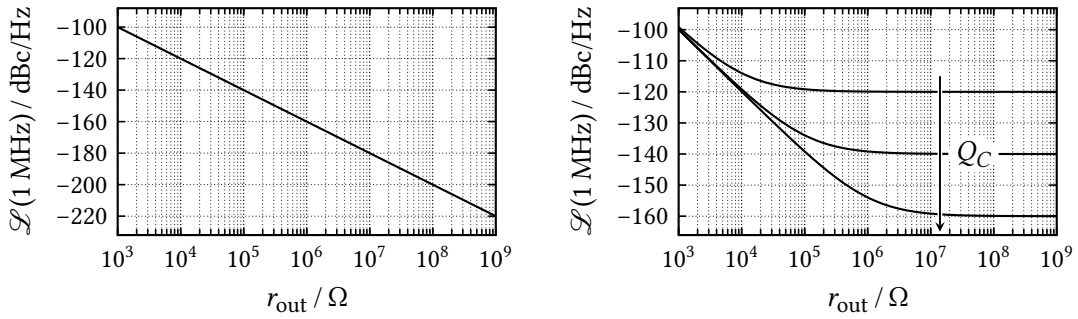

Figure 7.2. – Normalized phase noise of the oscillator in figure 7.1 with varying output resistance of the OTAs

This result is only true with ideal capacitors: Even if it were possible to build a perfect active inductor, the non-idealities of the capacitor would become noticable. This is shown in the right image of figure 7.2: At a certain point, increasing the output resistance of the OTAs does not improve phase noise. This can be seen easily in the model of figure 7.1: The degraded quality factor of the capacitors can be modeled with a parallel resistor, "replacing" the output resistor of the OTAs.

It is to be expected that the active gyrator, even if it were perfect, will introduce more noise in the tank than a conventional inductor. Furthermore, the injected noise of the passive inductor is inversely proportional to the quality factor: Q is determined by a *physical* resistor, which in turn also generates noise. The active inductor lacks this poperty. The output resistors of the OTAs determine the quality factor, but don't generate noise (they are *small signal* resistors). The noise is generated by the transistors and related to their transconductances. Therefore, for the active inductor it is possible to simultaneously get high noise and a high quality factor.

A note on the quality factor of the active inductor: Increasing the output resistance of the OTAs also increases their gain. This can also be acchieved by increasing their transconductances, but this changes the equivalent inductance. In order to keep the inductance constant (and therefore a constant oscillation frequency), the capacitances must be changed. In the end, it is possible to also improve the quality factor of the active inductor by changing the transconductances. Previously it was derived that the quality factor and the noise of the active inductor can be adjusted *independently*. How can this be true with considering the current discussion?

It is important to keep the wanted goald in mind: Improving phase noise without increasing power consumption. The phase noise can be decreased by either increasing the output resistances or the transconductances of the OTAs (with appropriate compensation of selected parameters like oscillation frequency). However, increasing transconductance always demands

proportionally more power, while increasing output resistance *does not*[2]. The output resistance of an OTA can be improved by many means, for example through the use of cascodes or cross-coupled pairs as additional loads.

Grözing et al. (see [GPB01]) proposed an active gyrator built from two OTAs whose output resistances are compensated by the means of cross-coupled pairs. Through changing their bias currents the (negative) compensation resistances can be tuned until they almost match the output resistances of the OTAs (they must not become larger or the circuit becomes unstable). The paper only shows simulation results, but here they reach a quality factor of a few hundreds. Stornelli et al. (see [Sto+16]) implement a bandpass filter based on an active inductor, which reaches a quality factor of 330. Furthermore, it can be assumed that active inductors with even higher quality factors are possible, therefore not limiting the total quality factor of the resonator. The main question is whether the extra noise of the active inductor, as compared to passive inductors, is compensated by the better quality factor of the capacitors (assuming the quality factor of the active inductors has no influence on phase noise).

Consider again Leeson's equation:

$$\mathscr{L}(\Delta\omega) = 10\log\left(\frac{2FkT}{P_{\text{tot}}} \cdot \left(1 + \left(\frac{\omega_0}{2Q\Delta\omega}\right)^2\right) \cdot \left(1 + \frac{\omega_{1/f}}{\Delta\omega}\right)\right)$$

which reduces in the ω^{-2}-region to

$$\mathscr{L}(\Delta\omega) = 10\log\left(\frac{2FkT}{P_{\text{tot}}} \cdot \left(\frac{\omega_0}{2Q\Delta\omega}\right)^2\right)$$

therefore[3]

$$\mathscr{L} \sim \frac{F}{Q^2}$$

The relation above shows that while the phase noise is linearily connected to the device excess noise, it decreases with the square of the total quality factor. This means that a tenfold increase in quality factor through active inductors can tolerate a *hundredfold* increase in device noise (with equal phase noise performance).

The analysis above has a flaw: It only considers the region of white noise and neglects flicker noise and constant phase noise (produced by white noise in the buffer of the oscillator). The latter is not of great concern for this discussion, the former however is. Here, the quality factor can not "compensate" the upconverted flicker noise. Usually, resistive lines (which are present in passive inductors) show little flicker noise. This means that the flicker noise region of the phase noise of oscillators based on active inductors will be significantly higher. However, since flicker noise occurs close to the intrinsic oscillator frequency, it could be filtered out by the phase-locked loop or injection-lock techniques within the oscillator. This must be considered in practical oscillator designs.

[2] Usually, techniques for increasing r_{out} do need a bit more power, but there is no direct proportionality as for g_m.

[3] Here, the 10 log() is dropped, since it is only used to express phase noise in dBc/Hz. The analysis does not change through this.

7.2. Comparison to other oscillator topologies

Table 7.1 compares the oscillator implemented in this work to other implementations. Since one of the key goals of this work is to present an alternative to classical topologies, the oscillator is compared to different structures. As reference, one oscillator each of the topologies relaxation oscillator, ring oscillator, LC oscillator and an oscillator based on active inductors is used. As

Topology & Work	Frequency (GHz)	Phase Noise @ 1 MHz (dBc/Hz)	Power (mW)	Area (mm^2)	FoM_T (dBc/Hz)
Ring Osc. [Liu+09]	7.3 — 7.86	−103.4	60	0.16 (0.13 µm)	−140.3
Relaxation Osc. [Ger+12]	0.001 — 0.012	−109 (@100 kHz)	0.09	0.03 (65 nm)	−145.6
LC Osc. [Zou+16]	3.61 — 5.26	−129.5 — −123.7	27	0.147 (180 nm)	−167.3 — −180.8
Active Inductor Osc.[LHL06]	0.5 — 3	−118 — −101	6 — 28	0.045 (180 nm)	−157.7 — −159.2
This work (∗)	0.625 — 2.9	−101 — −108	1.2 — 30	-	−158.3 — −164.0

Results marked (∗) denote simulation results.

Table 7.1. – Comparison of oscillator implementations

expected, the LC oscillator has the highest figure of merit and is followed by the oscillators based on active inductors. The ring oscillator shown here has a very bad FoM, they usually acchieve higher values. The oscillator implemented by Lu et al. only occupies a third of the area of the LC oscillator, but this has a much better phase noise performance with higher frequencies. Still, oscillators based on active inductors look promising and should be investigated further.

Unfortunately, there are many interesting oscillator designs with high tuning ranges, low phase noise and power consumption without any die photograph or mentioning of chip area. Therefore, these designs are not included in table 7.1, since one of the main objects of this work is the reduction of consumed chip area of oscillators.

7.3. Summary

This work presented an introduction to oscillators based on active inductors. For this, general discussions of oscillators were made in order to compare different oscillator topologies, since many already known principles can be used for active inductor oscillators. An existing topology was adapted and used to implement an oscillator in a smaller technology (65 nm), which does

not reach the performance of the reference LC oscillator. Still, the results show potential for further improvements.

7.4. Further prospects

There are research groups which investigate the implementation of active inductors. While there are some publications on oscillators, the main interest seems to be on general implementations and filter design, which may neglect certain effects influencing oscillator performance. For this, a rigorous analysis of active inductors for use in oscillators should be performed.

In my opinion, the discussion in section 7.1 should be evaluated empirically: By building an OTA with high output resistance, for example using the Grözing topology. As starting point, unrealistic conditions (neglecting mismatch and interconnect resistances) can be used in order to test the possibility of a high-Q oscillator. As was shown, with perfect capacitors the quality factor should be able to reach infinity. If high values can be reached, then the capacitors then can be made imperfect, making the model more and more accurate. For the series resistances of the capacitors, derived from specific quality factors, the following formula can be used:

$$R_s = \frac{1}{\omega_0 C Q}$$

where R_s is the series resistor, ω_0 the intrinsic oscillator frequency, C the associated capacitance and Q the corresponding quality factor.

Besides an OTA implementation of oscillators with active inductors, also the topologies using only a few transistors look promising, since here only very little devices add noise and the area can be very small.

Since stability is an issue with active inductors, perhaps this property can be used deliberately. Think for example of active inductors with OTA using the Grözing topology. Here, a cross-coupled pair is used to boost the output resistance, which is effectively parallel to the cross-coupled pair of the oscillator. In the right configuration it could be possible that one cross-coupled pair is not needed, therefore resulting in a topology with less devices and (possibly) less noise. In the big world of active inductor structures, there exist more with some kind of compensation circuit which can cause instabilities. Further investigations could reveal how these can be used constructively.

Appendix A.

Mathematical additions

A.1. Important trigonometric identities

$$\begin{aligned}
\cos(a)\cdot\cos(b) &= \frac{1}{2}\big(\cos(a-b)+\cos(a+b)\big)\\
\sin(a)\cdot\sin(b) &= \frac{1}{2}\big(\cos(a-b)-\cos(a+b)\big)\\
\sin^2(a) &= \frac{1}{2}\big(1-\cos(2a)\big)\\
\cos^2(a) &= \frac{1}{2}\big(1+\cos(2a)\big)\\
\sin(a\pm b) &= \sin(a)\cos(b)\pm\cos(a)\sin(b)\\
\cos(a\pm b) &= \cos(a)\cos(b)\mp\sin(a)\sin(b)\\
a\sin(x)+b\sin(x+\theta) &= \sqrt{a^2+b^2+2ab\cos(\theta)}\sin\Big(x+\arctan\big(b\sin(\theta),a+b\cos(\theta)\big)\Big)
\end{aligned}$$

A.2. Calculation of the ISF for the simple LC resonator

In this section, the ISF of the simple LC resonator (see figure 3.19) will be calculated analytically. First, the differential equation describing the resonator with injected current is solved. This serves as foundation for the calculation of the impulse sensitivity function.

A.2.1. Solution for the output voltage of the LC resonator under current injection

The basic differential equation is:

$$i_{\text{inj}} = i_0\delta(t-t_0) = i_C + i_L = C\frac{\partial}{\partial t}v_{\text{out}} + \frac{1}{L}\int_0^t v_{\text{out}}\,\mathrm{d}t$$

For easier analysis, this calculation will be performed in the s-domain:

$$i_0 \exp(-t_0 s) = C\big(sV_{\text{out}} - v_{\text{out}}(0)\big) + \frac{1}{sL} V_{\text{out}}$$

It is assumed that the capacitor is charged at the "beginning" ($t = 0$), so $v_{\text{out}}(0) = v_0$. Therefore,

$$\begin{aligned} i_0 \exp(-t_0 s) &= V_{\text{out}}\left(sC + \frac{1}{sL}\right) - Cv_0 \\ \iff V_{\text{out}} &= \frac{i_0 \exp(-t_0 s) + Cv_0}{sC + \frac{1}{sL}} = \frac{sL\big(i_0 \exp(-t_0 s) + Cv_0\big)}{s^2 LC + 1} \\ &= v_0 \frac{s}{s^2 + \omega_0^2} + \frac{i_0}{C} \exp(-t_0 s) \frac{s}{s^2 + \omega_0^2} \\ \iff v_{\text{out}}(t) &= v_0 \cos(\omega_0 t) + \frac{i_0}{C} \sigma(t - t_0) \cos(\omega_0 t) \end{aligned}$$

A.2.2. Calculation of the impulse sensitivity function

The above result can now be used to calculate the impulse sensitivity function. As reminder: the ISF is a periodic function, which gives the amount of phase change of an perturbed oscillator with the time of injection as parameter. To derive it, the phase change after the injection must be calculated. The oscillator waveform *after* the injection is of the form

$$v = v_0 \cos(\omega_0 t) + \Delta v \cos\big(\omega_0 (t - t_0)\big) \tag{A.1}$$

which can be written as:

$$v = a \sin(\omega_0 t + \theta) = a \cos\left(\omega_0 t + \theta - \frac{\pi}{2}\right) \tag{A.2}$$

With

$$a^2 = v_0^2 + \Delta v^2 + 2 v_0 \Delta v \cos(\omega_0 t_0) \tag{A.3}$$

$$\tan(\theta) = \frac{v_0 + \Delta v \cos\big(\omega_0 t_0\big)}{\Delta v \sin\big(\omega_0 t_0\big)} \tag{A.4}$$

The term $\omega_0 t_0$ can be expressed as ϕ_0 and is the phase at which the injection occurs. Here, only phases between 0 and 2π are considered. With this, the phase change can be calculated as

$$\begin{aligned} \Delta\phi &= \theta - \frac{\pi}{2} \\ \tan(\Delta\phi) = \tan(\theta - \frac{\pi}{2}) &= \frac{\sin\left(\theta - \frac{\pi}{2}\right)}{\cos\left(\theta - \frac{\pi}{2}\right)} \\ &= -\frac{\cos(\theta)}{\sin(\theta)} = -\frac{1}{\tan(\theta)} = -\frac{\Delta v \sin(\phi_0)}{v_0 + \Delta v \cos(\phi_0)} \end{aligned}$$

Now the ISF can be calculated to

$$\Gamma(\phi_0) = \arctan\left(-\frac{\Delta v \sin(\phi_0)}{v_0 + \Delta v \cos(\phi_0)}\right)$$

which reduces for small values of Δv to

$$\Gamma(\phi_0) \approx -\frac{\Delta v}{v_0} \sin(\phi_0)$$

For bigger values of Δv, the ISF is not really practical. Interestingly, the phase change is *not* proportional to Δv, which may be counter intuitive. Figure A.1 shows the deviation from the sinusoidal form of the ISF for larger values of Δv.

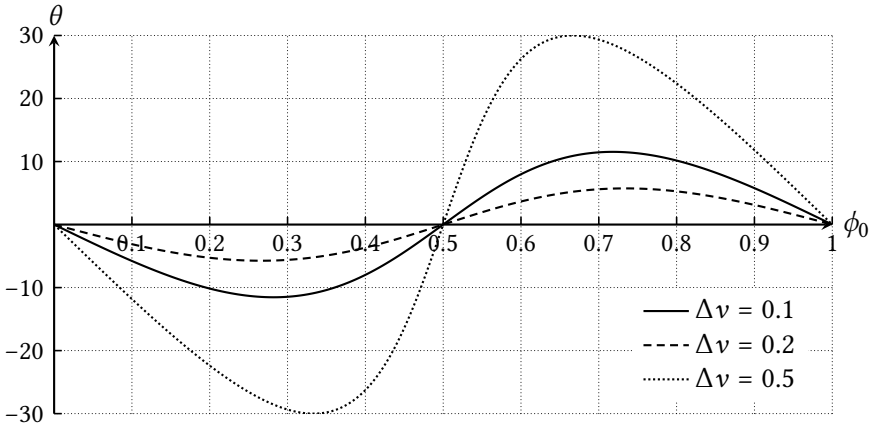

Figure A.1. – The impulse sensitivity function $\Gamma(\phi_0)$ for various values of Δv

For the ideal LC resonator, the ISF is sinusoidal, with a deviating waveform for bigger values of Δv. However, this is not important since the injection perturbance will always be small compared to the amplitude of the signal (recall that this discussion is about *noise*).

A.2.3. Injection without amplitude change

There exists a moment when the current injection causes no amplitude change. Contrary to many depictions[1], this generally *does not* coincide with the zero crossings of the oscillator waveform. Here, this point in time will be calculated using the above derived model for current injection in an ideal LC tank.

[1]For example does the original paper present it this way ([HL98]), as well as Razavi in his book on RF design ([Raz12]).

For zero-amplitude change, the following must hold (see Equation A.3 above):

$$\begin{aligned} v_0^2 &\stackrel{!}{=} a^2 \\ &= v_0^2 + \Delta v^2 + 2 v_0 \Delta v \cos(\omega_0 t_0) \\ \Delta v &= -2 v_0 \cos(\phi_0) \\ \Leftrightarrow \phi_0 &= \arccos\left(-\frac{\Delta v}{2 v_0}\right) \end{aligned}$$

The zero crossings of the (unperturbed) oscillator waveform occur at $\phi = \frac{n\pi}{2}$. At that points, Δv has to be 0 in order to have no amplitude change. But then there would be no charge injection at all, so a zero-amplitude change for injections at the zero crossings of the oscillator waveform is impossible.

Appendix B.

Simulation ressources

The following listing shows the used verilog-A module for simulating oscillators. It provides a negative, non-linear resistance in the form of a tanh-function. The maximum provided current ($I_{\max}$) and the slope in the origin (G_m) can be controlled. Furthermore, an offset can be specified, which shifts the current-voltage-characteristic voltage-wise. This can be used for single-ended simulations, but the operating point must be found by hand. In differential configurations this parameter should not be needed, since the mean of the differential voltage usually is 0.

```
`include "constants.vams"
`include "disciplines.vams"

module negative_resistance(p, n);
    electrical p, n;

    parameter real Imax = 1e-3;
    parameter real Gm = 1e-3;
    parameter real offset = 0;

    real V0 = Imax / Gm;

    analog begin
        I(p, n) <+ -Imax * tanh((V(p, n) - offset) / V0);
    end
endmodule
```

Bibliography

[Bae+16] W. Bae et al. “A 7.6 mW, 414 fs RMS-Jitter 10 GHz Phase-Locked Loop for a 40 Gb/s Serial Link Transmitter Based on a Two-Stage Ring Oscillator in 65 nm CMOS”. In: *IEEE Journal of Solid-State Circuits* 51.10 (Oct. 2016), pp. 2357–2367.

[Bes07] Roland E. Best. *Phase-Locked Loops: Design, Simulation and Applications*. 6th ed. McGraw-Hill Professional Engineering, 2007.

[CS66] L. S. Cutler and C. L. Searle. “Some Aspects of the Theory and Measurement of Frequency Fluctuations in Frequency Standards”. In: *Proceedings of the IEEE* 54.2 (Feb. 1966), pp. 136–154.

[Gar05] Floyd M. Gardner. *Phaselock Techniques*. 3rd ed. Wiley Publishing, 2005.

[Ger+12] Paul F. Geraedts et al. “Towards Minimum Achievable Phase Noise of Relaxation Oscillators”. In: (Feb. 2012).

[GPB01] M. Grözing, A. Pascht and M. Berroth. “A 2.5 V CMOS Differential Active Inductor With Tunable L And Q For Frequencies Up To 5 GHz”. In: *2001 IEEE Radio Frequency Integrated Circuits (RFIC) Symposium (IEEE Cat. No.01CH37173)*. May 2001, pp. 271–274.

[Gra+09] Paul R. Gray et al. *Analysis and Design of Analog Integrated Circuits*. 5th ed. Wiley Publishing, 2009.

[Gre07] A. Grebennikov. *RF and Microwave Transistor Oscillator Design*. John Wiley & Sons, Ltd., 2007.

[HL98] A. Hajimiri and T. H. Lee. “A general theory of phase noise in electrical oscillators”. In: *IEEE Journal of Solid-State Circuits* 33.2 (Feb. 1998), pp. 179–194.

[HRA15] Emad Hegazi, Jacob Rael and Asad Abidi. *The Designer’s Guide to High-Purity Oscillators*. 1st ed. Springer US, 2015.

[HSA01] E. Hegazi, H. Sjöland and A. Abidi. “A Filtering Technique to Lower Oscillator Phase Noise”. In: *2001 IEEE Internatinal Solid-State Circuits Conference. Digest of Technical Papers. ISSCC (Cat. No.01CH37177)*. Feb. 2001, pp. 364–365.

[Ito+06] Y. Ito et al. “A 0.98 to 6.6 GHz Tunable Wideband VCO in a 180nm CMOS Technology for Reconfigurable Radio Transceiver”. In: *2006 IEEE Asian Solid-State Circuits Conference*. Nov. 2006, pp. 359–362.

[Kim+05] Jonghae Kim et al. “A 44 GHz differentially tuned VCO with 4 GHz tuning range in 0.12μm SOI CMOS”. In: *ISSCC. 2005 IEEE International Digest of Technical Papers. Solid-state Circuits Conference, 2005.* Feb. 2005, 416–607 Vol. 1.

[Kun12] Ken Kundert. *Predicting the Phase Noise and Jitter of PLL-Based Frequency Synthesizers*. Version 4h. Mar. 2012. URL: `http://www.designers-guide.org/Analysis/PLLnoise+jitter.pdf`.

[Lee66] D. B. Leeson. "A Simple Model of Feedback Oscillator Noise Spectrum". In: *Proceedings of the IEEE* 54.2 (Feb. 1966), pp. 329–330.

[Lev+12] S. Levantino et al. "Efficient Calculation of the Impulse Sensitivity Function in Oscillators". In: *IEEE Transactions on Circuits and Systems II: Express Briefs* 59.10 (Oct. 2012), pp. 628–632.

[LHL06] L. H. Lu, H. H. Hsieh and Y. T. Liao. "A Wide Tuning-Range CMOS VCO With a Differential Tunable Active Inductor". In: *IEEE Transactions on Microwave Theory and Techniques* 54.9 (Sept. 2006), pp. 3462–3468.

[Lis+14] A. Liscidini et al. "A Power-Scalable DCO for Multi-Standard GSM/WCDMA Frequency Synthesizers". In: *IEEE Journal of Solid-State Circuits* 49.3 (Mar. 2014), pp. 646–656.

[Liu+09] H. Q. Liu et al. "A Low-Noise Multi-GHz CMOS Multiloop Ring Oscillator With Coarse and Fine Frequency Tuning". In: *IEEE Transactions on Very Large Scale Integration (VLSI) Systems* 17.4 (Apr. 2009), pp. 571–577.

[NLD05] R. Navid, T. H. Lee and R. W. Dutton. "Minimum achievable phase noise of RC oscillators". In: *IEEE Journal of Solid-State Circuits* 40.3 (Mar. 2005), pp. 630–637.

[Poo01] Rick Poore. *Phase Noise and Jitter*. Agilent EEsof EDA. 2001.

[PSL14] L. Pantoli, V. Stornelli and G. Leuzzi. "A single transistor post selector active tunable filter for radio receivers applications". In: *2014 International Workshop on Integrated Nonlinear Microwave and Millimetre-wave Circuit (INMMiC)*. Apr. 2014, pp. 1–3.

[PSL15] L. Pantoli, V. Stornelli and G. Leuzzi. "Class AB tunable active inductor". In: *Electronics Letters* 51.1 (2015), pp. 65–67.

[Rao70] T. N. Rao. "Stability of wide-band gyrator circuits". In: *IEEE Journal of Solid-State Circuits* 5.3 (June 1970), pp. 129–131.

[Raz01] Behzad Razavi. *Design of Analog CMOS Integrated Circuits*. 1st ed. McGraw-Hill, 2001.

[Raz12] Behzad Razavi. *RF Microelectronics*. 2nd ed. Pearson, 2012.

[Roh11] Ulrich Rohde. "A Novel Approach for Generating Active Inductors for Microwave Oscillators – Mathematical Treatment and Experimental Verification of Active Inductors for Microwave Applications". Habilitation. Brandenburgische Universität Cottbus-Senftenberg, 2011.

[SK06] B. Soltanian and P. R. Kinget. "Tail Current-Shaping to Improve Phase Noise in LC Voltage-Controlled Oscillator". In: *IEEE Journal of Solid-State Circuits* 41.8 (Aug. 2006), pp. 1792–1802.

[SOM11] T. Sato, K. Okada and A. Matsuzawa. "A New Figure of Merit of LC Oscillators Considering Frequency Tuning Range". In: *2011 0th IEEE International Conference on ASIC*. Oct. 2011, pp. 586–589.

[Sto+16] V. Stornelli et al. "An Assessment On Low-Voltage Low-Power Integrated Single Transisor Active Inductor Design for RF Filter Applications". In: *2016 International Conference on IC Design and Technology (ICICDT)*. June 2016, pp. 1–4.

[Tel48] B. D. H. Tellegen. "The Gyrator, an Electric Network Element". In: *Philips Technical Review* (1948).

[Tie06] Marc Tiebout. *Low Power VCO Design in CMOS*. Springer, 2006.

[Yua08] F. Yuan. *CMOS Active Inductors and Transformers. Principle, Implementation, and Applications*. Springer, 2008.

[Yua15] Fei Yuan. *CMOS Active Inductors*. Presentation Slides. 2015.

[ZB16] Z. Zahir and G. Banerjee. "A 1-2 GHz low phase-noise wide-band LC-VCO with active inductor based noise filter". In: *2016 12th Conference on Ph.D. Research in Microelectronics and Electronics (PRIME)*. June 2016, pp. 1–4.

[Zou+16] Wei Zou et al. "A low phase noise wideband VCO with 8-shaped inductor". In: *2016 International Symposium on Integrated Circuits (ISIC)*. Dec. 2016, pp. 1–4.